ACTIONS OF THE SULFUR MUSTARD ANALOGUE, NITROGEN MUSTARD, ON MOUSE SKIN AND POST EXPOSURE TREATMENT WITH CONNEXIN 43 ANTISENSE OLIGODEOXYNUCLEOTIDES

By

JAMES DANIEL WANG

A thesis submitted to the

Graduate School-New Brunswick

Rutgers, The State University of New Jersey

and

The Graduate School of Biomedical Sciences

University of Medicine and Dentistry of New Jersey

in partial fulfillment of requirements

for the degree of

Master of Science

Graduate Program in Toxicology

Written under the direction of

Dr. Donald R. Gerecke

and approved by

_____

_____

_____

_____

New Brunswick, New Jersey

May, 2014

ABSTRACT OF THE THESIS

Actions of the Sulfur Mustard Analogue, Nitrogen Mustard, on Mouse Skin and Post Exposure Treatment with Connexin 43 Antisense Oligodeoxynucleotides

By JAMES DANIEL WANG

Thesis Director:

Donald R. Gerecke, Ph.D.

Nitrogen mustard (NM), a less potent vesicant analog of sulfur mustard (SM), has very similar biological activity and function compared with SM. Connexin 43 (Cx43), the ubiquitously expressed gap junction protein in the skin, plays a significant regulatory role in wound repairs. In non-diabetic rodents and humans, there is a downregulation of Cx43 and an up-regulation of Connexin 26 and 30 (Cx26 and Cx30) in keratinocytes at the wound edges. The SKH-1 hairless mouse is a widely used wound healing model which has been used in SM research. The studies described here employed this model to examine the hypothesis that the changes in expression of Cx43 which are involved in diabetic and incisional/excisional wound healing play a role in the healing of NM chemical burn injuries as well. In addition, we hypothesize that Cx43 antisense oligodeoxynucleotides (Cx43 asODN) will facilitate the healing process after NM exposure as has been observed in the treatment of diabetic and incisional/excisional wounds. Using the SKH-1 mouse dorsal skin model, the present studies demonstrated that Cx43 was downregulated by NM at days 1, 3, 7, and 10 post-NM exposure, in a manner similar to that normally occurring in excisional/incisional wounds. In addition, Cx43 was further downregulated significantly by Cx43 asODN at day 3 and day 7. In

contrast, Cx26 and Cx30 were upregulated by NM for days 1, 3, 7, and 10 just has been observed in the diabetic and incisional/excisional wound models. In addition, Cx43 asODN significantly reduced expression of Cx26 and Cx30. Furthermore, Cx43 asODN reduced levels of the proinflammatory mediator interleukin 1B (IL-1B), COX-2 and increased interleukin 10 (IL-10), an anti-inflammatory cytokine. Finally, the histological examination of tissue sections of the mouse skin demonstrated that Cx43 asODN reduced inflammatory cell infiltration, hyperplasia, and thickening of the stratum corneum. The data suggest that Cx43, Cx26, and Cx30 play important roles in the healing of NM injuries in the SKH-1 hairless mouse dorsal skin model similar to that of the incisional/excisional wound model. In addition, post exposure treatment with Cx43 asODN leads to reduce expression of Cx43, Cx26, and Cx30 and facilitate wound repair.

Acknowledgements

The author wishes to express his gratitude to Dr. Donald Gerecke for his understanding, support, and valuable guidance during the course of this work.

Appreciation is also extended to Drs. Gisela Witz and Marion K. Gordon, members of my thesis committee, for their enormous help and valuable suggestions. Special thanks to Dr. Yoke-chen Chang, also a thesis committee member, for her coaching and guidance through the work.

I sincerely thank my colleagues Rita Hahn, Peihong Zhou, Iris Po, Andrea DeSantis Rodrigues and Alex Tang for their suggestions and help.

Table of Contents

Table of Contents (continued)

Page number

Table of Contents (continued)

Page Number

Table of Contents (continued)

Page Number

List of Tables

Page Number

List of Figures

Page Number

List of Figures (continued)

Page Number

List of Abbreviations

CEES	2 -chlorethylethyl sulfide
CCL-2	chemokine ligand-2
COX-2	cyclooxygenase-2
Cx43	connexin 43
Cx43 asODN	connexin 43 antisense oligodeoxynucleotides
Cx43 scODN	connexin 43 sense control oligodeoxynucleotides
Cx26	connexin 26
Cx30	connexin 30
DNA	deoxyribonucleic acid
DEPC	diethylpyrocarbonate
ECL	enhanced chemiluminescence
ECM	extracellular matrix
GAPDH	glyceraldehyde 3-phosphate dehydrogenase
H&E	haematoxyline and eosin stain
hr	hour
HRP	horseradish peroxidase
IL-1B	interleukin-1B
IL-6	interleukin-6
IL-10	interleukin-10
NM	nitrogen mustard
MMPs	matrix metalloproteinases
mRNA	messenger RNA
O.C.T.	optimal cutting temperature

List of Abbreviations (continued)

PGE-2	prostaglandin-2
PGES-2	prostaglandin E_2 synthase-2
qRT-PCR	quantitative reverse transcription polymerase chain reaction
SM	sulfur mustard
WB	western blotting

Introduction

1. Sulfur Mustard (SM) and its Analogs Nitrogen Mustard (NM) and 2-Chloroethyl Ethyl Sulfide (CEES)

Sulfur mustard (bis[2-chloroethyl] sulfide, SM, Figure 1) and its analog nitrogen mustard (bis(2-chloroethyl)methylamine, NM, Figure 1) are vesicants, i.e. blistering agents, with SM being the more reactive of the two. Both chemicals contain highly reactive bifunctional alkylating groups which can crosslink proteins, DNA, and other cellular components which can lead to disruption of tissue structure and loss of biological activity (Ghabili et al., 2011). SM was synthesized in 1822 and was first used as a chemical warfare agent in WWI by German troops. It was also used as recently as the 1980s Iraq-Iran war. In contrast to SM, NM was synthesized in the 1930s but was not produced in large amounts for warfare (Ganesan et al., 2010). SM exposure causes severe injure, while NM causes moderate to severe vesicant injury. CEES (2-chloroethyl ethyl sulfide, or half mustard, Figure 1) is a chemically related analog of sulfur mustard which shows relatively mild vesicant activity. NM and CEES are commercially available, less toxic and widely used as experimental alternatives to SM exposure in research laboratories (Sharma et al., 2008; Shakarjian et al., 2010). SM remains a significant military and civilian threat since its first use in WWI (Graham et al., 2009).

SM is a poorly volatile oily liquid which is barely soluble in water, but highly soluble in organic solvents. It ranges from light yellow to dark brown in color and has the odor of onion, garlic, or mustard. In its pure form, SM is a colorless, viscous liquid at room temperature, with a specific gravity of 1.27 and a melting point of 14°C. Other mustard agents differ in melting point and other physical properties but have broadly similar biological effects (Marrs et al., 1996). Sulfur and nitrogen mustards are lipophilic and readily

penetrate the skin (Ivarsson et al., 1992). After passing through the cellular membrane, sulfur mustards (SM and CEES) form highly reactive sulphonium ions, while nitrogen mustard forms an immonium ion. These intermediate ions are electrophilic and can attack nucleophilic sites in skin, lung and cornea. Both mustard ions irreversibly alkylate DNA, RNA, lipid and protein, which can result in cell death. An important target is DNA in which the purine bases are alkylated and damaged (Shakarjian et al., 2010).

Figure 1. Structures of sulfur mustard (SM), 2-chloroethyl ethyl sulfide (CEES, half-mustard), and nitrogen mustard (NM, HN2). All three agents induce blistering of the skin. Sulfur mustard is the most potent of these agents followed by NM and CEES. Adapted and modified from Shakarjian et al., Toxicol Sci. 114(1):5-19. 2010.

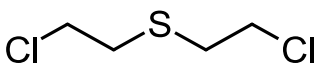

Sulfur Mustard (SM, HD)

bis(2-chloroethyl) sulfide

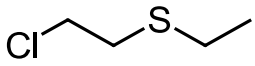

CEES (Half Mustard)
2-chloroethyl ethyl sulfide

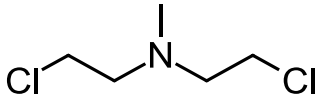

Nitrogen Mustard (NM, HN2)
bis(2-chloroethyl)methylamine

2. Acute and Chronic Effects to the Skin after SM Exposure

The primary targets of SM vapor exposure are skin, cornea, and respiratory tissues. SM affects the upper respiratory tract and the lungs and causes pulmonary edema. SM can also cause severe eye injuries and ultimately blindness. SM penetrates skin and causes extensive blistering after a latent period of several hours (This delay is observed in all tissues affected by mustards). The response of human skin to SM exposure is delayed onset of

erythema, followed by edema, inflammatory cell infiltration, the appearance of large blisters, and a prolonged healing period (Shakarjian et al., 2010). Exposed animal models show only microblisters, then shedding of the epithelium. The mechanism of blister formation is similar to Epidermolysis Bullosa (EB), a genetic human skin disease which produces fragility and blistering of the skin in mechanical trauma (Coulombe et al., 2009; Shakarjian et al., 2006). Matrix metalloproteinases (MMPs) play a role in both EB and SM-induced skin injury (Shakarjian et al., 2006). Skin blistering in both conditions is formed due to a separation of the epidermis from the dermis. In addition, separation of several proteins that attach basal keratinocytes to the basement membrane zone is observed (Monteiro-Riviere et al., 1999; Uitto and Pulkkinen, 2001).

In humans, usually no symptoms appear during the first hour after exposure, though occasionally there are signs of nausea, vomiting, and eye irritation (Ghabili et al., 2011). The effect to the eyes is faster than in the skin and the lung (Smith and Dunn, 1991). The threshold dose (the minimal dose for SM to cause damage) from skin exposure (200 μg x min/l) is much higher than the threshold dose of eye exposure (12 μg x min/l) (Smith and Dunn, 1991; Solberg et al., 1997). The respiratory tract, including the nasal, laryngeal, and tracheo-bronchial mucosa and the skin, are also the sensitive sites (Smith and Dunn, 1991). The onset of skin damage after SM exposure is slower than that observed in the eyes (Smith and Dunn, 1991). The initial signs of intense itching and erythema were observed around 6 hours post exposure (Smith and Dunn, 1991). Large round vesicles filled with a pale yellow liquid were observed 13 to 48 hours after exposure (Smith and Dunn, 1991). The vesicles may coalesce to form pendulous blisters. The blisters are formed due to separation of the epidermal and dermal layers with disruption of the basement membrane zone followed by edema (Zhang et al., 1995; Monteiro-Riviere et al., 1999). Subsequently, blisters burst and form either a necrotic layer or an eschar on the affected skin surface.

With respect to chronic effects in humans, the wounds may last 0–50 days and pigmentation changes may persist for months or years (Balali-Mood and Hefazi, 2005). The occurrence is directly related to the duration and severity of exposure. The most common long term cutaneous lesions are hyper-pigmentation, erythematous papular rash, dry skin, multiple cherry angiomas, atrophy, hypo-pigmentation, and hypertrophy (Balali-Mood and Hefazi, 2005). The healing of cutaneous SM injuries can take several months and can lead to long-term complications. Unlike other skin wounds, sulfur mustard injury is not reversible and doctors can only treat the symptoms. Currently, the standard or optimal methods of casualty management are still not well known, and no drugs are as yet known to be effective therapies. New strategies are needed for rapid and optimal methods to treat the wounds, and to improve long-term complications (Balali-Mood and Hefazi, 2006).

Figure 2 demonstrates the time course of pathophysiological responses following cutaneous SM exposure. Figure 3 depicts a hand with large blisters from exposure with SM.

Figure 2. Pathophysiological changes after dermal exposure to SM. After a latency period, the first sign of injury is erythema. Vesiculation starts between 13 and 22 hr after exposure and large blisters develop between 16-48 hr. It takes 2–3 weeks for vesicating lesions and several weeks for full-thickness erosions (Balali-Mood and Hefazi, 2005). Adapted from Shakarjian et al., Toxicol Sci. 114(1):5-19. 2010.

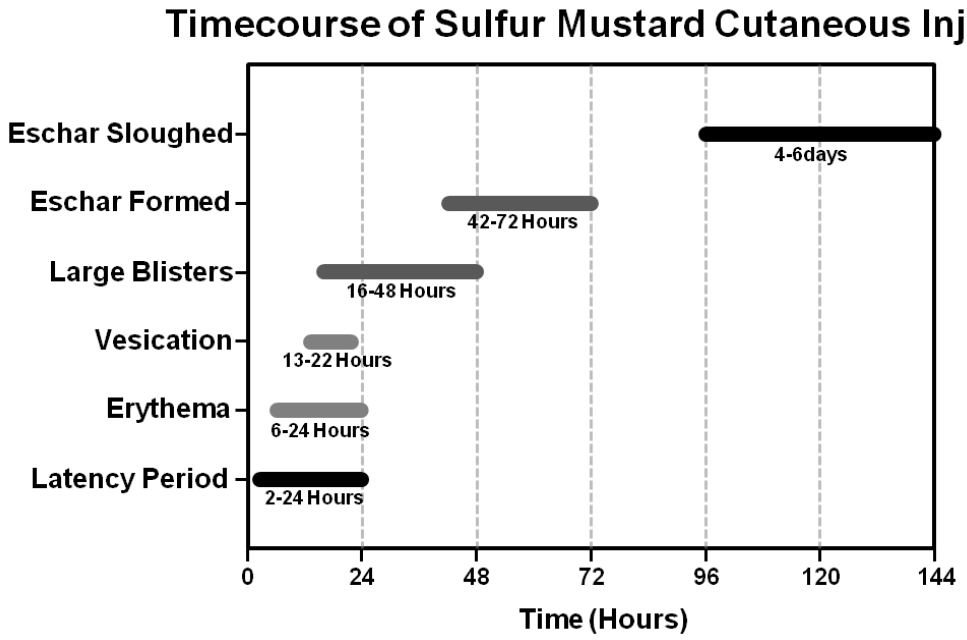

Figure 3. Large blisters on skin from exposure with SM. Blister formation due to separation of the epidermal and dermal layers occurs due to disruption of the basement membrane zone. Photo adapted from Zachary R. "mustard gas-blister." *Moriches Daily July 3, 2010. <http://morichesdaily.com/2010/08/toxic-munitions-dumping-sites-shores/mustardgas-blister/>*

3. Animal Model Systems to Study Skin Wound Healing after SM Exposure

Various animal models have been developed and used to study SM-induced toxicity in the skin. Species utilized are rabbits, guinea pigs, pigs, and mice (Smith et al., 1997; Tewari-Singh et al., 2009; Lindsay et al., 2004; Casillas et al., 1997). SM and other mustards were applied using a vapor cup or diluted with a suitable vehicle. Four stages (latency, erythema, vesiculation, and necrosis) of SM-induced injury were observed in the animal models. However, gross vesiculation characteristic of human exposures is not readily observed in animal models and only microblisters are detectable (Smith et al., 1997). Both the *in vivo* mouse ear and the *in vivo* hairless mouse models were initially considered to be used in our studies.

3.1. *In Vivo* Mouse EarModel to Study Skin Wound Healing after SM Exposure

The mouse ear model was first developed by Brinkley et al. (1989) to investigate SM-induced dermal changes. The model was further modified and characterized by Casillas et al. (1997) and named the mouse ear vesicant model (MEVM). Using male CD1 mice, liquid SM (0.04–0.64 mg in 5 μl dichloromethane) was applied to the medial surface in one ear with the other ear serving as the vehicle control. Samples were collected for analysis at 12, 18, and 24 hr post-exposure. Casillas et al. (1997) reported that after a latency period, the frequency and severity of histopathological markers, including epidermal necrosis, edema, and the formation of microblisters on medial and lateral surfaces, were increased and were dose-dependent. Based on edema response and histologic profiles, the optimal SM dose and exposure time for studies to develop pharmacological countermeasures using the MEVM was determined to be 0.16 mg/ear for a 24 hr exposure.

Due to technical drawbacks, the MEVM is not suitable for long-term studies (Dachir et al., 2010). It was found that the damage from liquid SM affects even the side of the ear not

exposed, developing “through and through” holes in the tissue. Since we planned to conduct a time course study for up to 10 days, we exposed the dorsal skin (which is thicker than ear skin) of the hairless mouse (SKH-1) model.

3.2. *In Vivo* Hairless Mouse Model to Study Skin Wound Healing after SM Exposure

SKH-1 mice (Figure 4) are an uncharacterized/non-pedigreed hairless strain of mice which was acquired by Temple University from a small commercial supplier in New York City. These mice were transferred in 1986 to Charles River from the Skin and Cancer Hospital at Temple University. This mouse is euthymic and immunocompetent. It has no obvious immunological deficiencies (Charles River Lab). SKH-1 hairless mice serve as a general rodent model for dermal research for safety and efficacy testing. They are particularly used in UV-induced skin damage studies and serve as a well characterized wound healing model (Anwar et al., 2008).

SKH-1 mice were used in CEES-induced skin injury for dose response (0.05–2 mg) and time dependency (3–168 hr) studies to investigate the expression of important inflammatory biomarkers (Tewari-Singh et al., 2009). Quantifiable inflammatory biomarkers of CEES-induced skin toxicity were determined and related to histopathological damage. Results showed most of the CEES-induced inflammatory response peaked near or after 9 hr and subsided within 72–168 hr (3-7 days) post-exposure. The inflammatory biomarkers investigated were edema, epidermal and dermal thickness, macrophage numbers, and neutrophil number. These were found to be useful for assessing the efficacy of therapeutic countermeasures being developed against SM-induced skin toxicity (Tewari-Singh et al., 2009).

More recently, Vallet et al. (2011) investigated acute and long-term (6 hr to 21 days) transcriptional upregulation in SM-exposed SKH-1 hairless mouse skin. The time-dependent

quantitative gene expression of various selected transcripts were determined up to 21 days post-exposure. These included the expression of two interleukins (IL-1β and IL-6), a macrophage inflammatory protein (MIP-2α, also called Cxcl2), tumor necrosis factor α (TNF-α), MIP-1αR (also called Ccr1), the laminin γ2 chain monomer (Lamc2), and two matrix metalloproteases (MMP-9 and MMP-2). The data showed that the mRNA levels for IL-6, IL-1β, Ccr1, and Cxcl2 were increased as early as 6 hr and remained up-regulated for 14-days. In addition, MMP-9, TNF-α, and Lamc2 expression were significantly up-regulated at specific time points during the 21 days assessed. However, MMP-2 mRNA levels remained unchanged even at day 21 post exposure. In addition, Joseph et al. (2011) used SM in a vapor cup model to expose the dorsal skin of these hairless mice with saturated SM vapor. The correlation of structural changes in the skin with inflammation and DNA damage was examined from full thickness skin punch biopsies collected at days 1, 3, 7 and 14 post-exposure. They found after 1 day, SM exposure resulted in epidermal thinning, stratum corneum shedding and neutrophil accumulation in the dermis. At day 3, a loss of epidermal structures was observed and cyclooxygenase-2 (COX-2) was upregulated. At day 14, epidermal regeneration with extensive hyperplasia was seen and COX-2 expression was reduced. The authors concluded that the data were consistent with the pathophysiology of skin injury in humans exposed to SM, validating the SKH-1 hairless mouse as a model to assess the dermal toxicity of vesicants.

Figure 4. A SKH-1 hairless mouse. SKH-1 mice are an uncharacterized/non-pedigreed hairless strain of mice which serve as a rodent model for dermal research for safety and efficacy testing. Photo adapted from Charles River-SKH-1 mouse. *http://www.criver.com/EN-US/PRODSERV/BYTYPE/RESMODOVER/RESMOD/Pages/SKH1Mouse.aspx*

4. Role of Connexins in the Skin and Wound Healing

Local cell-cell communication plays a significant regulatory role in wound repair of skin (Mori et al., 2006). This local communication requires the gap-junction (GJ) proteins, connexins (Cxs) (Figure 5) (Goodenough and Paul, 2009), in order to maintain homeostasis and to directly influence wound repair. Gap junction channels allow the direct exchange of small molecules between cells. Local injury causes a complex response leading to the healing of injured tissues, and cellular regeneration. The initiation, maintenance, and resolution of those responses require gap junction cellular communication (Chanson et al., 2005).

Gap junctions are specialized cell–cell connections that directly link the cytoplasm of neighboring cells. The channels span the two plasma membranes and are formed by the alignment of two hemichannels, each consisting of an oligomer of a structural subunit known as a connexin. Six connexins oligomerize to form the hemichannels referred to as ‘‘connexons’’ (Goodenough and Paul, 2003). A gap junction channel is created when one hemichannel docks with a second one in an opposing cell (Burra and Jiang, 2011). Groups of

these intercellular channels (termed gap junctional plaques) mediate the passage of amino acids, second messengers (eg. cyclic AMP), electrical signals, ions (Ca^{2+}), and other molecules of molecular weight <1000 Da (eg. glucose and prostaglandins such as PGE-2) through the connected cytoplasmic domains (Lampe and Lau, 2004; Sohl et al., 2005; Oyamada et al., 2005). Data acquired from connexin (eg. Cx47) knockout mice indicated that gap junction communication is critical for tissue functions and organ development (Oyamada et al., 2005).

In forming a gap junction channel, the membranes of two adjacent cells must come close to each other, but must leave a 2–4 nm intercellular space (gap) (Meşe et al., 2007). The pores of gap-junction channels are then wide enough (approximately 1.2 nm) to be permeable to a wide variety of molecules (up to about 1 kDa in molecular mass) (Hervé and Derangeon, 2013).

The opening or closure of gap junctional channels is controlled by gating mechanisms that include calcium ion concentration, pH, transjunctional membrane potential (voltage dependence), and protein phosphorylation. However, the exact mechanism of opening and closing remains unclear (Bajpai et al., 2009, Hervé and Derangeon, 2013). The controlled gating through gap junctions is highly essential for keeping cells functioning normally. Phosphorylation of intracellular regions of the connexins is known to alter the gating and permeability of the gap junction channels (Lampe and Lau, 2004; Cooper and Lampe, 2002; Cameron et al., 2003). The half-life of connexins is short and does not exceed more than a few hours. Formation and degradation of connexins is a dynamic process. Connexins are degraded through either proteasomes or lysosomes (Dbouk et al., 2009).

Thus far, 21 human and 20 mouse connexin genes have been identified (Sohl and Willecke, 2003). Connexin expression can be regulated at steps from DNA to RNA to protein

but transcriptional control is one of the most important (Oyamada et al., 2005). Among connexins, connexin-43 (Cx43) is the most ubiquitously expressed connexins. It is endogenously expressed in over 35 cell types including keratinocytes, endothelial cells, cardiomyocytes, and astrocytes (Nicholson, 2003; Oyamada et al., 2005; Matsuo et al., 2007; Laird, 2006).

Figure 5. Structures of connexin, connexon (hemichannel) and gap junction. Schematic model illustrating assembly of connexins into gap junctions. Six connexin subtypes oligomerize into connexons or hemichannels. Two connexons combine into a gap junction. (Adapted and modified from Wagna, C. (2008). Function of connexins in the renal circulation. *Kidney International.* 73: 547–555.)

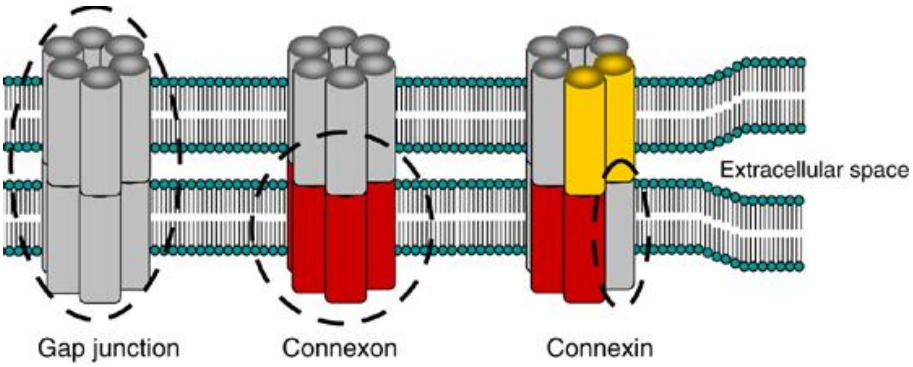

4.1. Role of Connexin 43 (Cx 43), Cx26 and Cx30 in the Skin and Wounds

Connexins play an essential role in tissue and organ homeostasis via gap junction communications during keratinocyte growth and differentiation. Mutations in connexin genes lead to several human hereditary diseases. At least nine connexin genes, including those for Cx43, Cx26, Cx30, Cx30.3 and Cx31, are expressed during the differentiation of keratinocyte (Di et al., 2001; Langlois et al., 2007). It was reported that Cx43 and Cx26 collectively co-regulate epidermal differentiation from basal keratinocytes (Langlois et al., 2007). Cx43,

Cx26, and Cx30, a close homologue of Cx26, are co-expressed in human and rodent epidermis (Richard, 2000).

The expression pattern of connexins in human epidermis is depicted in Figures 6 and 7. In human interfollicular skin, Cx43 is mainly expressed in the suprabasal layers, with the highest expression in the granular layer. Cx30 is expressed in the granular layer, while Cx26 is expressed in the basal layer and granular layer of palmoplantar skin. In contrast, in adult rodents, Cx43 is predominantly expressed in the basal layer and Cx26, Cx30 in the suprabasal layers (Scott et al., 2012). The histological images of SKH-1 hairless mouse dorsal skin and ear skin are depicted in Figure 7.

Both Cx26 and Cx43 are expressed in the hair follicles and sweat glands (Salomon et al., 1994). Cx43 is expressed in multiple cell types in the skin and is involved in many stages of tissue repair. The levels of Cx26 and Cx30 are extremely low in the normal unwounded epidermis. In the epidermis, Cx26 and Cx30 have a negative correlation with proliferation, while Cx43 has a positive correlation (Coutinho et al., 2003). In the adult human epidermis, connexins have distinct as well as overlapping expression patterns. However, under pathological conditions, the normal distribution of connexins is altered.

Though the role of connexins during keratinocyte differentiation is still not well understood, the correlation of different skin pathologies with mutations in the genes of Cx43, Cx26, Cx30, Cx30.3, and Cx31 indicate that intercellular communication during development and differentiation of the epidermis is very important (Richard, 2005). Mutations (dominant) in the gene encoding Cx43 leads to the pleiotropic developmental disorder ODDD (Oculodentodigital Dysplasia) (Meşe et al, 2007). A brief summary of skin epidermal connexins and associated disorders is listed in Table 1.

Table 1. Skin epidermal connexins and associated disorders in humans (Table adapted and modified from G Meşe et al, 2007).

Gene	Hereditary disease
GJB4(Cx30.3)	Autosomal-dominant erythrokeratodermia variabilis
GJB3(Cx31)	Autosomal-dominant and -recessive erythrokeratodermia variabilis Autosomal-dominant and -recessive nonsyndromic sensorineural hearing loss (DFNA3)
GJB2(Cx26)	Autosomal-recessive nonsyndromic sensorineural hearing loss (DFNB1) Autosomal-dominant nonsyndromic sensorineural hearing loss (DFNA3) Vohwinkel syndrome Keratitis–ichthyosis–deafness syndrome Palmoplantar keratoderma associated with sensorineural hearing loss Bart–Pumphrey syndrome
GJB6(Cx30)	Autosomal-recessive nonsyndromic sensorineural hearing loss (DFNB1) Autosomal-dominant nonsyndromic sensorineural hearing loss (DFNA3) Clouston syndrome (Hidrotic ectodermal dysplasia)
GJA1(Cx43)	Oculo–dento–digital dysplasia

Figure 6. Expression pattern of connexins in human epidermis. At least nine different connexins have been identified during epidermal morphogenesis, which is likely to represent the pattern of connexins in injured skin. Adapted from Gülistan Meşe, Gabriele Richard and Thomas W. White. Gap Junctions: Basic Structure and Function. *Journal of Investigative Dermatology* (2007) 127, 2516–2524.

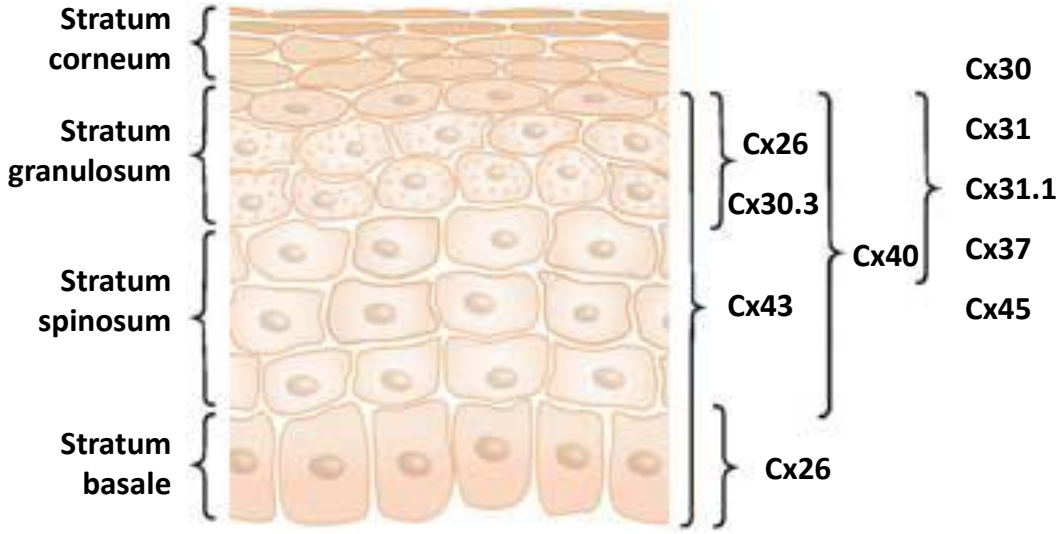

Figure 7. Expression pattern of connexins in human epidermis and histological images of SKH-1 hairless mouse dorsal skin and ear skin.

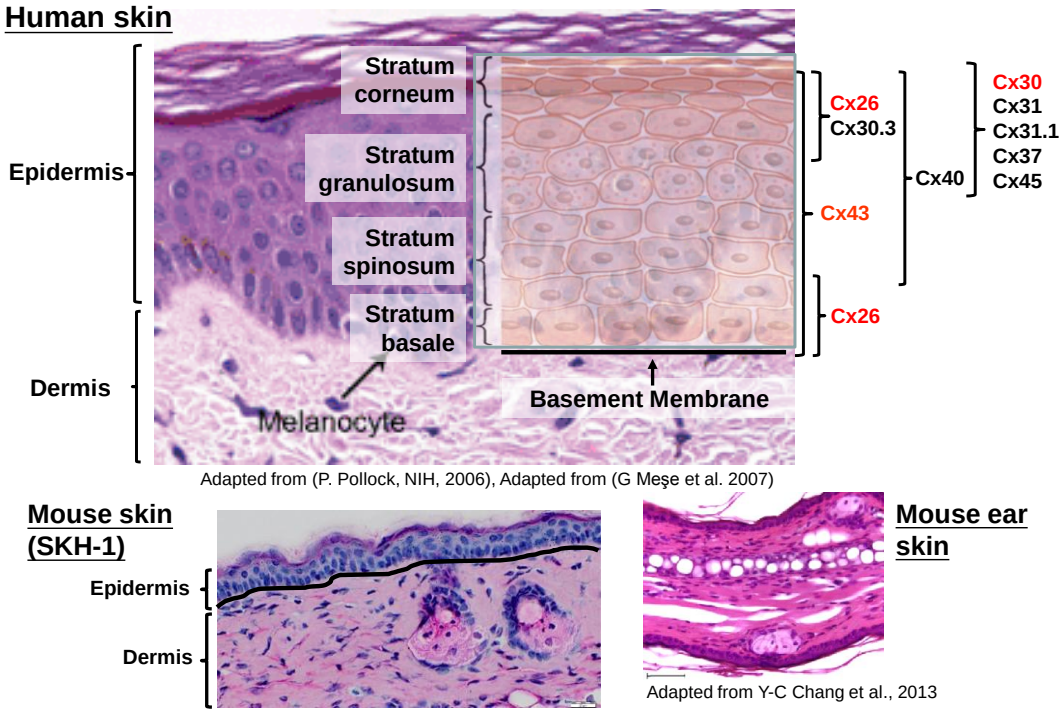

Local skin injury results in a complex response for the healing of the injured tissue and the regeneration of cells. The initiation, maintenance, and resolution of these responses require cellular communication via connexins (Chanson et al., 2005). Epidermal recovery is a critical part of cutaneous wound healing because it leads to closure of the wound and restores the important barrier function of the skin. The process involves the proliferation and migration of immature keratinocytes at the wound margins and the differentiation of the immature keratinocytes in the regenerated epidermis. Cx43, being the most broadly expressed connexin in epidermis (Meşe et al, 2007), is expressed in multiple cell types of the skin, including keratinocytes and dermal fibroblasts. It is involved in many stages of tissue repair (Coutinho et al., 2003). As mentioned, cell-cell communication through Cx43 plays a major role in the wound healing process, and the junctional protein is known to be regulated by glucose, nitric oxide, TGF-β, and TNF-α. However, the mechanisms by which they regulate Cx43 are still not clear (Bajpai et al., 2009). Cx43 is also expressed by most of the immunocompetent cells including macrophages, neutrophils, mast cells, and lymphocytes (Oviedo-Orta and Howard, 2004).

In rodents and humans there is a downregulation of Cx43 and an up-regulation of Cx26 and Cx30 in keratinocytes at the wound edges (Brandner et al., 2004; Coutinho et al., 2003; Goliger and Paul, 1995). The expression of connexin proteins after wounding is regulated at both the transcriptional and translational levels, with a sequence of dynamic changes occurring during wound closure. It was found that Cx43 and Cx31.1 start to be downregulated in the keratinocytes of the wound edge within six hours and are nearly undetectable by 24–48 hours (Coutinho et al., 2003; Goliger and Paul, 1995). Like keratinocytes, Cx43 is downregulated in wound edge dermal fibroblasts in the first 24–48 hours after wounding as they start to migrate into the wound bed and form new granulation tissue (Mori et al., 2006). However, Cx26 and Cx30 appear to be associated with keratinocyte

migration, since they are upregulated in the same leading-edge cells that migrate using lamellipodia to crawl forward and close the wound. The levels of Cx26 and Cx30 are extremely low in the unwounded epidermis in mice (Coutinho et al., 2003). Once the wound is closed, Cx26 and Cx30 downregulate to their apparent normal levels within the differentiated epidermis. The expression of Cx43 and Cx31.1 then return as the epidermis regains its characteristic laminar architecture (Brandner et al., 2004). Brandner et al. (2004) reported evidence that keratinocytes grafted into a wound bed appear to help to reconstitute a tissue gap junction network dominated by Cx26 and Cx30, which should facilitate healing. Therefore, downregulation of Cx43 appears to improve healing.

Cx43 is upregulated in the epidermis, dermis, and granular tissues in diabetic and chronic skin wounds, while it is downregulated in normal incisional and excisional wounds (Bajpai et al., 2009). In streptozotocin (STZ)-induced diabetic rats, Cx43 protein levels are significantly reduced in the intact epidermis, but increased in the intact dermis. However, following excisional wounding of STZ-induced diabetic rats, Cx43 protein levels dramatically increase in the epidermal leading edge keratinocytes. Reepithelialization does not begin until 2 days later, when excess Cx43 is diminished. This upregulation of Cx43 is thought to be one of the causes for delayed diabetic wound healing (Wang et al., 2007). In addition, the upregulation of Cx43 was identified in human venous leg ulcers (Mendoza-Naranjo et al., 2012) and in human middle ear cholesteatoma (Choung et al., 2006), both of which are chronic conditions.

4.2. Antisense Therapy and the Effect of Cx43 Antisense Oligodeoxynucleotides (Cx43 asODNs) in Wound Healing

The existence of antisense oligonucleotides in cells was known as early as 1959, but only in recent years have they been used as potential chemotherapeutic agents (Rapaport et

al., 1992). Synthetic oligonucleotides were administered exogenously to inhibit the replication and expression of Rous sarcoma virus in 1978 (Rapaport et al., 1992).

Antisense therapy can be a useful treatment for genetic disorders or infections. Because mRNA has to be single stranded for it to be translated, a strand of nucleic acid (DNA, RNA, or a chemical analogue) can be synthesized which will bind to specific sequences on the mRNA and inactivate it. Thus if the sequence of a specific gene is known, the gene can be inactivated. The gene's messenger RNA is called the "sense" sequence and the synthesized nucleic acid is an "anti-sense" oligonucleotide because its base sequence is the complement of the gene's messenger RNA. Antisense oligonucleotides are thus highly selective and less toxic than conventional drugs. Antisense therapy is ultimately to prevent protein production from the targeted gene. However, the exact mechanism remains unclear. Antisense therapies have been used or attempted for treatment of various diseases, including cancers, hemorrhagic fever viruses, HIV/AIDS, asthma, and cardiovascular and renal diseases (Crooke, 2000; Saonere, 2011). Synthetic oligodeoxynucleotides (ODNs) have been reported to inhibit viral and cellular gene expression by sequence-specific antisense (AS) hybridization. AS ODNs inhibit specific proteins from being synthesized (Rapaport et al., 1992).

In incisional and excisional skin wound healing models in mice, a single topical gel application of Cx43 antisense oligodeoxynucleotide (Cx43 asODN) (Cx43 5’-GTAATTGCGGCAGGAGGAATTGTTTCTGTC-3’), was effective in a transiently downregulating Cx43 protein levels in and around the wound within 2 hr, with the level recovering by 24 hr (Qiu et al., 2003). Cx43 knockdown reduced inflammation macroscopically (reduced in swelling and redness) and microscopically (decreased neutrophil number in the tissue around the wound site). The Cx43 knockdown led to a dramatic increase

in the rate of wound healing. This suggested that Cx43 asODN treatment may be an effective and safe wound healing therapy in tissue repair (Qiu et al., 2003).

Mori et al. (2006) conducted a study to compare physiological and cell biological responses of the repair process in the presence and absence of Cx43 asODN treatment *in vivo* and in a cell culture model in mice. The results indicated that Cx43 asODN reduced protein levels of Cx43 in the epidermis and dermis within 2 hours of treatment. One day after full-thickness excisional wounds in mice, expression of Cx43 mRNA in Cx43 asODN-treated wounds was significantly reduced. However, by 7 days after the injury, expression levels were similar in the treated and untreated wounds (Mori et al., 2006). It was also reported that a single treatment of excisional wounds with Cx43 asODN gel in STZ-induced diabetic rats prevented the initial upregulation of Cx43 in response to the excision injury. The treated wounds in these diabetic rats were found to have better wound healing, as assessed by their ability to re-epithelialize at the same rate as control wounds in non-diabetic rats (Wang et al., 2007).

It is important to note that though treatment of the wound with Cx43 antisense dramatically increased the rate in wound healing, the effects of Cx43 antisense were transient so that the re-expression of Cx43 in later post-wounding stages was not affected. It is possible that down-regulating Cx43 in basal epithelial cells of the epidermis favors the transformation or dedifferentiation of keratinocytes into a migrating phenotype (Chanson et al., 2005). Similar observations were found in wound healing experiments in mice with a skin-specific deletion of Cx43 (Kretz et al., 2003). Cx43 asODN was delivered in 30% Pluronic (a registered trademark of BASF) F-127 gel in DEPC water. Pluronic F-127 is a non-ionic copolymer surfactant used in insect cell culture as an antifoaming agent (Sigma Aldrich). Pluronic F-127 gel is liquid at 0-4 ºC, but sets rapidly when warmed by living tissue at higher temperatures. Technically, the mix of Cx43 asODN in pluronic gel is critical to

enhance the delivery of Cx43 asODNs since they are rapidly broken down (half-life 20–30 minutes) when they contact cells or sera if not applied in the gel, They can only act locally for a short time if not in the gel. However, pluronic gel in the wound site provides a slow-release reservoir that can maintain delivery of active Cx43 asODN for several hours (Becker et al., 1999). In addition, because the half-life of Cx43 in normal keratinocytes is about 1.5 hours, it is rapidly depleted once its messenger RNA is destroyed by Cx43 asODN (Becker, 2009).

In humans and rodents, a downregulation of Cx43 and an up-regulation of Cx26 and Cx30 in keratinocytes at the wound edges have been recognized as appropriate response to injury. The down-regulation of Cx43 was accompanied by increased levels of type I collagen, TGF-β, and decreased levels of tumor necrosis factor alpha (TNF-α), chemokine ligand-2 (Ccl-2), as well as reduced infiltration of neutrophils, and macrophages at the wound site. The down-regulation of Cx43 also resulted in enhanced fibroblast migration and keratinocyte proliferation, leading to faster wound closure (Mori et al., 2006; Qiu et al., 2003; Brandner et al., 2004; Coutinho et al., 2003). In addition, an increase in phosphorylation of Cx43 at serine 368 may be associated with decreased gap junctional communication (Richards et al., 2004). Effects of down-regulation of Cx43 that enhance wound healing are depicted in Figure 8.

Figure 8. Effects of down-regulation of Cx43 (with Cx43 asODN) (Mori et al., 2006; Qiu et al., 2003; Bajpai et al., 2009**).** Figure adapted and modified from Bajpai et al., 2009.

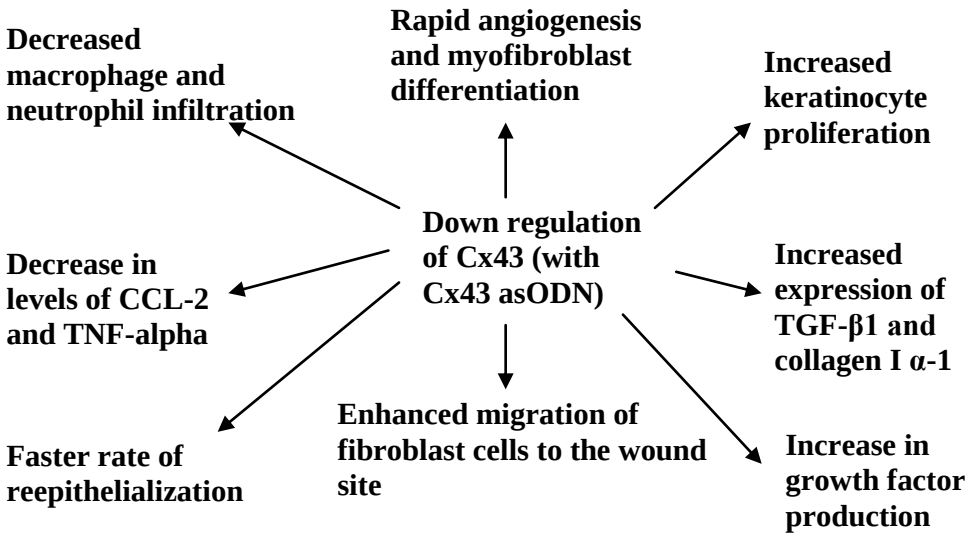

Mori et al., 2006; Qiu et al., 2003; Bajpai et al., 2009

5. Role of Selected Biomarkers of Inflammation and Granulation Tissue Remodeling

It is known that SM upregulates many inflammation mediators, including IL-1α, IL-1β, IL-6, IL-8, tumor necrosis factor-α (TNF-α), and others (Arroyo et al., 2000; Kehe et al., 2009). It was reported that mRNA levels of IL-6, IL-1β, Ccr1, CxCl2 increased as early as 6 hr and up to 14 days after exposure of SKH-1 mouse skin to SM. A topical application of SM also significantly up-regulated MMP-9, TNF-α, and Lamc2 expression at specific time points. However, the mRNA levels of MMP-2 remained unaffected by SM (Vallet et al., 2011).

CEES (2-chloroethyl ethyl sulfide) was found to upregulate several enzymes responsible for the synthesis of prostaglandins and leukotrienes, including cyclooxygenase-2 (COX-2) and microsomal prostaglandin E synthase-2 (mPGES-2) (Black and Hayden et al.,

2010). PGE-2 level increase significantly in inflammatory skin diseases supporting the observation for PGES-2 upregulation after injury with CEES (Reilly et al., 2000). Mechanical stimulation of osteocytes leads to an adaptive release of PGE-2 via Cx43 hemichannels. The hemichannels gradually close after 24 hr of continuous shear stress and Cx43 expression on the cell surface is reduced (Siller-Jackson et al., 2008).

The pro-inflammatory cytokine tumor necrosis factor-α (TNF-α) downregulates Cx43 and inhibits gap-junctional intercellular communication in corneal fibroblasts (Kimura and Nishida, 2010). In addition, TNF-α reduces the expression of Cx43 at the protein and mRNA levels in HaCaT cells, an immortalized keratinocyte cell line (Tacheau et al., 2008). Three progressive but overlapping phases, including inflammatory, proliferative and remodeling (maturation) phase, have been recognized in the wound healing process (Stramer et al., 2007). In the present studies, inflammatory biomarkers (IL-1B, IL-6, IL-10, COX-2 and PGES-2) and enzyme biomarkers for granulation tissue wound remodeling (MMP-2, MMP-9 and MMP-12) were selected to support the effect of Cx43 asODN as an therapy to facilitate wound healing in NM-exposed mouse skin.

5.1. Interleukin 1B (IL-1B), Interleukin 6 (IL-6) and Interleukin 10 (IL-10)

Cytokines are small, secreted proteins that affect the behavior of immune and other cells. Cytokines include interleukins, lymphokines, and several related signaling molecules such as tumor necrosis factor-α (TNF-α) and interferons. After incisional wounding of mice skin, expression of IL-1α, IL-1β, IL-6, and TNF-α were upregulated during the inflammatory phase of healing. In skin, the interleukin 1 (IL-1) cytokine family acts as a proinflammatory mediator (Werner and Grose, 2003). On exposure to pathological agents, IL-1B is produced by activated leukocytes and leads to inflammatory responses (Werner and Grose, 2003). IL-1α and/or IL-1β are also produced by keratinocytes in the epidermis and endothelial cells

(Matsushima et al., 2010). The expression changes of cytokines can serve as biomarkers for cutaneous inflammatory responses after SM exposure (Arroyo et al., 2000).

IL-6 is a multifunctional cytokine produced by a variety of cells, including fibroblasts, and can function as an autocrine or paracrine mediator (Liu et al., 2007). By using a full-thickness punch biopsy wounding model, it was found that wounds took up to three times longer to heal in IL-6 knock-out mice than those of wild-type controls (Werner and Grose, 2003), indicating IL-6 is needed for appropriate wound healing.

IL-10 is an anti-inflammatory cytokine. The IL-10 family of cytokines is produced by various immune cells. They are essential for maintaining the integrity and homeostasis of epithelial layers. These cytokines have diverse host defense mechanisms in epithelial cells and can enhance the tissue-healing process in injuries as a consequence of viral and bacterial infections. IL-10 can repress pro-inflammatory responses and limit unnecessary tissue damages caused by inflammation. IL-10 family cytokines have important functions in many infectious and inflammatory diseases. Many chronic bacterial and viral infections show increased IL-10 expression (Ouyang et al., 2011). Enk and Katz have demonstrated that murine keratinocytes are capable of producing IL-10 mRNA and protein (Enk and Katz, 1992). After incisional wounding of mice, levels of IL-10 mRNA increase with a peak at 60 min after injury. IL-10 has been found to inhibit inflammation and scar formation (Werner and Grose, 2003). Vallet et al. (2011) investigated the time-dependent quantitative gene expression after dorsal skin exposure to SM saturated vapor in SKH-1 hairless mice. Specific transcript RT-PCR analysis demonstrated that the mRNA levels of IL-1B, IL-6, Ccr1, and Cxcl2 increased as early as 6 hr in SM-exposed skins and remained up-regulated over a 14-day period (Vallet et al., 2011). Thus, pro-inflammatory mediators IL-1B, IL-6 and the anti-inflammatory mediator IL-10 may play important roles in NM injury.

5.2. Cyclooxygenase-2 (COX-2)

CEES was found to upregulate several enzymes required for the synthesis of prostaglandins, including cyclooxygenase-2 (COX-2) and microsomal prostaglandin E synthase-2 in mouse keratinocytes (Black and Joseph et al., 2010). Concentration- and time dependent increases in mRNA and protein expression of COX-2 and microsomal prostaglandin E synthase-2 were observed in CEES-treated full-thickness human skin equivalents (Black and Hayden et al., 2010). COX-2 is the rate-limiting enzyme in prostaglandin synthesis and prostaglandin E2 induces Cx43 expression. However, the COX-2 specific inhibitor, celecoxib, did not reduce Cx43 expression *in vivo* in mouse intestinal tissues (Husøy et al., 2005).

To examine the role of COX-2 in sulfur mustard-induced skin toxicity, Wormser et al. (2004) applied SM to the ears of COX-2-deficient and wildtype (WT) mice. It was found that ear swelling was significantly reduced ($P < 0.05$) by 55% and 30%, respectively 24 hr and 48 hr after exposure in COX-2-deficient treated vs. WT mice. These findings suggest that COX-2 may participate in the early stages of SM-induced acute skin wounds (Wormser et al., 2004). In addition, COX-2 was identified in the epidermis of SM-treated mice (Nyska et al., 2001). Joseph et al. (2011) exposed the dorsal skin of SKH-1 hairless mice to saturated SM via vapor cup to study the correlation of structural changes in the skin with inflammation and DNA damage over the course of 14 days following exposure. It was reported that at 3 days post exposure, COX-2 was upregulated, and at 14 days the expression of COX-2 was reduced (Joseph et al., 2011). Based on these findings, it is possible that nitrogen mustard upregulates COX-2 in order to induce synthesis of PGE-2 (the signaling molecule), and PGE-2 in turn induces Cx43 to release additional PGE-2 from the cells. Thus, COX-2 may have an important role in NM injury.

5.3. PGE_2 synthase-2 (PGES-2)

PGES-2 is a membrane-bound prostaglandin E synthase that catalyzes the conversion of prostaglandin H2 (PGH-2) to PGE-2. Thus far, three prostaglandin E synthases have been identified. Membrane-bound (Microsomal) prostaglandin E synthase 2 (mPGES-2 or PGES-2) and cytosolic prostaglandin E synthase (cPGES) are constitutive enzymes which are involved in basal PGE-2 production. The third identified PGES (mPGES-1) is also a membrane bound enzyme that is an isomerase that can be induced by inflammatory cytokines to play major pathophysiological roles leading to inflammation, pain, fever and stroke (Samuelsson et al., 2007). The level of PGE-2 is dependent on the PGES-2 which is analyzed in the current studies.

PGE-2 is one of the most abundant prostaglandins which is well characterized in animal species, and displays various biological activities. PGE-2 contributes to the pain, redness, and swelling associated with inflammation. Prostaglandins may function in both the promotion and resolution of inflammation (Ricciotti et al., 2011). *In vitro* SM-exposure studies using organ cultures of full-thickness human skin explants demonstrated that prostaglandin E2 is involved in early stages of the inflammatory response. PGE-2 was assayed with the AMI PGE-2 Enzyme Immunoassay Kit and levels of PGE-2 were found to be elevated after exposure of skin to SM (Rikimaru et al., 1991). After CEES exposure of the human skin substitutes, Skin2 (differentiating keratinocytes on a fibroblast-collagen matrix) and EpiDerm (differentiating keratinocytes), it was found that the release of extracellular PGE-2 increased (Blaha et al., 2000). The PGE-2 was analyzed using either radioimmunoassay (RIA) or enzyme-linked immunosorbent assay (ELISA) (Blaha et al., 2000).

PGE-2 induces Cx43 expression. Since COX-2 is the rate-limiting enzyme in prostaglandin synthesis (Husøy et al., 2005), PGES-2 and PGE-2 may play an important Cx43-related role in NM injury and healing.

5.4. Matrix Metalloproteinase 2 (MMP-2), Matrix Metalloproteinase 9 (MMP-9) and Matrix Metalloproteinase 12 (MMP-12) - Remodeling Biomarkers

The remodeling of granulation tissue to a scar is dependent on collagen turnover processing at a biologically related slow rate. Collagen breakdown is controlled by matrix metalloprotinases (MMPs) which are secreted by epidermal cells (MMP-2), fibroblasts (MMP-9), and macrophages (MMP-12) (Nagase et al., 2006; Vaalamo et al., 1999). Matrix metalloproteinases, a family of extracellular matrix (ECM) degrading enzymes, are classified as collagenases (MMP-1, -8, and -13), gelatinases (MMP-2 and -9), stromelysins (MMP-3, -7, -10, and -12), membrane-type MMPs (MT-MMPs), and other MMPs (Salmela et al., 2001). MMPs are a group of zinc-dependent extracellular proteinases and their proteolytic activities assist in degradation of ECM and basement membrane. MMPs are essential in inflammatory and immune responses, and in epidermal differentiation. MMPs remodel the extracellular matrix and contribute to structural integrity (Tan and Tsai, 2012).

MMP-2 and MMP-9, the gelatinase group, mainly digest gelatin, the denatured form of collagen. MMP-2 and MMP-9 also digest a number of ECM molecules including laminin-111 and collagens types IV, V, and XI. MMP-2, but not MMP-9, digests denatured collagens I, II, and III chains. MMP-2 is the major gelatinolytic MMP produced in skin keratinocytes. MMP-2 and MMP-9 are normally inactive in skin but are expressed during injury. They degrade collagen IV and other critical components of the basement membrane zone that separates the epidermis from the dermis (Nagase et al., 2006).

MMP-9 is an inducible MMP that plays a role in tissue injury. The biological behaviors (proliferation, viability, collagen secretion, horizontal migration, and vertical

migration) of fibroblasts in a cell culture (CRL-1213, ATCC) were inhibited by high levels of MMP-9 (Xue et al., 2012). Likewise, MMP-9 expression prolonged the healing of diabetic foot ulcers by inhibiting the biological effects of fibroblasts (Liu et al., 2009).

Vallet et al. (2011) quantitated the time-dependent expression of gelatinases and other wound markers after dorsal skin exposure to SM in the SKH-1 hairless mouse. Using the qRT-PCR method, it was found that topical application of SM significantly up-regulated the mRNA level of MMP-9 (48-168 hr), TNF-α (72-168 hr), and Lamc2 at specific time points. However, MMP-2 mRNA levels remained unaffected by SM over the time-period examined (Vallet et al., 2011). These observations confirmed those reported by Shakarjian et al (2006) in the mouse ear vesicant model. Shakarjian found the relative levels of MMP-9 mRNA were increased 27-fold in the absence of observable increases in the MMP-2 mRNA levels.

MMP-12 (Human macrophage metalloelastase) is expressed primarily in macrophages and osteoclasts. It digests elastin and a number of ECM molecules. It is essential in macrophage migration (Nagase et al., 2006). MMP-12 was originally found in the alveolar macrophages of cigarette smokers. The enzyme degrades soluble and insoluble elastin, type IV collagen, laminin, and fibronectin (Salmela et al., 2001; Vaalamo et al., 1999). It is also upregulated in inflammatory bowel disease (Salmela et al., 2001) and its expression in macrophages under the shedding intestinal epithelium in inflammatory bowel diseases suggests MMP-12 participates in the degradation of basement membrane components of the bowel. MMP-12 may facilitate macrophage migration through the epidermal and vascular basement membranes in inflammatory skin diseases (Vaalamo et al., 1999). Thus, at least MMP-2, MMP-9 and MMP-12 may play important roles in NM injury.

6. Thesis Research Rationale

Several different animal models, including rabbits, guinea pigs, and mice, have been developed for investigating the mechanisms involved in sulfur mustard-induced toxicity of the skin (Vallet et al., 2011). A mouse ear vesicant model (MEVM) was developed (Casillas et al., 1997) to screen pharmacological compounds able to treat SM-induced skin damage. In this mouse model, liquid SM (0.04-0.64 mg in 5 μl) was applied to the inner surface in one ear and the other ear served as the vehicle control. As mentioned, the major drawback for MEVM model is that it is not appropriate for long-term study (Section 3.1, Dachir et al., 2010). The SKH-1 hairless mouse is a popular rodent model used in dermal research for safety and efficacy testing. It is particularly useful for UV-induced skin damage studies and serves as a wound healing model (Anwar et al., 2008). Dorandeu et al. (2011) applied SM both as a vapor and as a liquid in a solvent to the skin of hairless mice (SKH-1) to study the inflammatory responses induced by the agent. In addition, Tewari-Singh et al. (2009), using SKH-1 hairless mice, showed that liquid CEES induced quantifiable inflammatory biomarkers. The dose range in the study was 0.05-2 mg and the skin samples were collected and analyzed from 3 to 168 hr post exposure. Joseph et al. (2011) used vapor cup SM exposure of the dorsal skin of SKH-1 hairless mice to study the correlation of structural changes in the skin with inflammation and DNA damage over the course of 14 days. It was concluded that the results were consistent with the pathophysiology of skin after humans were exposed to SM, therefore, the SKH-1 hairless mouse has been validated as a model to assess the dermal toxicity of vesicants. Studies using this mouse model are suitable for acute and long-term cutaneous vesicant studies.

SM is a potent vesicant which has been extensively investigated in animal models and in *in vitro* studies, as well as in humans due to exposures during the Iran-Iraq war. NM, a

chemotherapeutic agent that is a less potent analog of SM, has not been fully characterized for its vesicating potential. Due to structural homology, NM was presumed to have a similar biological activity as SM and this has been demonstrated (Gordon et al., 2010; Shakarjian et al., 2010; Sharma et al., 2008). Because of restrictions on using SM outside of specific government approved facilities, we proposed to use the less toxic, but commercially available NM as a comparable vesicant. In addition, in order to perform a time course study, we proposed to use the more applicable hairless mouse (SKH-1) model rather than the mouse ear vesicant model (MEVM). Briefly, we decided to expose hairless mouse (SKH-1) dorsal skin to evaluate the injury induced by NM and whether Cx43 antisense oligodeoxynucleotides (Cx43 asODNs) were effective as a therapy against NM-induced skin damage.

Cx43 is the most broadly expressed connexin in the epidermis (Meşe et al, 2007). It is expressed in multiple cell types, including keratinocytes and dermal fibroblasts. Furthermore, it is involved in many stages of tissue repair (Coutinho et al., 2003). In rodents and humans Cx43 is downregulated while Cx26 and Cx30 are upregulated in keratinocytes at the wound edges (Brandner et al., 2004; Coutinho et al., 2003; Goliger and Paul, 1995). Mori et al. (2006) compared physiological and cell biological responses of the repair process in the presence and absence of Cx43 antisense oligodeoxynucleotide (Cx43 asODN) treatment in male, 8 week old ICR (CD-1®) mice and cell culture models, and found that the protein levels of Cx43 in the epidermis and dermis were reduced within 2 hours of treatment and that healing was faster. Also, Qiu et al. (2003) showed Cx43 asODN downregulated Cx43 which reduced the inflammatory response and shortened the time for wound repair in both the incisional and burned skin wound healing models. Therefore, we used the hairless mouse (SKH-1) dorsal skin model to evaluate the effectiveness of Cx43 asODNs as a therapy for nitrogen mustard exposure. Assessment was by histology (H&E histology), macroscopic appearance of the mouse skin, expression levels of Cx43, Cx26 and Cx30, as well as levels of

selected inflammation and remodeling biomarkers. By comparing control and treated groups, it appears that Cx43 asODN is a good potential therapy for NM-exposed mouse skin, and should be investigated further to determine if it should be pushed forward toward FDA approval for use on SM-exposed human skin. The work presented here is the first step toward the pre-clinical animal trials.

Statement of Hypothesis

The chemical structures of nitrogen mustard (NM) and sulfur mustard (SM) are similar and reports in the literature indicate that they have similar biological activity and pathological effects. The similarity between NM and SM was demonstrated in cornea toxicity using an *ex vivo* culture model (Gordon et al., 2010). We hypothesize that NM-induced injury of mouse dorsal skin is comparable to the established injury induced by SM in the mouse dorsal skin model (Joseph et al., 2011; Vallet et al., 2011; Dorandeu et al., 2011).

In addition, evidence suggests the upregulation of Cx43 is associated with prolonged diabetic wound healing and that connexin 43 antisense oligodeoxynucleotides (Cx43 asODN) treatment improves the healing rate. Since NM-induced skin wounds show delayed healing, we hypothesize that Cx43 will be upregulated in NM-induced skin wounds as is seen in diabetic wounds. In addition, we hypothesize that Cx43 asODN will facilitate the healing process after NM exposure in a manner similar to diabetic wounds.

Specific Aims

Specific Aim 1: To determine whether the injury induced by NM in the mouse dorsal skin vesicant model resembles the injury previously observed from SM injury in this animal model and in the CD-1 mouse ear vesicant model. Three types of sample analysis, including macroscopic appearance, H&E histology and quantitative reverse transcription polymerase chain reaction (qRT-PCR), were performed to address this.

Specific Aim 2: To determine levels of Cx43, Cx26 and Cx30 in mouse dorsal skin after NM exposure and how treatment with connexin 43 antisense oligodeoxynucleotides (Cx43 asODN) affects these levels. Four types of sample analysis, including macroscopic appearance, H&E histology, qRT-PCR (Cx43, Cx26 and Cx30) and western analysis (Cx43), were performed to determine this.

Specific Aim 3: To evaluate the effects of Cx43 asODN on biomarkers of both inflammation (Il-1B, IL-6, IL-10, PGES-2 and COX-2) and the remodeling phase of wound healing (MMP-2, MMP-9 and MMP-12) in NM-exposed mouse skin. To evaluate this, qRT-PCR analysis was performed.

Materials and Methods

1. Chemicals and Reagents

HPLC grade unmodified Cx43-AntiSense-Oligodeoxynucleotides (Cx43 asODN) (Cx43 5'-GTAATTGCGGCAGGAGGAATTGTTTCTGTC-3') and Sense Control-Oligodeoxynucleotides (Cx43 scODN) (Cx43 5'-GACAGAAACAATTCCTCCTGCCGCAATTTAC-3') were purchased from Integrated DNA Technologies (IDT) (Coralville, Iowa). The sequence of Cx43 asODN is the same as Cx43 asODN used by Qiu et al. (2003). Pluronic F-127 (P2443), nitrogen mustard (NM, as a hydrochloride salt), methylene chloride, and acetone were purchased from Sigma-Aldrich (St. Louis, MO). Pluronic gel is liquid at 0-4ºC, but sets rapidly when warmed by living tissue at higher temperatures. Pluronic F-127 is a non-ionic copolymer surfactant qualified for use in insect cell culture as an antifoaming agent (Sigma Aldrich). Acuderm Acu-Punch biopsy punches and 10% formalin were purchased from Fisher Scientific (Pittsburgh, PA). Trizol reagent was obtained from Invitrogen Corporation (Carlsbad, CA) and High Capacity cDNA Reverse Transcription Kit with RNase Inhibitor was obtained from Applied Biosystems (Foster City, CA). Rabbit anti-mouse Cx43 antibody (ab11370) was purchased from Abcam and GAPDH primary antibody (G9545) was purchased from Sigma. Gene-specific primers for Cx43, Cx26, Cx30, IL-6, IL-1B, IL-10, MMP-2, MMP-9, MMP-12, COX-2, PGES-2, and GAPDH (used as an endogenous control) were purchased from IDT Integrated DNA Technologies. Rapid Chrome™ H & E Frozen Section Staining Kit (REF 9990001) was purchased from Thermo Scientific. Nitrocellulose transblot membrane (0.2 μm) was purchased from Bio-Rad Laboratories, Life Sciences Group, Hercules, CA, USA.

2. Animals

Female SKH-1 hairless mice (5-7 weeks old) were purchased from Charles River Laboratories (Wilmington, MA). All animal studies were conducted in accordance with the protocol approved by Laboratory Animal Services (LAS), Rutgers University.

3. Determination of the Dose of NM for the Exposure to SKH-1 Mouse Dorsal Skin and the Dose of Cx43 asODN for Post Exposure Treatment

For NM, we chose the dose based on the published literature. NM was used as a substitute to mimic the vesicant effects of SM in a study to treat NM induced dermal wound with doxycycline hydrogels in SKH-1 mouse dorsal skin (Anumolu et al., 2011). NM (5 μmoles in acetone) was applied topically once to mouse dorsal skin and the skin samples or punch biopsies were collected at days 1, 3, 7 and 10 post exposure (Anumolu et al., 2011). Skin samples were sectioned and subjected to H & E stain for the histological evaluation. The typical vesicant toxicities, including inflammatory cell infiltration, edema, epidermal necrosis and hyperplasia, separation of epidermal and dermal layers and degradation of the dermis were observed (Anumolu et al., 2011). Since all animals survived at day 10 and the toxic effects to the skin were observed in their study, we decided to choose 5 μmoles of NM for our first study.

For Cx43 asODN, we also chose the dose based on the literature search. Qiu et al. found the optimal dose for a single topical application of Cx43 asODN to downregulate Cx43 and increase the rate of wound closure in incisional and excisional skin wound healing models in adult mice was 0.05 nmoles (50 μl of 1 μM) (Qiu et al., 2003). In addition, after a single topical application of 50 μl of 1 μM (0.05 nmoles) of Cx43 asODN in 30% Pluronic F-127 gel to full-thickness excisional wounds in mice dorsal skin, an acute downregulation of Cx43 and markedly improvement the rate and quality of skin healing was observed (Mori et al., 2006).

Furthermore, it was found after a topical application of 50 μl of 10 μM (0.5 nmoles) of Cx43 asODN in 30% Pluronic F-127 gel to full-thickness excisional wounds in STZ (streptozotocin) induced diabetic adult male Sprague-Dawley rats resulted in downregulation of Cx43 and increase the wound healing rate to normal rate (Wang et al., 2007). In consideration that both NM induced chemical wound and diabetic wounds have prolonged wound healing time and the weight of mice (20 gm) vs. rats (350-400 gm), we decided to initiate the first study in SKH-1 mice with 0.15 nmoles of Cx43 asODN.

4. Use of CY3-tagged ODNs to Evaluate the Penetration of Cx43 asODN into NM Wounded Tissue.

Female SKH-1 hairless mice aged 6 weeks (4 per group) were used as an *in vivo* animal model to assess Cx43 asODN treatment penetration into wounded areas following NM exposure. Three groups of mice were used in a 1 day study (mice sacrificed at 2, 6, 24 hr following exposure); all groups received NM exposure to dorsal skin followed by CY3-tagged connexin 43 Antisense Oligodeoxynucleotide (CY3-tagged Cx43 asODNs) treatment. Cy3 is a cyanine dye, shows yellow-green fluorescence (excitation wavelength at ~550 nm and emission wavelength at ~570 nm). A standard circular template (15 mm) was used to ensure a uniform exposure area of NM on all mice. Mice were anaesthetized by isoflurane inhalation during NM exposure and Cx43 asODN treatment. Topical wounds were created by application of 5 μmoles NM (100 μl of 50 mM in acetone) in the mid back region. Following exposure, Elizabethan collars were placed on each mouse to prevent disruption of the wounding site. Two hours after NM exposure, a single topical application of 0.15 nmoles Cx43 antisense ODNs tagged with the CY3 fluorophore (Sigma- Aldrich) was applied. ODNs were delivered in 30% Pluronic F-127 gel (Sigma- Aldrich, Dorset, UK) in 1x TE buffer (10mM Tris-HCL, 1mM EDTA pH 7.4). An aliquot of 1.0 μM CY3-tagged Cx43 asODN in 30% of Pluronic F-127 gel was prepared and set on ice before use. Cx43 asODNs

was delivered in 30% Pluronic F-127 gel (Sigma- Aldrich, Dorset, UK) in DEPC water. Pluronic gel is liquid at 0-4ºC, but sets rapidly when warmed by living tissue at higher temperatures. Pluronic F-127 is a non-ionic copolymer surfactant qualified for use in insect cell culture as an antifoaming agent (Sigma Aldrich). Theoretically, the mix of Cx43 asODN in pluronic gel is critical to enhance the delivery of Cx43 asODNs. Cx43 asODN is rapidly broken down (half-life 20–30 minutes) when it contacts cells or sera, so it can only act locally or topically. However, pluronic gel in the wound site provides a slow-release reservoir that can maintain delivery of active Cx43 asODN for several hours (Becker et al., 1999). In addition, because the half-life of Cx43 in normal keratinocytes is about 1.5 hours, it is rapidly depleted once its messenger RNA is destroyed by Cx43 asODN (Becker, 2009). Collars were kept on the mice overnight to prevent disruption of the gel. The mice were euthanized by CO_2 gas and punch biopsies (12 mm in diameter) were collected at 2 hr, 6 hr, and 1 day after exposure to evaluate the penetration of CY3-Cx43 asODN to NM wounded tissue. The weight of the tissue was measured for edema. The skin samples were dissected into 2 sections and fresh frozen in O.C.T. (optimal cutting temperature compound) in liquid nitrogen for histology evaluation.

5. Study 1 - A Study of the Effects of CX43 asODN on NM-Exposed SKH-1 Mouse Dorsal Skin

SKH-1 female hairless mice aged 5-6 weeks, four or five mice in each group, purchased from Charles River Laboratories (Wilmington, MA) were used as an *in vivo* animal model to assess NM dermal wound progression and to evaluate the effectiveness of the subsequent treatment with Cx43 asODN to NM-exposed dorsal skin. Five groups of mice (weight ranged from 23.1 to 25.3 gm) were used in Study 1 including group1: NM-exposed dorsal skin, group 2: NM-exposed dorsal skin with Cx43 asODN treatment, group 3: NM-exposed dorsal skin with Cx43 scODN treatment and group 4 (Vehicle control): methylene

chloride exposed dorsal skin with 30% Pluronic F-127 in PBS treatment. One group of mice was taken at day 10 as naïve (unexposed) control. Mice were anesthetized by isoflurane inhalation during NM exposure and Cx43 asODN treatment. Topical wounds were created by application of 5 μmoles of NM in methylene chloride to the dorsal skin of mice. A standard circular template (15 mm in diameter) was used to ensure uniform exposure area of NM on all mice. A single topical application of 0.15 nmoles Cx43 AntiSense Oligodeoxynucleotides (Cx43 asODNs), or sense control ODNs (scODN) in 30% Pluronic F-127 gel were applied to the wound 2 hours after NM exposure. The mice were euthanized by CO_2 gas and punch biopsies (12 mm in diameter) were collected at 1, 3, 7, and 10 days after NM exposure. Macroscopic images were taken, and graded by at least 3 people. The most representative samples were chosen. The 12 mm punch biopsies were weighed and the percent relative skin weights, an assess of edema, was calculated as 100 x [NM-exposed biopsy weight – vehicle control biopsy weight]/[vehicle control biopsy weight]. Each biopsy sample was cut into 4 equal sections, two sections were frozen in liquid nitrogen for protein and RNA extractions, one section was fresh frozen in O.C.T. in liquid nitrogen and one section was fixed in 10% formaldehyde. The section fixed in 10% formaldehyde was shipped to AML Laboratories, Inc. (Baltimore, MD 21206) for histological evaluation. No Elizabethan collars were used in this study.

6. Study 2 - A Time-dependent Study of the Effects of CX43 asODN on NM-Exposed SKH-1 Mouse Dorsal Skin

SKH-1 hairless mice (5 mice per group, weight ranging from 22.7 to 26.9 gm) were used as an *in vivo* animal model to assess NM dermal wound progression. Five groups of mice were used in Study 2 including group1: NM-exposed dorsal skin; group 2: NM-exposed dorsal skin with Cx43 asODN treatment; group 3: NM-exposed dorsal skin with Cx43 scODN treatment and group 4: vehicle controls (exposed to acetone and treated with 30%

Pluronic F-127 in PBS). One group of mice was taken at 0 time point as naïve (unexposed) control. A standard circular template (15 mm in diameter) was used to ensure a uniform exposure area of NM on all mice. Mice were anaesthetized by isoflurane inhalation at NM exposure and Cx43 asODN treatment. Topical wounds were created by application of 5 μmole of NM in acetone (100 μl of 50 mM) to the dorsal skin of mice. Following exposure, Elizabethan collars were placed on each mouse to prevent disruption of the wounding site, and removed 1 day post treatment. A 1 ml aliquot of 1μM Cx43 asODN (1:200 dilution from 200 μM stock ODNs) in 30% of Pluronic F-127 gel (Sigma- Aldrich, Dorset, UK) in PBS or DEPC water was prepared and set on ice before use. A single topical application of 0.15 nmole (150 μl of 1 μM) of Cx43 antisense ODNs or sense control ODNs (Sigma-Aldrich) was applied to the wound 2 hours after NM exposure. The mice were euthanized by CO_2 gas and punch biopsies (12 mm in diameter) were collected from the wounded skin at 0, 1, 3, 7, and 10 days after exposure to evaluate the effectiveness of Cx43 asODN to NM on chemical dermal wound formation. Macroscopic images were taken, and graded by at least 3 people. The most representative images were chosen. The 12 mm punch biopsies were weighed and the percent relative skin weights, an assess of edema, was calculated as 100 x [NM-exposed biopsy weight – vehicle control biopsy weight]/[vehicle control biopsy weight]. The skin samples were dissected into 4 sections, two sections were taken in liquid nitrogen for protein and RNA extractions, one section was fresh frozen in O.C.T. on dry ice, and one section was fixed in 10% formaldehyde for histological evaluation.

7. Extraction of Total Protein from Mouse Skin Samples

Frozen skin samples were mixed with extraction buffer (EB) containing protease inhibitor (1 tablet per 10 ml buffer) (Roche 04693124001) and pulverized twice on dry ice. Extraction buffer is composed of modified RIPA buffer (50 mM Tris-HCL PH7.4, 150 mM NaCl, 1 mM

EDTA, 1% NP-40, 1% Na-deoxycholate and 0.1% SDS in water). Tissue was then lysed using a GenoGrinder 2000 at 200 rpm 2 min x3 or 300 rpm 3 min x2 and incubated on ice for 20 min. After heating samples to 60ºC for 4 min (vortexing every 30sec), samples were centrifuged at highest speed (>12,000 rpm) for 20 min at 4ºC. The supernatant was removed and stored at -20ºC until used. Total protein concentration was determined using BCA Assay (Thermo Scientific).

8. Histology

For histological evaluation, skin samples were fresh frozen in O.C.T. in liquid nitrogen. Samples were placed on ice for 15 min and then immediately frozen in liquid nitrogen, and were stored at -80 ºC until analysis. Skin samples were sectioned at -15 ºC to - 20 ºC at a thickness of 10μm. Skin sections were stained using a Rapid Chrome™ H & E frozen section staining kit (Thermo Scientific, REF 9990001). The stained slides were cover-slipped with Permount. Skin sections were viewed with an OLYMPUS® VS120® Virtual Microscopy System equipped with 2x, 10x, 20x, 40x OLYMPUS UPLSAPO objective lenses.

9. Western Blotting

Pooled protein samples per group (total protein = 15 μg) were heated at 95-100º C for 5 min, centrifuged and then applied onto a sodium dodecyl sulfate polyacrylamide electrophoresis gel (SDS-PAGE) for 1hr at 100 volts to separate proteins. Gels were transferred onto nitrocellulose transblot membranes (0.2 μm, Bio-Rad Laboratories, Life Sciences Group, Hercules, CA, USA) for 1 hr at 100 volts. Membranes were placed in 5% blocking buffer (5% milk powder with TBST) for 1 hr or overnight at 4ºC and then washed 10 min with 1x TBS/0.2% Tween-20 buffer (TBST) for 3 times. Membranes were incubated in a rabbit anti-mouse Cx43 antibody (1:12,000 dilution, Abcam, ab11370) in 1% bovine

serum albumin BSA in TBST for 1 hr. Blots were washed in 1 x TBST and then incubated in Goat anti-rabbit IgG conjugated to horseradish peroxidase (HRP) conjugated secondary antibodies (1:15,000 dilution, Bio-Rad Laboratories) (in 5% milk + TBST or 1% BSA). Membranes were treated with detecting solution: Pierce SuperSignal West Pico Chemiluminescent Substrate (Prod 34080) before exposure to X-ray film. Membranes were washed with TBST for 5 min, water for 5 min, stripped with 0.2N HCl for 7 min, water for 5 min, TBST for 5 min, and blocked with 5% blocking buffer for reprobing rabbit anti GapDH primary antibody (1:20,000) (Sigma G9545) and Goat anti-rabbit secondary antibody (1:15,000, Bio-Rad Laboratories) as a loading control.

10. Isolation of RNA

Frozen skin samples were prepared for the isolation of RNA using Sigma TRI Reagent (TRIzol, T9424). Frozen samples were pulverized 2-3 times to crush tissue and then mixed with RLT buffer (a lysis buffer and a proprietary component of RNeasy Kit from Qiagen) in tubes using Genogrinder. The tissue was ground 3 times at 300 rpm for 3 min and rested 1 min on ice each time. TRI reagent, 500 µl (Sigma) was added to each tube, the tube was mixed well by inversion. The mixed solution was incubated at RT for 5 min. Chloroform was added and each tube vortexed for 15 seconds and then incubated for 2-3 min. The tubes were then centrifuged at 12,000 xg, 4°C, for 15 min. The aqueous phase (top layer) was removed by aspiration and transferred to a new sterile RNase-free tube. The sample (up to 700 µl) was loaded into an RNeasy column (Qiagen) seated in a 2.0 ml collection tube. The column was spun at ≥8,000 xg, for 30 sec. The flow through was discarded. RWI buffer (350µl, a buffer for washing membrane bound RNA and a proprietary component of RNeasy RNA isolation Kit, Qiagen) was added onto the column and the column was spun at ≥8,000 xg, for 30sec. DNase I (Qiagen Cat#: 79254) incubation mix (80 µl) was added

directly to the RNeasy spin column membrane and incubated at room temperature (RT) for 15 min. Fresh 350 µl buffer RW1 was added onto the column and the column was spun at ≥8,000 xg, for 30 sec one more time. The column was transferred into a new collection tube, and washed twice with 500 µl buffer RPE (a proprietary component of RNeasy RNA isolation kit from Qiagen for washing membrane bound RNA) with spinning. The column was transferred to a new 1.5 ml collection tube. RNase-free water 30-50 µl (eluent) was pipetted directly onto the column. The column was spun at ≥8,000 xg for 1 min to elute RNA after sitting at RT for 1-2 min. Isolated RNA was stored at -80^{o}C.

11. Quantitative reverse transcription–polymerase chain reaction (qRT-PCR) Analysis

RNA (0.4 µg) was reverse-transcribed into 20µl cDNA using SuperScript® II Reverse Transcriptase (Invitrogen). Gene-specific primers for Cx43, Cx26, Cx30, IL-6, IL-1B, IL-10, MMP-2, MMP-9, MMP-12, COX-2, PGES-2, and GAPDH (used as an endogenous control) were purchased from IDT Integrated DNA Technologies. SYBR Green (Applied Biosystems) RT-PCR (1:3 cDNA dilution, 300 nM primers) was performed on a ViiA™ 7 system (Applied Biosystems).

Expression of a target gene was normalized to the expression of a reference gene GAPDH (target gene/GAPDH gene). After normalization, data were expressed as the fold change of mRNA relative to naïve (unexposed control) or as fold change to the vehicle control. The latter is methylene chloride and 30% Pluronic F-127 in PBS for Study 1, and acetone and 30% Pluronic F-127 in PBS for Study 2. Why and how this calculation was made is explained below. The control was assigned a value of 1 and treated samples calculated relative to control (mRNA fold change of treated sample target gene/mRNA fold change of the control). When compared to the control, a value greater than 1 indicates gene expression is upregulated and less than 1 indicates downregulation.

It was imperative to address changes due to a vehicle effect occurring in some samples, since some target genes from some of the animals in the vehicle control groups showed substantial differences in mRNA expression when compared to the naïve controls (see section 6 of Discussion). To normalize the data to remove the potential vehicle effect and understand only the effect on the target genes, the data were expressed as fold change relative to vehicle controls, which normalizes the mRNA expression to both GAPDH and the vehicle. For example, as stated in Results section 4.2.1, "After NM exposure, the mRNA of Cx43 was statistically significantly down-regulated at day 1 (fold change = 0.39) when compared to the vehicle control (fold change = 1.0) (Figure 16A)." The fold change of 0.39 was calculated as follows:

	A	B	C	D	E	F
	Day Treatment Mouse #	mRNA GAPDH	mRNA Cx43	relative quantification rQ (Cx43/GAPDH)	mRNA Fold Change	mRNA Avg. Fold Change
1	**1d VC #1**	**51.469**	**129.007**	**2.507**	**0.919**	**1.00**
2	1d VC #2	54.158	136.657	2.523	0.925	
3	1d VC #3	39.941	72.641	1.819	0.667	
4	1d VC #4	30.833	116.535	3.780	1.386	
5	1d VC #5	42.852	129.017	3.011	1.104	
6				Average from 5 VC mice rQ (Cx43/GAPDH) **2.728**		
7	**1d NM #1**	**93.323**	**150.068**	**1.608**	**0.590**	**0.39**
8	1d NM #2	100.330	132.528	1.321	0.484	
9	1d NM #3	92.953	117.698	1.266	0.464	
10	1d NM #4	118.785	113.236	0.953	0.349	
11	1d NM #5	180.228	81.487	0.452	0.166	
12	1d NM #6	107.719	87.196	0.809	0.297	

Calculation examples given for row 1 and row 7:

Row 1:
The Cx43 mRNA level for mouse #1 from vehicle control group at day 1 (**1d VC #1**) was normalized to GAPDH mRNA level. The resulting rQ (Cx43/GAPDH) was then divided by the average rQ (Cx43/GAPDH) from all 5 mice in the vehicle control (VC) group to get the fold change (FC) as follows:

Items in [brackets] correspond to the row and column of the above Table.

rQ (Cx43/GAPDH)=129.007 [C1]/51.469 [B1]=2.507 [D1]
FC=2.507 [D1]/2.728 (Average of 5 VC mice) [D6] = 0.919 [E1]
Average FC for 5 mice in vehicle control group at day 1= average of [E1] to [E5]= 1.00

Row 7:
The mRNA level of Cx43 for mouse #1 from NM-exposed group at day 1 (**1d NM#1**) was normalized to the mRNA level of GAPDH. The resulting rQ (Cx43/GAPDH) was then divided by the average rQ (Cx43/GAPDH) from all vehicle control (VC) mice to get the fold change (FC) as follows:

Items in [brackets] correspond to the row and column of the above Table.

rQ (Cx43/GAPDH)=150.068 [C7]/93.323 [B7]=1.608 [D7]
FC=1.608 [D7]/2.728 [D6] = 0.590 [E7]
Average FC for 6 mice in NM-exposed group at day 1= average of [E7] to [E12]= 0.39

12. Statistics

Data were reported as mean ± SE. For RT-PCR analysis, the fold change over time was assessed with the Student's *t*-test (unpaired *t*-test) to determine the probability (P) values. Statistical analyses were conducted using 2-tailed *t*- test with equal variance for groups. A p value of <0.05 was defined as significant.

Results

Results for Specific Aim 1

Specific Aim 1: To determine if NM (nitrogen mustard) mouse dorsal skin vesicant model resembles the previously established SM (sulfur mustard) mouse dorsal skin vesicant model. Three types of sample analysis, including macroscopic appearance, histologic assessment of sections stained with H&E (haematoxylin and eosin stain) and quantitative reverse transcription polymerase chain reaction (qRT-PCR), were performed.

1. Animal Survival

In preliminary Study 1, it was noted that some mice did not survive for 10 days after NM exposure and that the NM powder was not dissolved completely in methylene chloride (dichloromethane). Also, white residue was observed on the skin of some mice and it was observed that they were licking the site where NM was applied. Therefore, the more polar solvent, acetone was used as the vehicle for the main study, i.e., Study 2. The dielectric constant for acetone is 21, while that of methylene chloride is only 9.1. In addition, to prevent licking of the applied vehicle plus or minus NM, Elizabethan collars (24h) were used. In this way, mice were unable to ingest any residue.

Preliminary Study 1 determined the conditions that would favor survival of the animals being exposed to NM and treatment with Cx43 asODN (connexin 43 antisense oligodeoxynucleotides). Table 2 shows the survival rate of mice for both preliminary Study 1 and the main body of work, Study 2. In Study 1, all mice survived at days 1, 3 and 7. At day 10, only 60% of mice in the NM-exposed group survived. Those living had a white residue remaining on the skin from the exposure and were lethargic, sluggish and had dyspnea. Saline was given subcutaneously starting from day 7, as required by our animal protocol for

any animals losing more than 10% of their body weight. In Study 2, even though the mice in NM-exposed group were weak, all the mice survived the full 10 days and white residue was never present on their skin. Since only the vehicle had been changed from methylene chloride to acetone, it appeared that methylene chloride was reducing survival. Therefore, acetone was used as the vehicle solvent and Elizabethan collars were employed for the NM exposures in Study 2. All subsequent data presented in the Results section will be from Study 2. Data from preliminary Study 1 using methylene chloride as solvent is included in Appendix A to Appendix E.

Table 2. The survival of SKH-1 mice after exposure with nitrogen mustard in Study 1 and Study 2. Nitrogen mustard (NM, 5 μmoles) dissolved in methylene chloride (Study 1) or acetone (Study 2) and Cx43 scODN (0.15 nmoles) or Cx43 asODN (0.15 nmoles) each dissolved in a vehicle consisting of 30% Pluronic F-127 in PBS were applied to the skin of SKH-1 mice as described in Materials and Methods. The "vehicle control" consisted of methylene chloride (Study 1) or acetone (Study 2) and 30% Pluronic F-127 in PBS. VC=vehicle control. NM=Nitrogen mustard. sC=Sense control, Cx43 scODN. As=Antisense, Cx43 asODN.

Group	VC	NM	NM + sC	NM + As
Day	**No. of surviving mice/No. of total mice per group**			
STUDY 1				
1	4/4	5/5	4/4	5/5
3	4/4	5/5	4/4	5/5
7	4/4	5/5	4/4	5/5
10	4/4	3/5	3/4	5/5
Survival	**100%**	**60%**	**75%**	**100%**
STUDY 2				
1	5/5	6/6	5/5	5/5
3	5/5	6/6	5/5	5/5
7	5/5	6/6	5/5	5/5
10	5/5	6/6	5/5	5/5
Survival	**100%**	**100%**	**100%**	**100%**

2. Skin Injury Induced by NM in the SKH-1 Hairless Mice

The extent of injury on the skin of the SKH-1 hairless mice following NM exposure was evaluated based on the macroscopic appearance, edema as determined by biopsy weights, histologic examination of tissue sections and analysis of the mRNA expression levels of inflammatory biomarkers IL-1B (interleukin-1B), IL-6 (interleukin-6), COX-2 (cyclooxygenase-2), and remodeling biomarkers MMP-2 (matrix metalloproteinase-2) and MMP-9 (matrix metalloproteinase-9).

2.1 Macroscopic Appearance and Histology Post NM-Exposure

The macroscopic appearance as presented in Figure 9 showed lesions of the skin of NM exposed mice for all the time points studied (Figure 9, panels E-H). The unexposed control groups (Figure 9, panels A-D) was unaffected by the acetone vehicle without NM. On day 1 after NM exposure, erythema and edema of the skin was observed. On day 3, erythema was still present and formation of a scab was noted. At day 7, the scab became more prominent. After 10 days, the scab appeared to be desicated and the skin appeared more fragile and showed signs of flaking.

The biopsy weight changes that occurred from 1 to 10 days post exposure with NM are listed in Table 3. Changes in the percent relative skin weights (Casillas et al., 1997; Shakarjian et al., 2006) were used to assess NM-induced adverse edema effect. There were significant increases in the relative skin weights in the NM-exposed groups at each time point compared with the vehicle controls, indicating the degree of abnormal edema in the NM-exposed skin. The relative skin weights were 276, 117, 103 and 69% greater than the vehicle control skin at days 1, 3, 7 and 10, respectively. Edema was maximal at day 1 and then steadily decreased throughout the study.

The H&E stained sections of the normal unexposed skin tissues of SKH-1 mice demonstrated the expected tight stratum corneum, an epidermis with 3-5 layers of epithelia, the dermis, and a normal distribution of resident dermal cells and inflammatory cells, and regularly spaced appendages of the skin (Figure 10, panels A and F). The appendages of the skin include the hairs, hair follicles, sweat glands and the sebaceous glands. These help maintain body homeostasis.

As indicated in Figure 10 (panels B-E), NM exposed tissue sections showed signs of tissue disruption with separation of the epidermis from the dermis, shedding of the stratum corneum and formation of a scab in the epidermis, and signs of edema (an increase in epidermal and dermal thickness). At day 1, NM exposure consistently resulted in separation of the epidermis from the dermis (black arrowheads, Figure 10, panel G) and shedding of the stratum corneum (blue arrow, Figure 10, panel G). Three days after NM exposure, epidermal hyperplasia (h, dotted black arrow, Figure 10, panel H) was commonly observed in the mouse skin. At day 7, formation of an eschar (scab) in the epidermis (s, black arrow in Figure 10, panel I) and inflammatory cell infiltration in the dermis (i, dotted black arrow in Figure 10, panel I) were observed. At day 10, thickening of the stratum corneum (sc) (black arrow in Figure 10, panel J) and epidermal hyperplasia (h, dotted black arrow, Figure 10, panel J) were frequently observed.

These histological changes are the expected phenotype of toxicity to skin. Hyperplasia is commonly associated with inflammatory skin diseases and therefore serves as an indicator of the inflammation in tissues (Lee et al., 1994) along with edema. In the current study, hyperplasia was observed in the NM-exposed mouse skin from day 3 through day 10, suggesting inflammation of the skin. Experiments were not performed longer to determine when this would resolve. Also, the presence of many inflammatory cells in the dermis of the NM-exposed skin confirmed inflammation following exposure to NM (Figure 10, panel I).

2.2 mRNA Expression Levels of Inflammation and Remodeling Biomarkers Following NM-Exposure

The expression levels of markers of inflammation (IL-6, IL-1B and COX-2), and markers of remodeling **(**MMP-2 and MMP-9) for various time points post NM exposure were determined by qRT-PCR and shown in Figures 11-12. The mRNA expression of the target genes was normalized to glyceraldehyde 3-phosphate dehydrogenase (GAPDH), and then expressed as fold change relative to vehicle control, which consists of acetone and 30% Pluronic F-127 in PBS. The mRNA from vehicle control divided by vehicle control arbitrarily assigned the number 1. The detailed step-by-step explanation for the calculation of expression level of a target gene is described in section 11 of Materials and Methods. Due to potential vehicle effects on the analysis of Cx43, IL-10, MMP-12 and PGES-2, data were expressed as fold change relative to vehicle controls rather than naïve controls. The effect of NM-exposure was determined by comparing the data from the NM-exposed group to the unexposed vehicle control group. The mean fold changes relative to naïve controls for the target genes at each time point are included in Appendix A.

Compared to controls, the proinflammatory cytokine IL-6 mRNA was significantly increased 30 fold at one day after NM exposure and steadily declined to basal levels over time (20 fold at 3 days, 5 fold at 7 days and basal level at 10 days) (Figure 11A). IL-1B (Figure 11B) mRNA was significantly increased 140 times in the one day post NM exposure samples, after which the increase lessened to 10 times the vehicle control at day 3, 40 times at day 7 and 11 times at day 10. COX-2 mRNA (Figure 11C) was consistently increased for all time points after NM-exposure being 11 fold higher at 1 day, 17 fold higher at 3 days, 22 fold higher at 7 days and 10 fold higher at 10 days.

The mRNA levels of MMP-2 (Figure 12A) and MMP-9 (Figure 12B) increased later than the inflammatory mRNAs, increasing at 7 days post exposure. The fold change in

mRNA values for MMP-2 relative to the vehicle control was 0.12 and 0.16 at day 1 and day 3, respectively, but increased to 7 and 5 fold higher at day 7 and day 10, respectively (Figure 12A). Similarly, the fold changes for MMP-9 mRNA compared with the vehicle control were 0.35 and 0.44 at day1 and day 3, respectively, increasing to 4 and 2 fold at day 7 and day 10, respectively, relative to the vehicle control (Figure 12B).

2.3 Results Summary for Specific Aim 1

NM induced skin lesions on the backs of SKH-1 mice resemble the lesions observed when SM is used as the vesicant. Edema increased over all time points. The macroscopic appearance displayed erythema, edema and formation of scabs on the skin. Histologic examination of NM exposed mouse skin tissue sections showed that NM caused separation of the epidermis from the dermis, as well as shedding and thickening of stratum corneum, formation of scabs, hyperplasia. In addition, more inflammatory cells accumulated in the dermis. The significant upregulation of mRNA levels of proinflammatory biomarkers (IL-1B (days 1, 7, 10), IL-6 (days 1, 3, 7), COX-2 (days 1, 3, 7, 10)) and remodeling biomarkers (MMP-2 (days 7, 10) and MMP-9 (days 7, 10)) also agreed with what has been shown after SM injury in this mouse model. Therefore, NM is a good substitute agent for studying skin injury induced by SM.

Figure 9. Macroscopic appearance from NM-exposed mouse skin. Macroscopic appearance of the skin in SKH-1 hairless mice with and without topical application of 5 μmoles of NM in acetone for 1, 3, 7 and 10 days post-exposure as described in Materials and Methods. Mice from unexposed groups are depicted in the left panels (panels A-D). Mice from NM-exposed groups are depicted in the right panels (panels E-H).

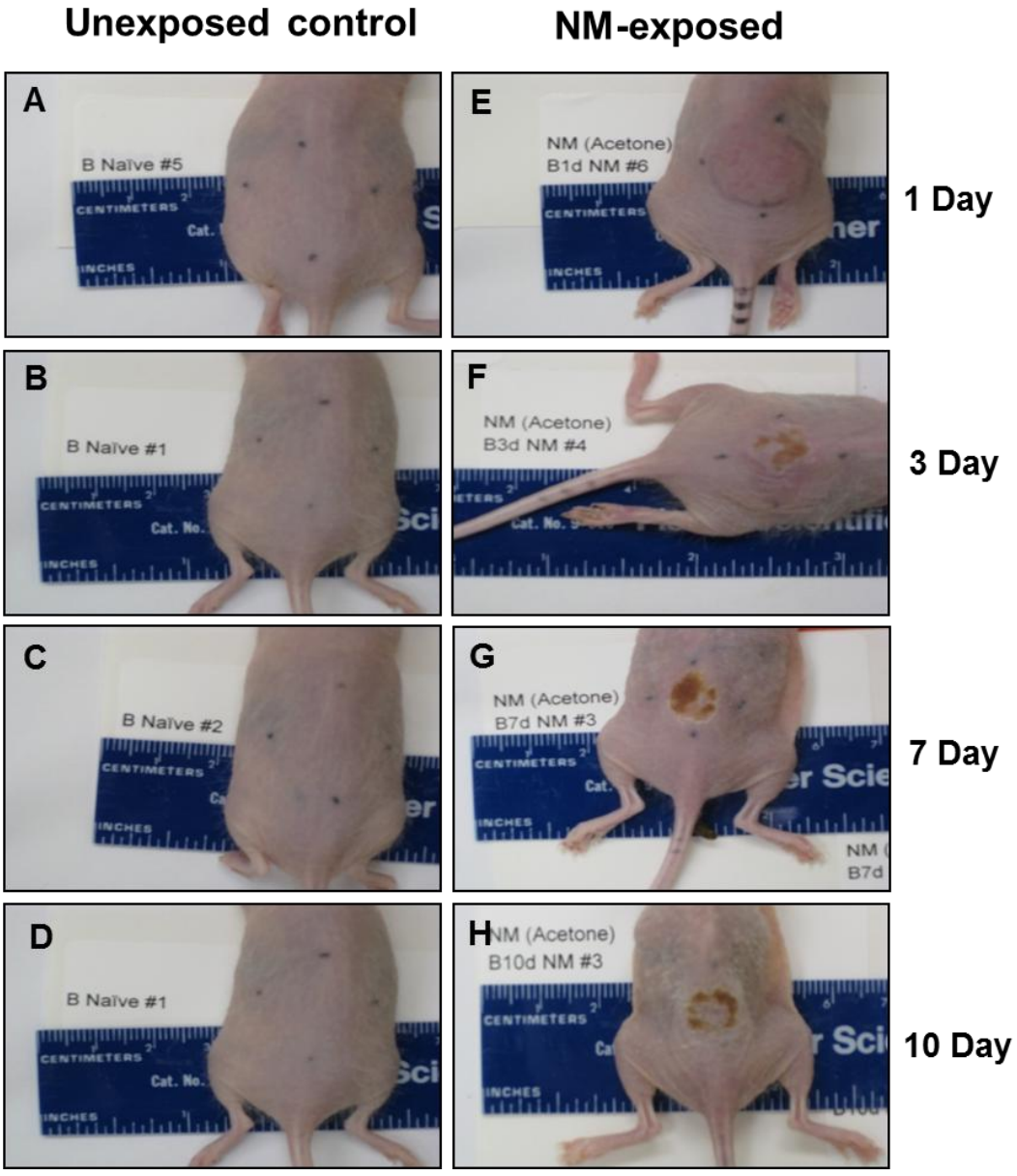

Table 3. Weight changes of biopsy samples 10 days post NM exposure. The punch biopsies (12 mm in diameter) were collected at 1, 3, 7, and 10 days after NM (5 μmoles in acetone) exposure. Weight changes were evaluated as described in Materials and Methods. Data reported as mean ± SE; VC: Vehicle Control; NM: NM-exposed. Significantly different from vehicle control: * NM (n = 6) vs. VC (n = 5) ($p < 0.05$).

Relative skin weight (%) = 100 x [NM-exposed biopsy weight – vehicle control biopsy weight]/[vehicle control biopsy weight]

Day post exposure	VC (g)	NM (g)	Relative skin weight (%)
1	0.068 ± 0.003	0.254 ± 0.011	276*
3	0.077 ± 0.008	0.167 ± 0.027	117*
7	0.066 ± 0.004	0.134 ± 0.004	103*
10	0.067 ± 0.004	0.114 ± 0.011	69*

Figure 10. H&E Histology of dorsal skin biopsies of SKH-1 hairless mice treated with NM. Hematoxylin and eosin stained sections of skin tissue in mice following either no treatment (panels A and F, day 0), or exposure to 5 µmoles of NM in acetone (Study 2) (panels B-E, G-J). NM exposed biopsies were obtained at day 1 (panels B, G), day 3 (panels C, H), day 7 (panels D, I) and day 10 (panels E, J) post exposure, as described in Materials and Methods. Right panels (F-J) are higher magnifications of rectangles from left panels A-E. Abbreviations: hf (hair follicle), h (hyperplasia), s (scab), sc (stratum corneum), i (inflammatory cell). The black arrow heads in panel G show the separation of epidermis from dermis. The blue arrow in panel G shows shedding of stratum corneum. Bar = 200 µm (panels A-E) and bar = 50 µm (panels F-J).

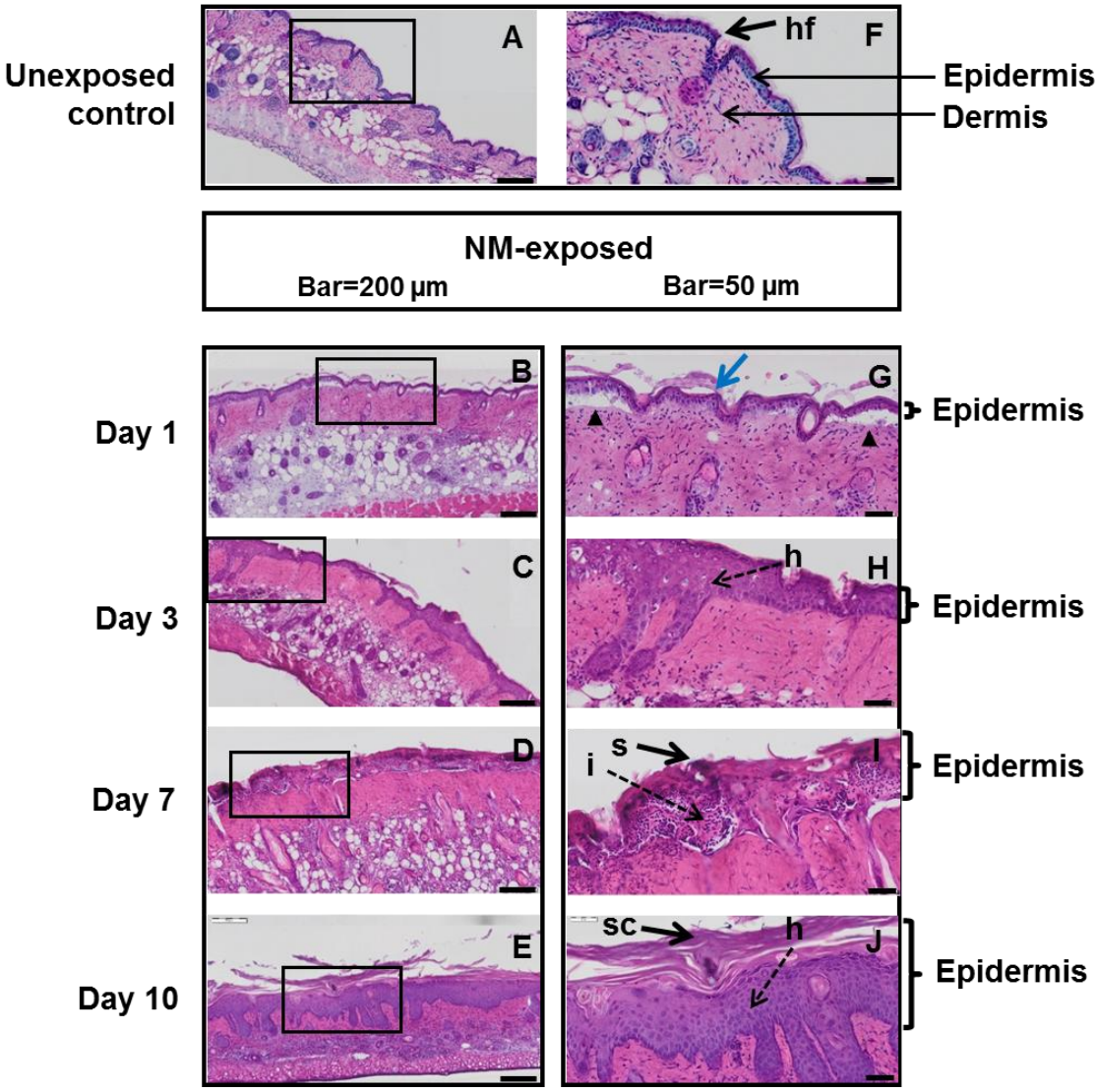

Figure 11. mRNA expression levels of proinflammatory biomarkers IL-6, IL-1B and COX-2 following NM-exposure. qRT-PCR analysis of Il-6 (A), IL-1B (B), COX-2 (C) gene expression of skin biopsies at days 1, 3, 7, 10 post exposure of SKH-1 mouse dorsal skin to 5 μmoles NM in acetone (Study 2) as described in Materials and Methods. mRNA expression of biomarkers was normalized to GAPDH and expressed as fold changes (as described under Results) relative to vehicle control (mRNA of vehicle control divided by vehicle control was assigned the number 1 and is shown as a dotted line). Data reported as mean ± SE. VC: Vehicle Control; NM: NM-exposed. Significantly different from vehicle control: * NM (n=6) vs. VC (n=5) ($p < 0.05$).

A. IL-6

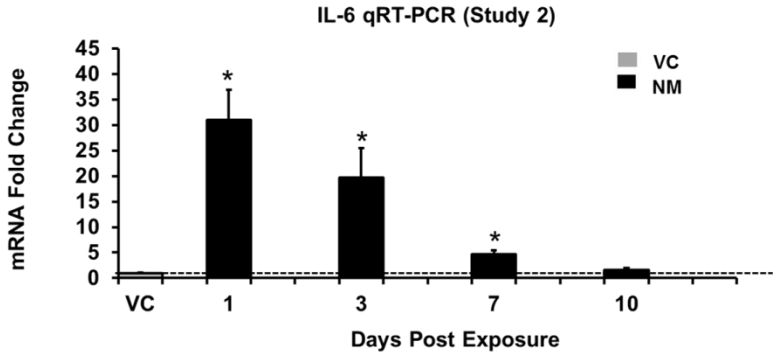

B. IL-1B

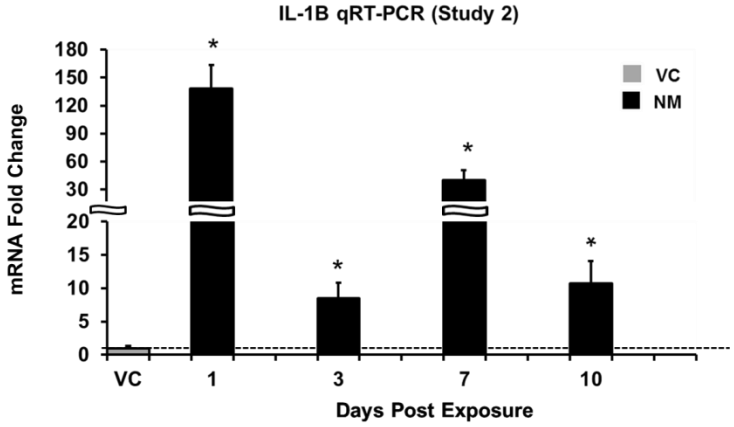

C. COX-2

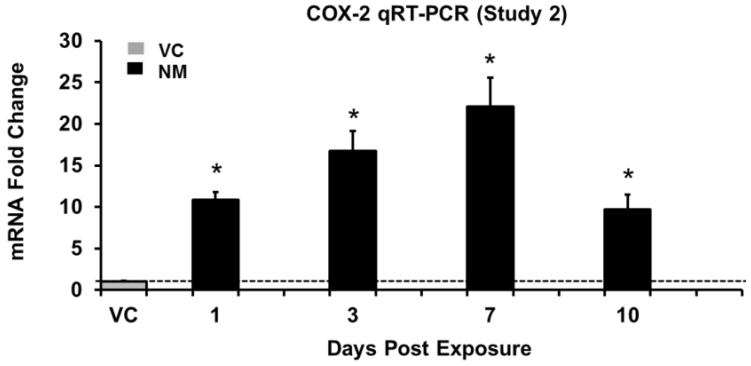

Figure 12. mRNA expression levels of remodeling biomarkers MMP-2 and MMP-9 following NM-exposure. qRT-PCR analysis of MMP-2 (A) and MMP-9 (B) gene expression for mouse skin biopsies at days 1, 3, 7, 10 post NM-exposure (5 μmoles in acetone, Study 2). mRNA expression of biomarkers was normalized to GAPDH and expressed as the fold change (as described under Results) relative to vehicle control (mRNA of vehicle control divided by vehicle control was assigned the number 1 and is shown as a dotted line). Data are reported as mean ± SE. VC: Vehicle Control; NM: NM-exposed. Significantly different from vehicle control: * NM (n = 6) vs. VC (n = 5) ($p < 0.05$).

A. MMP-2

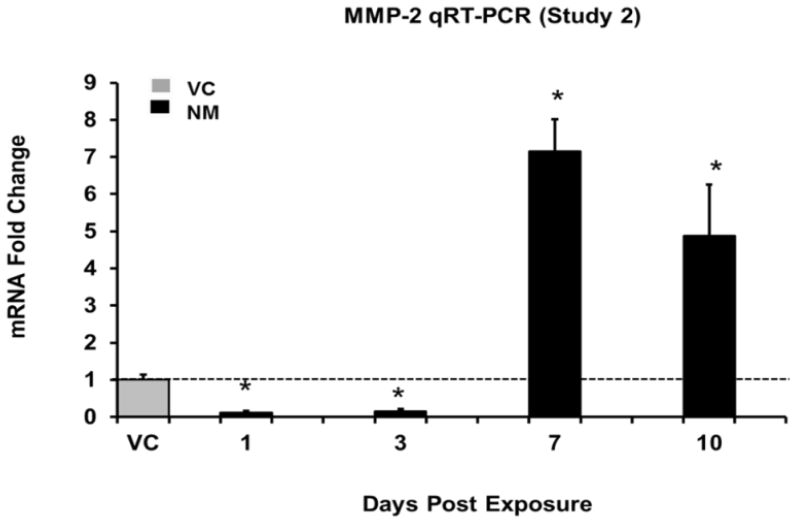

B. MMP-9

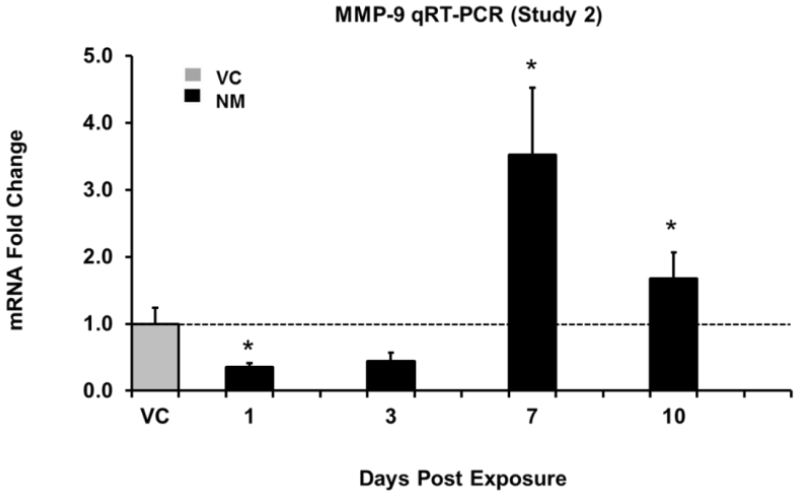

Results for Specific Aim 2

Specific Aim 2: To determine levels of Cx43, Cx26 and Cx30 after NM exposure and treatment with Cx43 asODN in mouse skin. Four types of sample analysis, including macroscopic appearance, H&E histology, qRT-PCR (Cx43, Cx26 and Cx30) and western blot (Cx43), were performed.

3. Penetration of Cx43 asODN into Wounded Tissue as Determined by Using CY3-Tagged Cx43 asODN

CY3 tagged Cx43 asODN was used to determine the penetration of the Cx43 asODN into the wounded area at 2, 6, and 24 hr post NM exposure, as shown in Figure 13. The fluorophore demonstrated that Cx43 asODN penetrated well into the wounded area (Figure 13, red color). CY3-tagged Cx43 asODN penetrated throughout the epidermis and hair follicles by 2 hr. The label appeared more punctate by 6 hr and appeared to reach the bottom of papillary dermis by 24 hr.

Figure 13. Penetration of CY3-tagged Cx43 asODN into NM exposed mouse skin. Control (naïve) and NM (5 μmoles in acetone) exposed skin sections collected at 2, 6, and 24 hr after treatment with CY3-tagged Cx43 asODN (0.15 nmoles in 30% Pluronic F-127 in PBS) as described in Materials and Methods. Red fluorescence indicates the penetration of CY3-tagged Cx43 asODN into the injured skin and white arrows indicate the penetration through hair follicles. Blue fluorescence indicates nuclei stained with DAPI. Images were taken at 200x on Zeiss Axio Observer. Scale bars represent 20 μm.

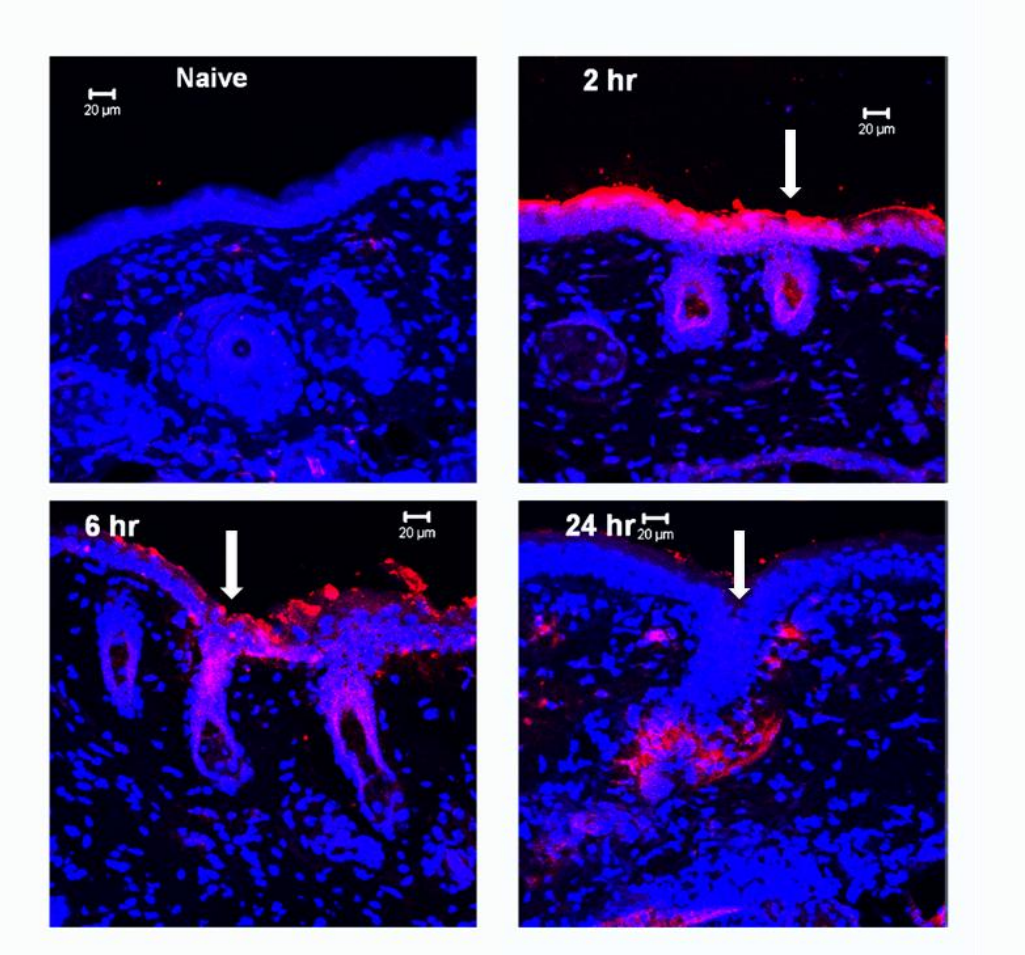

4. Effects of Cx43 asODN on the Skin of Hairless Mice Post NM Exposure

The effects of Cx43 asODN on the skin of mice following NM exposure were evaluated based on the macroscopic appearance, histologic examination of tissue sections, qRT-PCR analysis of the mRNA expression levels of Cx43, Cx26, Cx30, and western blot analysis of the protein levels of Cx43. The Cx43 asODN was added 2 hours after the NM

exposure. All analyses were performed at 1, 3, 7, and 10 days after NM exposure with or without Cx43 asODN treatment.

4.1. Effects of Cx43 asODN on the Macroscopic Appearance and Histology of NM Exposed Mouse Skin

Macroscopic images of the mouse skin were taken and graded by at least 3 people. The most representative samples were chosen which are shown in Figure 14 for all the time points examined.

With post exposure Cx43 asODN treatment, the macroscopic appearance showed reduced erythema of the mouse skin for day 1 (Figure 14A, panel C) when compared to NM-exposure alone (Figure 14A, panel B). At day 3, compared to NM-exposure alone (Figure 14B, panel B), Cx43 asODN treatment (Figure 14B, panel C) resulted in reducing edema and scab formation. Reducing scab formation and less flaking of the skin were also seen with Cx43 asODN treatment at day 7 (Figure 14C, panel C), compared to NM-exposure alone (Figure 14C, panel B). For day 10, there does not seem to be any significant difference in reducing scab size between the Cx43 asODN treated and untreated groups when looking at the gross pathology (Figure 14D, panels B and C).

Examination of representative tissue sections suggested less shedding and slightly less thickening of the stratum corneum for the Cx43 asODN treated group (Figure 14A, panels F and I) at day 1 post exposure as compared to the untreated NM-exposed group (Figure 14A, panels E and H). For day 3, less scab area and less epidermal hyperplasia were observed in the group treated with Cx43 asODN (Figure 14B, panels F and I). The wounds treated with Cx43 asODN seemed to progress toward healing at a quicker rate than NM-exposed skin receiving no antisense treatment. At day 7, Cx43 asODN treatment resulted in less necrosis of the superior dermis with less destruction of cell adhesion in the tissue and less inflammatory cell infiltration into the dermis (Figure 14C, panels F and I) as compared to

the NM-exposed groups alone (Figure 14C, panels E and H). In addition, on day 7, histology showed that the Cx43 asODN treatment groups (Figure 14C, panels F and I) seemed to have a faster rate of re-epithelization when compared to the NM exposed group alone which remained as an open, exposed wound longer (Figure 14C, panels E and H). At day 10, the Cx43 asODN treated group (Figure 14D, panels F and I) demonstrated less thickening of the stratum corneum and less hyperplasia of the epidermis as compared to the NM-exposed mouse skin (panels E and H of Figure 14D) indicating the healing effect of Cx43 asODN treatment.

In an additional set of representative mice, the histologic examination of skin tissue sections (Figure 15) also suggested that post-exposure treatment with Cx43 asODN resulted in less separation of epidermis from dermis (Figure 15, panel F), reduced epidermal hyperplasia (Figure 15, panels G) and less thickening of the stratum corneum (Figure 15, panels I), compared to the NM-exposed mouse skin receiving no treatment (Figure 15, panels B, C and E, respectively). In addition, with Cx43 antisense treatment, NM exposed mouse skin showed fewer inflammatory cells at all time points examined in mice (Figure 15, panels F- I). The histologic examination suggested that Cx43 asODN attenuates NM-induced inflammation.

In summary, from the gross pathology and H&E histology there seems to be a trend toward faster progression of wound healing and a faster rate of re-epithelization following treatment with Cx43 asODN post NM exposure.

The macroscopic appearance and H&E histology from all individual mice of Study 2 using acetone as vehicle for NM are included in Appendix C.

Figure 14. Effects of Cx43 asODN on the macroscopic appearance and H&E histology of mouse skin at days 1, 3, 7 and 10 post NM exposure. Macroscopic appearance (panels A-C) and H&E histology of mouse skin sections (panels D-I) at day 1 (A), day 3 (B), day 7 (C) and day 10 (D) for unexposed control (panels A, D, G), NM exposed (5 µmoles in acetone) (panels B, E, H) or NM exposed plus Cx43 asODN treatment (0.15 nmoles in 30% Pluronic F-127 in PBS) (panels C, F, I). Samples are dorsal skin biopsies of mice as described for Study 2 in Materials and Methods. Panels G, H, I are higher magnifications of rectangles in panels D, E, F, respectively. Bar= 200 µm (panels D-F) and bar = 50 µm (panels G-I).

A. 1 day post exposure

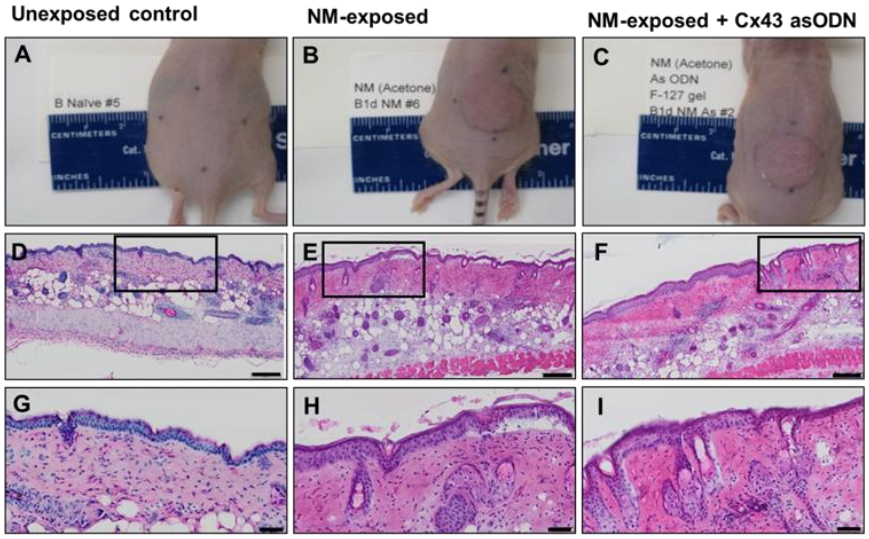

B. 3 days post exposure

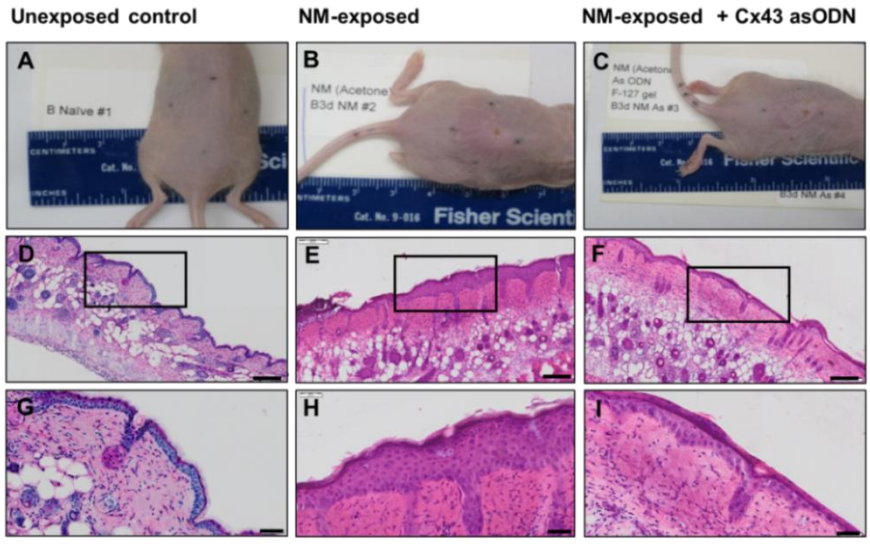

C. 7 days post exposure

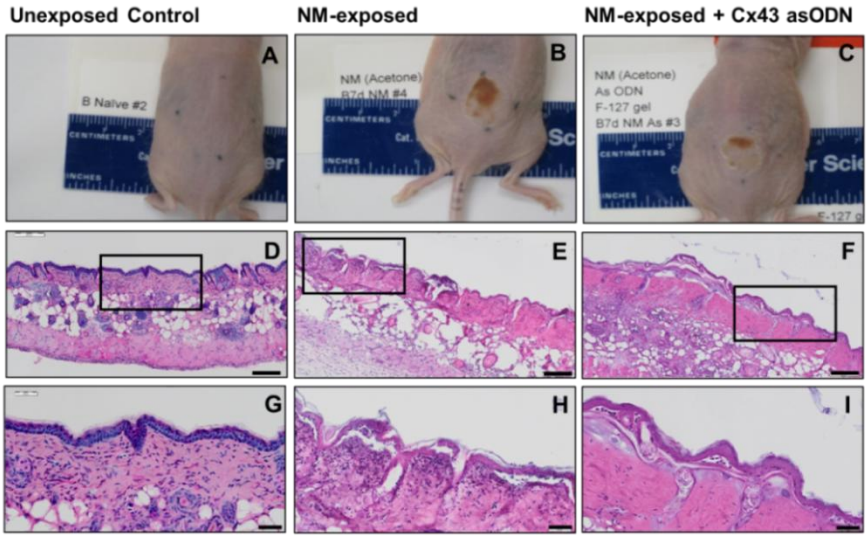

D-F: Bar=200 μm; G-I: Bar=50 μm

D. 10 days post exposure

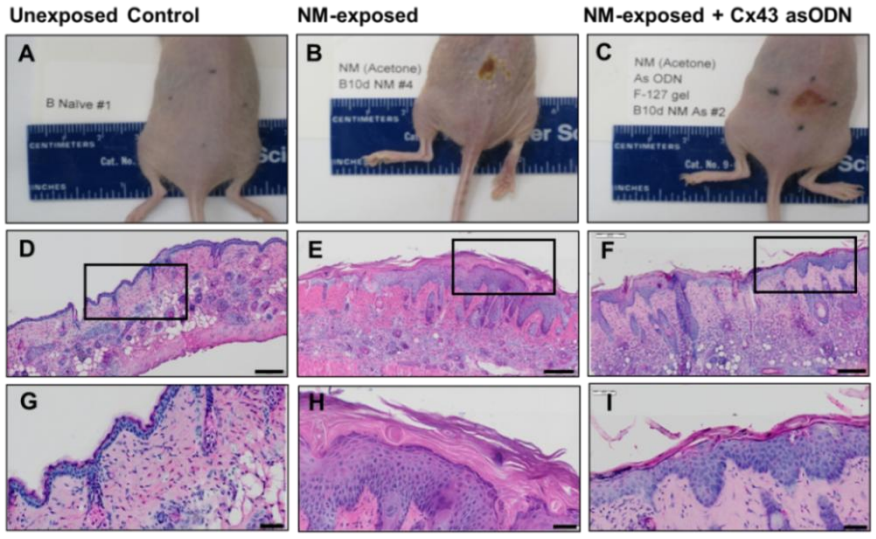

D-F: Bar=200 μm; G-I: Bar=50 μm

Figure 15. Histologic features indicating degree of inflammation in mouse skin after NM exposure and post-exposure treatment with Cx43 asODN. Hematoxylin and eosin histology of additional representative mouse skin sections for unexposed control (A), NM exposed (5 μmoles in acetone) (panels B-E) or NM exposed plus Cx43 asODN treatment (0.15 nmoles in 30% Pluronic F-127 in PBS) (panels F-I) as described for Study 2 in Materials and Methods. Bar = 50 μm. With Cx43 asODN treatment, NM exposed mouse skin shows fewer inflammatory cells at days 1, 3, 7 and 10 (panels F. G, H. I), less thickening of the stratum corneum at days 7 and 10 (panels H and I), as well as less hyperplasia at days 3, 7 and 10 (panels G, H, I).

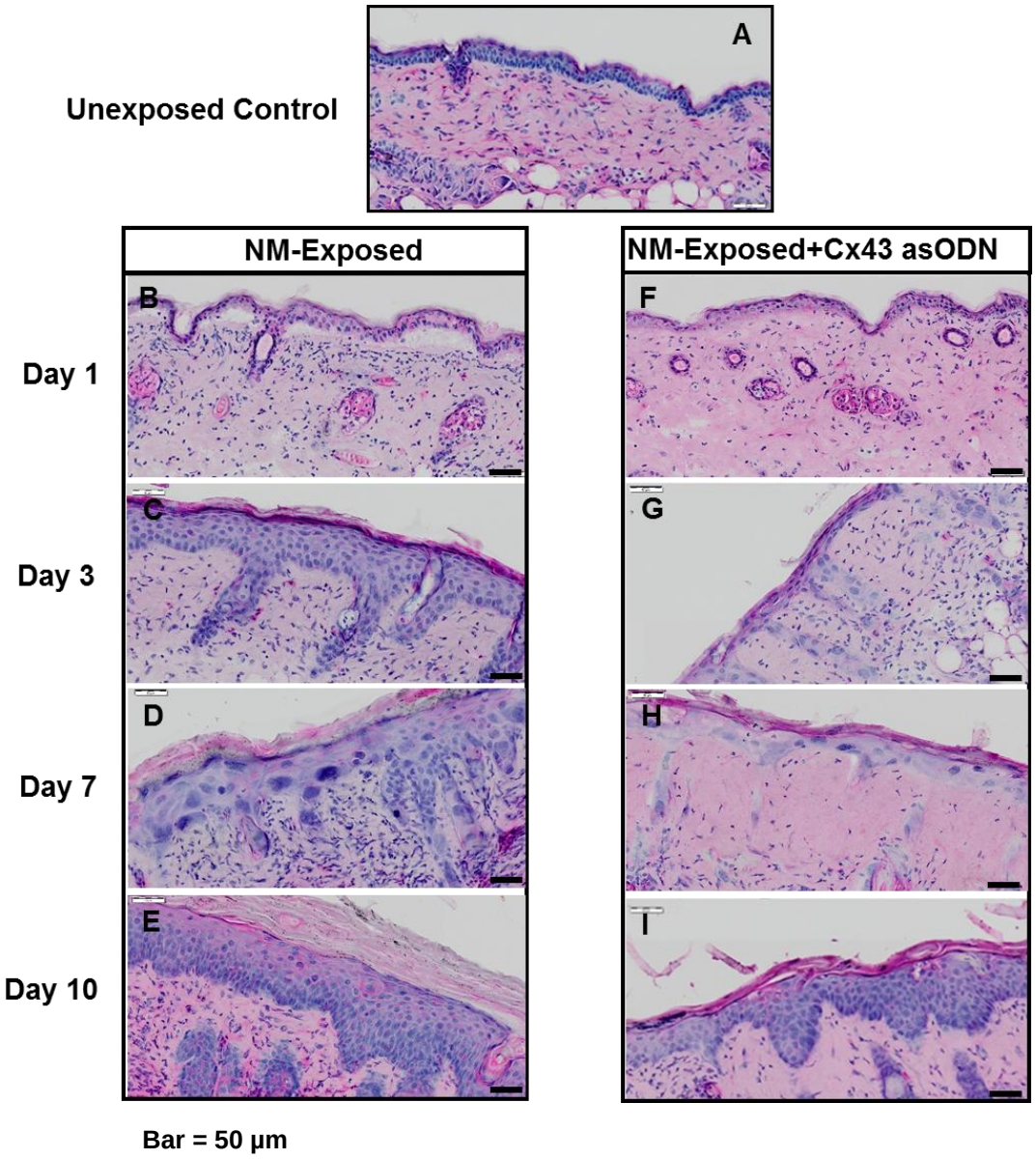

4.2. Effects of Cx43 asODN on the mRNA Expression of Connexins (Cx43, Cx26, Cx30) in NM Exposed Mouse Skin

Connexins 43, 26 and 30 (Cx43, Cx26 and Cx30) are known to play important roles in wound healing. In rodents and humans there is a downregulation of Cx43 and an up-regulation of Cx26 and Cx30 in keratinocytes at the wound edges (Brandner et al., 2004; Coutinho et al., 2003; Goliger and Paul, 1995). Once the wound is closed, Cx26 and Cx30 downregulate to their initial normal levels within the epidermis. Finally, the expression of Cx43 returns to normal as the epidermis regains its characteristic laminar architecture (Brandner et al., 2004).

The mRNA expression of Cx43 and other target genes evaluated in the study were normalized to GAPDH. Due to potential vehicle effects on the analysis of Cx43, IL-10, MMP-12 and PGES-2, data were expressed as fold change relative to vehicle controls. mRNA fold change of vehicle control group represents 1 after normalization to GAPDH as described in section 11 of Materials and Methods. The effect of Cx43 asODN was statistically analyzed by comparing the data from the NM-exposed group treated with Cx43 asODN to the NM exposed group not receiving post exposure Cx43 asODN. The qRT-PCR data in this section are results from Study 2. The results of qRT-PCR analysis from Study 1 are included in Appendix D. Fold changes relative to unexposed (naïve) controls at each time point are included in Appendix A.

4.2.1. qRT-PCR Analysis of Cx43

After NM exposure, there was a statistically significant down regulation on Cx43 mRNA (black bars) at day 1 (fold change = 0.39), day 7 (fold change = 0.67), and day 10 (fold change = 0.82) when compared to the vehicle control (grey bar, fold change = 1.0, dotted line on graph) (see Figure 16A). At day 3, Cx43 was down-regulated (fold change = 0.70) but the reduction was not statistically significant. The mRNA levels of Cx43 in the

NM-exposed without Cx43 asODN treatment samples were down-regulated as compared to those vehicle control samples from day 1 to day 10 with the lowest level of Cx43 at day 1 and the highest level of Cx43 at day 10.

Cx43 asODN treatment (white bars) resulted in a further significant reduction of Cx43 mRNA ($P<0.05$) for day 3 (a 35% reduction or 2.9 (1/0.35) fold less) and day 7 (a 36% reduction or 2.8 fold less) when compared to NM-exposure alone (* in Figure 16A). Cx43 was still down-regulated after antisense treatment by day 10 (a 15.7% reduction), however, this reduction was not a statistically significant change. The Cx43 mRNA level slightly increased (16.6% increase) after Cx43 asODN treatment at day 1 but the difference was not significant. The results indicated that, in general, treatment with Cx43 asODN post NM exposure attenuates the mRNA level of Cx43.

4.2.2. qRT-PCR Analysis of Cx26

Compared to the vehicle control, the expression of Cx26 mRNA was statistically significantly up-regulated in the NM-exposed group not receiving Cx43 asODN for all the time points studied (# in Figure 16B). The mRNA level of Cx26 changed in these samples from a 2-fold increase at day 1 to a 5 fold, 7 fold and 6-fold increase at days 3, 7 and 10, respectively, compared to vehicle controls.

Cx26 mRNA was also upregulated from day 1 to day 10 when a single dose of Cx43 asODN treatment was employed after NM exposure as compared to vehicle controls. However, the increase was not as extensively as after NM exposure without Cx43 asODN treatment. Compared to NM exposure alone, Cx43 antisense treatment resulted in reduction of the Cx26 mRNA expression from day 1 to day 10. The reduction was statistically significant for day 1 (a 25% reduction or 4 fold less) and day 3 (a 30% reduction or 3.3 fold

less) (* in Figure 16B). The data suggest that treatment with Cx43 asODN also attenuates the expression of Cx26 mRNA post NM exposure.

4.2.3. qRT-PCR Analysis of Cx30

A statistically significant up-regulation of Cx30 mRNA was observed after NM exposure (without Cx43 asODN treatment) for all-time points studied when compared to the vehicle control (# in Figure 16C). The mRNA level of Cx30 was increased 5 fold at day 1 and 10.5, 15.0, 9.5 fold at days 3, 7 and 10, respectively, as compared to the vehicle control. The mRNA expression levels increased peaking at day 7 and then began decreasing. Between day 7 and day 10, the mRNA level went from 15 times that of the vehicle control to only 9.5 times of the control.

A statistically significant ($P<0.05$) reduction of Cx30 mRNA level by Cx43 asODN treatment was observed for day 1 (a 58% reduction or 1.7 fold less) in the NM exposed/Cx43 asODN treated group (* in Figure 16C) as compared to NM-exposed group alone. Cx30 mRNA was also reduced by Cx43 antisense treatment at days 3, 7 and 10. The data suggest that treatment with Cx43 asODN post NM exposure also attenuates the mRNA expression of Cx30.

4.3. Immunoblots and Densitometry of Cx43 in Mouse Skin

Western blot analysis (Figure 17A) supported the mRNA data with few exceptions. The protein expression level of Cx43 decreased in NM exposed groups without Cx43 asODN treatment when compared to the vehicle control groups at all the time points studied. Following Cx43 antisense treatment, western blot analysis also showed the further reduction of Cx43 protein levels for all the time points in the NM-exposed/Cx43 asODN treated groups (NM+As) compared to NM-exposed groups alone (NM) (Figure 17A). The intensity of the WB bands were evaluated by densitometry (Figure 17B). The densitometric analysis showed

the level of Cx43 protein decreased in NM exposed mouse skin as compared to the vehicle control groups (assigned a value of 1) for all time points studied. The levels of Cx43 were 0.4, 0.83, 0.17 and 0.53 for days 1, 3, 7 and 10, respectively. The levels of Cx43 were further reduced after Cx43 asODN treatment to 0.37, 0.63, 0.14 and 0.36 for days 1, 3, 7 and 10, respectively (Figure 17B).

4.4. Results Summary for Specific Aim 2

Cx43 mRNA was downregulated, while Cx26 and Cx30 mRNAs were upregulated in NM-exposed mice skin. This upregulation of Cx26 and Cx30 was maximum at 7 days post NM exposure. In addition, treatment with Cx43 asODN post NM exposure resulted in further downregulation of Cx43, and an attenuation of the increase in Cx26 and Cx30 mRNA. Densitometric analysis of the Cx43 protein on western blots supports the mRNA data. Based on histological examination and macroscopic appearance, downregulation of Cx43 by Cx43 asODN resulted in attenuating the injury as well. Overall, the data indicate that changes in expression of Cx43 occur in NM injury. Cx43 asODN facilitates the healing process of these wounds by further downregulating Cx43. In addition, the data also suggest that Cx26 and Cx30 may have a role in NM injuries since Cx43 asODN decreases the mRNA expression of both Cx26 and Cx30 after NM exposure. Immunoblots and Densitometry of Cx43 in mouse skin from Study 1 are included in Appendix D.

Figure 16. Effects of Cx43 asODN on mRNA expression levels of connexins Cx43, Cx26 and Cx30 following NM exposure and post-exposure treatment with Cx43 asODN. Cx43 (A), Cx26 (B) and Cx30 (C) mRNA levels were determined at days 1, 3, 7 and 10 by qRT-PCR analysis of skin biopsies of SKH-1 mice exposed to 5 μmole of NM (in acetone) plus and minus treatment with 0.15 nmoles of Cx43 asODN in 30% Pluronic F-127 in PBS as described for Study 2 in Materials and Methods. mRNA expression of Cx43, Cx26 and Cx30 was each normalized to GAPDH and expressed as fold changes (as described under Results) relative to vehicle control (mRNA of vehicle control divided by vehicle control was assigned the number 1 and is shown as a dotted line). Data reported as mean ± SE. VC: Vehicle Control; NM: NM-exposed; NM+As: NM-exposed treated with Cx43 asODN. # $p < 0.05$ (NM vs. VC); * $p < 0.05$ (NM+As vs. NM).

A. Cx43

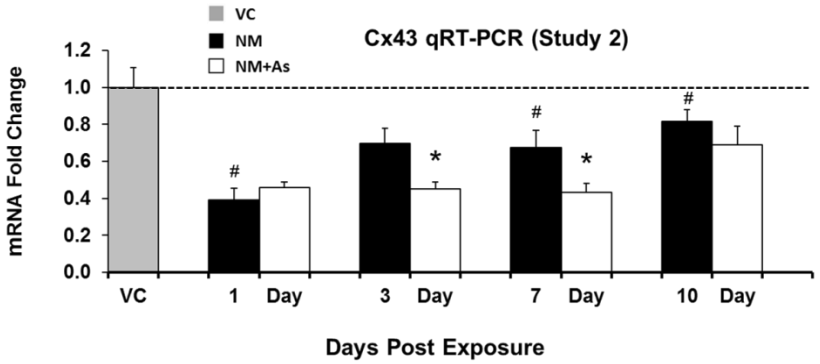

B. Cx26

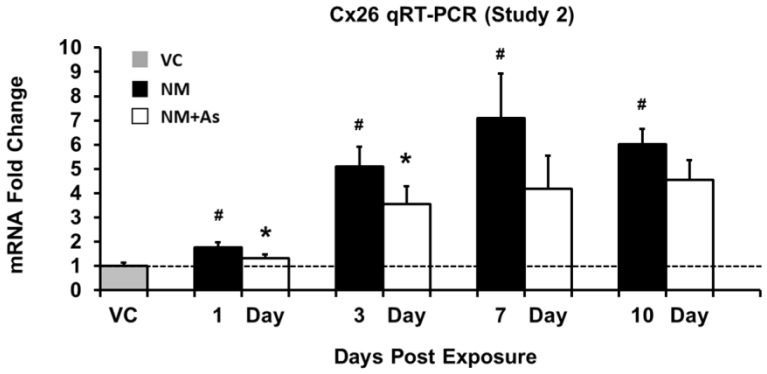

C. Cx30

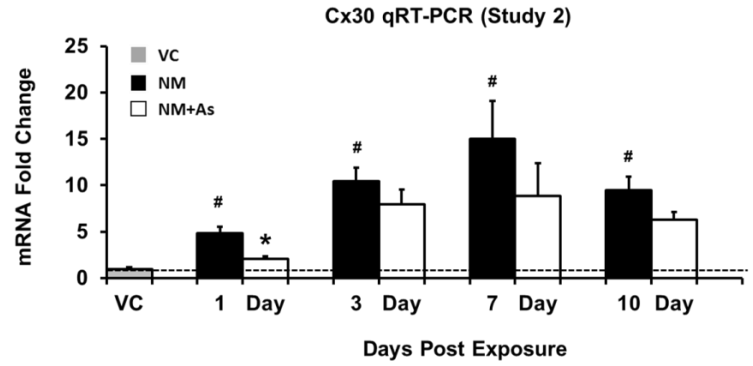

Figure 17. Effect of Cx43 asODN on Cx43 protein levels following NM exposure plus and minus post-exposure treatment with Cx43 asODN or Cx43 scODN. Cx43 protein levels were determined at days 1, 3, 7 and 10 by immunoblots (A) of skin biopsies of SKH-1 mice exposed to 5 μmoles of NM (in acetone) and treated with 0.15 nmoles of Cx43 asODN in 30% Pluronic F-127 in PBS or 0.15 nmoles of Cx43 scODN as described for Study 2 in Materials and Methods. The western blot band density was evaluated by densitometry (B). Protein levels of Cx43 in unexposed control (UC), vehicle control (VC, exposed to acetone and treated with 30% Pluronic F-127 in PBS), NM exposed (NM), NM exposed treated with Cx43 scODN (NM + sC) and NM exposed treated with Cx43 asODN (NM + As) mice skin at days 1, 3, 7 and 10 post-exposure. GAPDH was used as equal protein loading controls.

A. Immunoblots of Cx43:

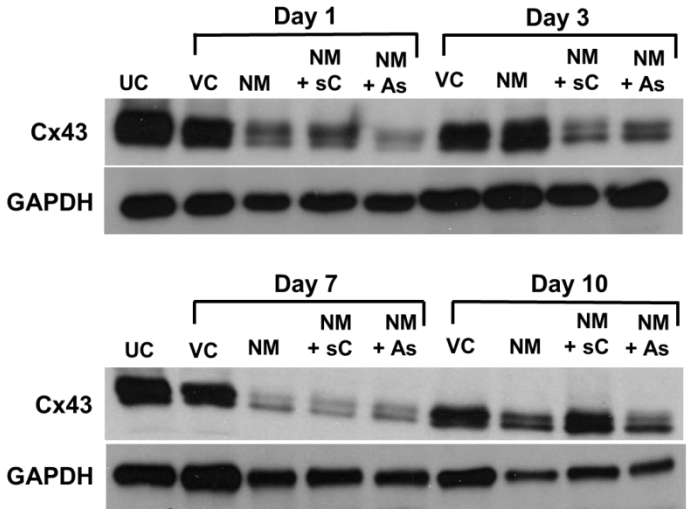

B. Densitometry of Cx43:

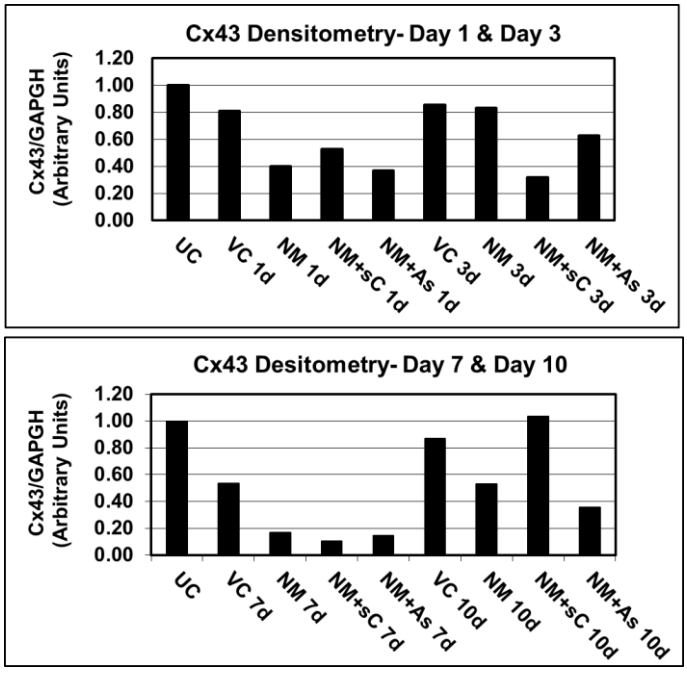

Results for Specific Aim 3

Specific Aim 3: To evaluate the effects of Cx43 asODN on biomarkers of both inflammation (IL-6, IL-1B, IL-10, PGES-2 and COX-2) and the remodeling phase of wound healing (MMP-2, MMP-9 and MMP-12) in NM-exposed mouse skin. qRT-PCR analyses were performed to analyze these biomarkers of injury and healing.

5. Effects of Cx43 asODN on Biomarkers of Both Inflammation and the Remodeling Phase of Wound Healing in NM-Exposed Mouse Skin

To evaluate the effects of Cx43 asODN on biomarkers of both inflammation (IL-6, IL-1B, IL-10, COX-2 and PGES-2) and the remodeling phase of wound healing (MMP-2, MMP-9 and MMP-12) in NM-exposed mouse skin, the mRNA expression of IL-1B, IL-6, IL-10, COX-2, PGES-2, MMP-2, MMP-9,and MMP-12 in mouse skin were determined by qRT-PCR analysis. The effect of Cx43 asODN was determined by comparing the data from the NM exposed group receiving no subsequent treatment, to the NM-exposed group treated with Cx43 asODN. The data presented are the results from Study 2. Results from Study 1 are tabulated in Appendix D.

5.1. qRT-PCR Analysis of Biomarkers of the Inflammation Phase (IL-6, IL-1B, IL-10, COX-2 and PGES-2) in NM-Exposed Mouse Skin

Compared to the vehicle controls, IL-6 mRNA, a proinflammatory cytokine, was significantly upregulated in the NM-exposed group at days 1, 3 and 7 (Figure 18A). IL-6 mRNA was increased 30 fold one day after NM exposure. A steady decline in expression was observed over time (at 3 days, 20 fold; at 7 days, 5 fold, and at10 days, it was back to the basal level). Comparing the NM exposed group to the samples treated with Cx43 asODN post-NM exposure, qRT-PCR analysis showed IL-6 mRNA in the Cx43 asODN treated group was higher than in the NM-exposed group without treatment at days 3, 7 and 10. At day 7, the difference was significant (5-fold). The IL-6 mRNA levels in the day 3 and day 10,

Cx43 antisense treated post NM exposure groups were also higher than the NM-exposed group alone, but the differences were not statically significant. The fold changes were 31 vs. 20 and 8 vs. 2, for day 3 and day 10, respectively (Figure 18A). At day 1, the IL-6 mRNA level in the NM exposed, Cx43 asODN treated group did not exceed that of NM-exposed samples.

The mRNA of IL-1B, also a proinflammatory cytokine, was upregulated in the NM-exposed group at day 1 (140-fold). By day 3 it was reduced to 10 fold. Compared to vehicle controls, a 40 fold increase was seen at day 7, but at day 10, this level fell to 11-fold (Figure 18B). The mRNA levels of IL-1B in the NM-exposed group demonstrated the upregulation of IL-1B after NM exposure for all time points studied, with the greatest upregulation at 1 day after exposure. The mRNA level of IL-1B was reduced in NM exposed groups receiving Cx43 asODN treatment at day 1 post exposure (120-fold vs. 140-fold), but this reduction was not significant. After day 1, the pattern changed. With Cx43 asODN treatment, the mRNA level of IL-1B remained upregulated with a peak at day 3 (400 fold, 260 fold and 60 fold higher than the vehicle controls at days 3, 7 and 10, respectively). Cx43 antisense significantly increased the mRNA levels of IL-1B at days 7 and 10 post NM exposure. It appears that it takes more than 1 day for IL-1B to increase in response to NM exposure.

The mRNA level of IL-10 (an anti-inflammatory marker) was downregulated in the NM-exposed group for all the time points studied when compared to the vehicle controls but the difference was only significant at day 1 (50% of the vehicle control). The mRNA levels increased from day 1 to day 7 with the peak observed at day 7 and then decreased at day 10 after NM exposure (Figure 18C). The mRNA fold changes were 0.48, 0.75, 0.97 and 0.69 at days 1, 3, 7 and 10, respectively. IL-10 mRNA was further reduced by Cx43 asODN treatment at all-time points studied but the difference was not statistically significant when

compared to NM-exposed group (Figure 18C). The IL-10 mRNA level was not changed significantly by Cx43 asODN treatment.

The mRNA levels of COX-2 in the NM-exposed group alone were significantly upregulated compared to the vehicle control for all time points studied after NM-exposure (1 day-11 fold, 3 day-17 fold, 7 day-22 fold and 10 day-10 fold) (Figure 18D). Following post NM exposure treatment with Cx43 asODN, qRT-PCR analysis showed a significant ($P<0.05$) reduction of COX-2 at day 1 when compared to the NM-exposed group (fold change: 7 vs. 11, a ~35% reduction) (Figure 18D). However, in these NM exposed and Cx43 asODN treated samples, the mRNA expression of COX-2 was increased at days 3, 7 and 10 with the maximal level occurring at day 3 post-exposure (66 fold).

Prostaglandins may function in both the promotion and resolution of inflammation (Ricciotti et al., 2011). Membrane-bound PGES-2 (prostaglandin E_2 synthase-2) catalyzes the conversion of prostaglandin H2 (PGH-2) to prostaglandin-2 (PGE-2). PGE-2 contributes to the pain, redness, and swelling associated with inflammation. The level of PGE-2 is dependent on the level of its synthase PGES-2. Data from qRT-PCR analysis showed PGES-2 was significantly downregulated after NM exposure at all time points examined (43-66% of the fold change of vehicle controls, ~35-60% reduction) when compared to the vehicle controls. Addition of Cx43 asODN appeared to have no effect on the downregulation of PGES-2 (Figure 18E).

In summary, after exposure with NM, the mRNA expression of IL-1B, IL-6 and COX-2 were upregulated but the levels of IL-10 and PGES-2 mRNA were downregulated. The mRNA level of COX-2 at day 1 was significantly reduced after Cx43 antisense treatment (a ~35% reduction). Treatment with Cx43 asODN resulted in further upregulation of IL-1B, IL-6 and COX-2 at days 3, 7 and 10. The treatment with Cx43 asODN has no significant influence on the mRNA levels of IL-10 and PGES-2.

Figure 18. Effects of Cx43 asODN on mRNA expression levels of inflammatory biomarkers IL-6, IL-1B, IL-10, COX-2 and PGES-2. qRT-PCR analyses of IL-6 (A), IL-1B (B), IL-10 (C), COX-2 (D) and PGES-2 (E) mRNAs in skin biopsy samples were performed following exposure of 5 μmoles of NM in acetone to SKH-1 mouse skin for 2 hours and treated with 0.15 nmoles of Cx43 asODN for 1, 3, 7, 10 days post exposure as described for Study 2 in Materials and Methods. mRNA expression of biomarkers was normalized to GAPDH and expressed as fold changes (as described under Results) relative to vehicle control (mRNA of vehicle control divided by vehicle control was assigned the number 1 and is shown as a dotted line). Data reported as mean ± SE. VC: Vehicle Control (exposed to acetone and treated with 30% Pluronic F-127 in PBS); NM: NM-exposed; NM+As: NM-exposed treated with Cx43 asODN. $^{\#}$ $p < 0.05$ (NM vs. VC); * $p < 0.05$ (NM+As *vs* NM).

A. IL-6

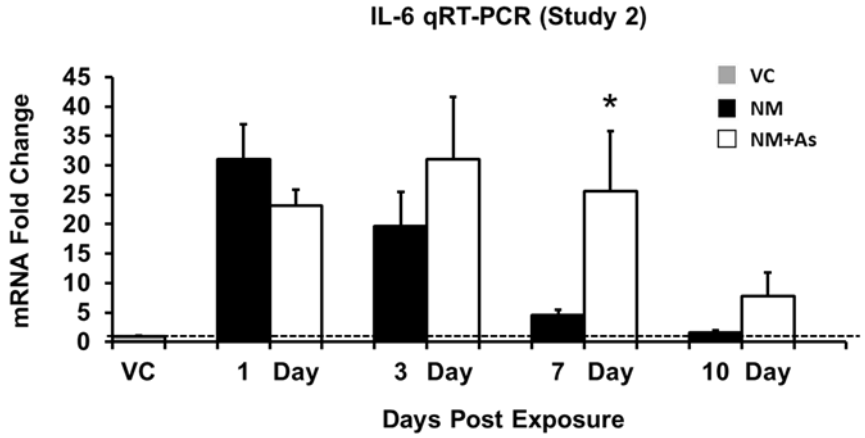

B. IL-1B

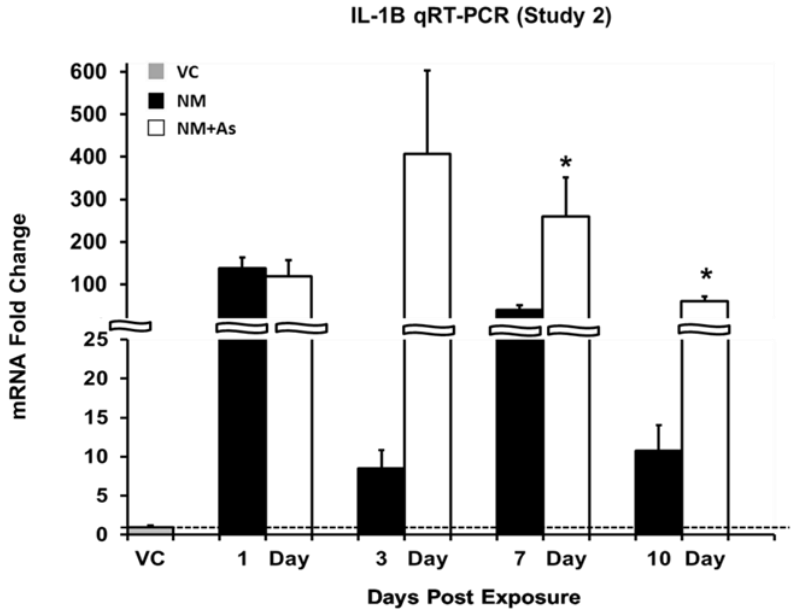

C. IL-10

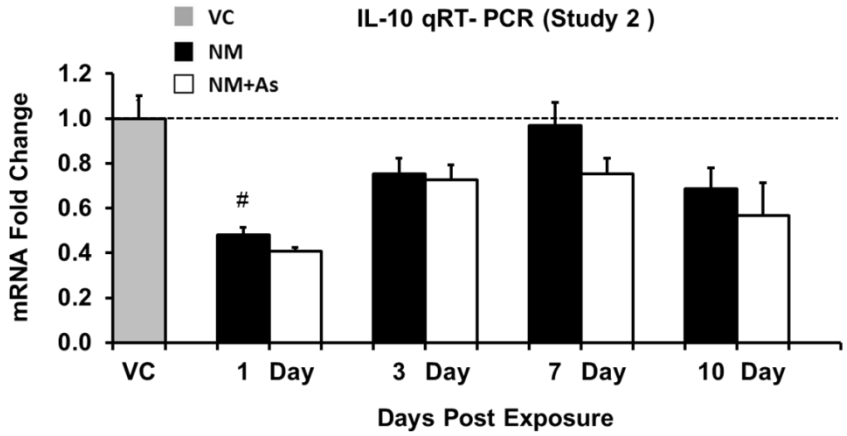

D. COX-2

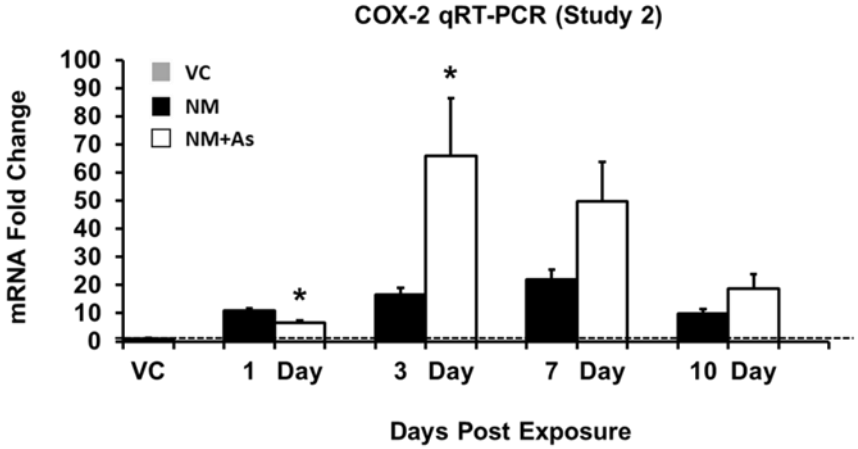

E. PGES-2

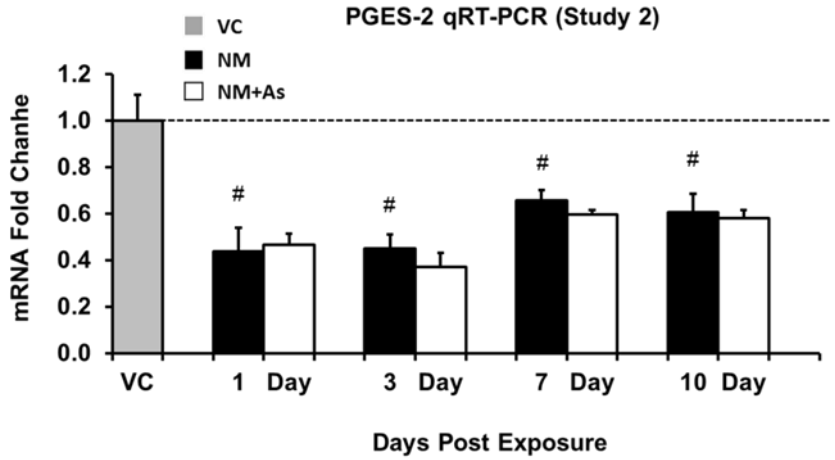

5.2. qRT-PCR Analysis of Biomarkers of the Remodeling Phase of Wound Healing (MMP-2, MMP-9 and MMP-12) in NM-Exposed Mouse Skin

To evaluate the effects of Cx43 asODN on biomarkers of the remodeling phase of wound healing (MMP-2, MMP-9 and MMP-12) in NM-exposed mouse skin, the mRNA expression of MMP-2, MMP-9, and MMP-12 were determined by qRT-PCR analysis from biopsies. The effect of Cx43 asODN was determined by comparing the data from NM exposed skin with that of NM exposed treated with Cx43 asODN. Presented are the results from Study 2. Appendix D contains the results of qRT-PCR analysis from Study 1.

5.2.1. qRT-PCR Analysis of MMP-2

MMP-2 mRNA was not produced at day 1 and day 3 after NM exposure but was upregulated at day 7 (mRNA fold change was 7) and day 10 (mRNA fold change was 5) compared to the vehicle control (Figure 19A).The peak level of MMP-2 mRNA was observed at day 7 after NM exposure. Cx43 asODN treatment increased MMP-2 mRNA levels slightly at days 7 and 10, but the differences were not significant.

5.2.2. qRT-PCR Analysis of MMP-9

qRT-PCR analysis of NM-exposed mouse skin showed MMP-9 mRNA levels were minimally synthesized at day 1 and day 3 but were upregulated at day 7 (mRNA fold change = 3.5) and day 10 (mRNA fold change = 1.7) (Figure 19B) indicating the MMP-9 mRNA peaked at day 7 but was halved by day 10 post NM exposure. Cx43 asODN treatment after NM exposure resulted in a minor difference in MMP-9 mRNA expression for day 10 (mRNA fold change was 2). The data suggest that Cx43 asODN has no significant influence on MMP-9 mRNA expression.

5.2.3. qRT-PCR Analysis of MMP-12

MMP-12 has been suggested to help macrophage migration through the epidermal and vascular basement membranes in inflammatory skin diseases (Vaalamo et al., 1999).

Therefore, the enzyme could play a role in healing of mustard exposure. The analysis of NM-exposed mouse skin showed MMP-12 mRNA was expressed at a level lower than vehicle control mouse skin at days 1 and 3 which is consistent with MMP-2 and MMP-9 data. No published data regarding MMP12 mRNA level from incisional/excisional and SM wounds are available for comparison. The levels were greater than vehicle control levels by days 7 and 10 (Figure 19C). However, Cx43 asODN treatment resulted in no significant change of the MMP-12 mRNA levels after NM exposure.

5.3. Results Summary for Specific Aim 3

After NM exposure, the mRNA levels of inflammation biomarkers IL-6, IL-1B, and COX-2 were upregulated within 24 hr and remained upregulated throughout study time points. In contrast, after exposure to NM, the mRNA of IL-10, an anti-inflammatory cytokine, and PGES-2 were downregulated at all time points studied. The mRNA levels of biomarkers for the remodeling phase of wound healing, MMP-2, MMP-9 and MMP-12 were upregulated at later time points, day 7 and day 10 after NM exposure.

When Cx43 antisense treatment was applied after NM exposure, the mRNA level of COX-2 at day 1 was significantly reduced. In addition, at day 1, the IL-6 and IL-1B mRNA levels in the NM exposed, Cx43 asODN treated group did not exceed that of NM-exposed samples. The treatment with Cx43 asODN at 3, 7, and 10 day post NM exposure resulted in further upregulation of IL-1B, IL-6 and COX-2. In contrast, the treatment with Cx43 asODN had no significant influence on the mRNA levels of IL-10 and PGES-2. In addition, Cx43 asODN treatment resulted in no significant changes of the mRNA levels of MMP-2, MMP-9 and MMP-12, suggesting Cx43 asODN treatment has no significant effect on these biomarkers of wound healing in NM-exposed mouse skin.

Figure 19. Effects of Cx43 asODN on mRNA expression levels of biomarkers of the remodeling phase of wound healing MMP-2, MMP-9 and MMP-12. qRT-PCR analyses of MMP-2 (A), MMP-9 (B), and MMP-12 (C) gene expression of skin biopsy samples were performed following exposure of 5 μmoles of NM (in acetone) to SKH-1 mouse skin and treated with 0.15 nmoles of Cx43 asODN (30% Pluronic F-127 in PB) for 1, 3, 7, 10 days post exposure as described for Study 2 in Materials and Methods. mRNA expression of MMPs was normalized to GAPDH and expressed as fold changes (as described under Results) relative to vehicle control (mRNA of vehicle control divided by vehicle control was assigned the number 1 and is shown as a dotted line). Data reported as mean ± SE. VC: Vehicle Control (exposed to acetone and treated with 30% Pluronic F-127 in PBS); NM: NM-exposed; NM+As: NM-exposed treated with Cx43 asODN. # $p < 0.05$ (NM vs. VC); * $p < 0.05$ (NM+As *vs* NM).

A. MMP-2

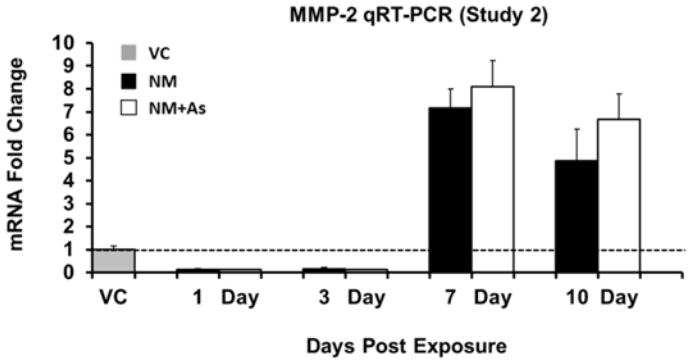

B. **MMP-9**

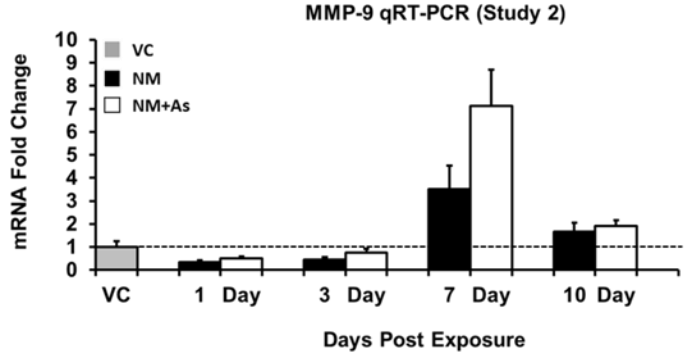

C. MMP-12

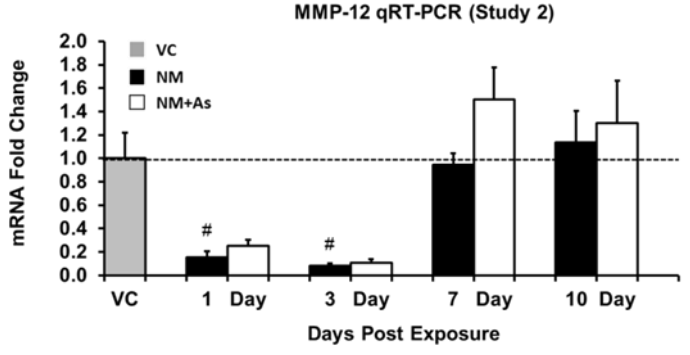

Discussion

1. NM Injury in the SKH-1 Hairless Mouse Model Compared to SM Injury in the SKH-1 Hairless Mouse and the CD-1 Mouse Ear: Macroscopic Appearance and Histology.

The present studies showed that the skin injury caused by NM exposure using the SKH-1 hairless mouse dorsal skin model resembles the injury induced by SM in the SKH-1 hairless mouse dorsal skin model (Joseph et al., 2011; Vallet et al., 2011, Dorandeu et al., 2011). It is also consistent with the injury induced by SM in the CD-1 Mouse Ear Vesicant Model (MEVM) (Casillas, et al., 1997; Shakarjian et al., 2006). Our endpoints for vesicant action comparison were the macroscopic appearance (erythema, edema and scab), the histology of skin biopsies (separation of epidermis from dermis, shedding and thickening of stratum corneum, hyperplasia and increased numbers of inflammatory cells over time after NM exposure), and the upregulation of mRNA for inflammation and wound remodeling biomarkers, IL-1B, IL-6, COX-2 and MMP-9.

In our studies, lesions to the dorsal skin were observed in mice for days 1, 3, 7 and 10 post exposure to 5 μmole NM. The macroscopic appearance showed erythema and edema of the skin at day 1 and scab formation (necrotic brown lesions) was seen at day 3. Necrotic brown lesions became severe at day 7. After 10 days, the scab appeared to be desicated and the skin appeared more fragile and showed signs of flaking (Figure 9). Our data are comparable to the macroscopic appearance reported by Dorandeu et al. (2011) for exposing SKH-1 mouse dorsal skin (0.28 cm^2) with 2 μl neat liquid SM (2.54 mg, purity >95%). The Dorandeu mice were kept under observation for up to 30 days and showed that erythema developed quickly after the SM exposure. At day 1, the skin was brownish in color. At day 2, necrosis was seen. After 3 days, necrosis became very severe and the skin was severely depressed being thinner than the original surface. Even after 30 days, a severe full thickness

burn was present. None of the mice died from their exposure conditions (Dorandeu et al., 2011).

Edema was also observed in the SKH-1 hairless mouse dorsal skin model post SM exposure (Dorandeu et al., 2011). A significant 200% increase in the biopsy weights, expressed as % of control, was reported 3 days after the exposure to1 µl liquid SM (Dorandeu et al., 2011). This is the only time point for the 1 µl exposure appearing in the report. SM-induced edema was also reported in the CD-1 Mouse Ear Vesicant Model (Shakarjian et al., 2006). Significant increases were observed in the percent relative ear skin weight of punch biopsies exposed to SM (0.08 mg in methylene chloride) assessed at 6 hr (29%), 12 hr (135%), 1 day (169%) and 3 day (207%) post-exposure (Shakarjian et al., 2006). Edema in our NM-exposed SKH-1 mice showed similar increases. In our studies, significant increases were observed in the % relative skin weight in NM-exposed punch biopsies at day 1 (276%), day 3 (117%), day 7 (103%) and day 10 (69%) (Table 3). NM-induced edema was greatest at 1 day, while SM edema was greatest at 3 days. This effect is the apparent result of replacing the nitrogen with sulfur atom.

Lesions to the dorsal skin were observed histologically in our NM-exposed mice for days 1, 3, 7 and 10 (Figure 10). At day 1, shedding of the stratum corneum and separation of the epidermis from the dermis was observed. After 3 days, epidermal hyperplasia was noted. At day 7, an eschar (scab) formed in the epidermis and there were more inflammatory cells in the dermis. At day 10, hyperplasia and thickening of the stratum corneum were observed. Increased numbers of inflammatory cells appeared in the dermis (Figures 10 and 15), indicating inflammation of the skin following NM exposure. The aforementioned histologic data from our studies are comparable with the findings from Joseph et al. (2011), which studied SM-induced lesions on SKH-1 mouse dorsal skin after the exposure (vapor form, 10 µl neat SM, 1.4 g/m^3 for 6 min). In Joseph et al. study, full thickness skin punch biopsies

were collected at days 1, 3, 7 and 14 post-exposure. The major difference in the study design between this study and ours was that we applied NM dissolved in a vehicle. Joseph et al. found that, after 1 day, SM exposure resulted in epidermal thinning, stratum corneum shedding and neutrophil accumulation in the dermis. At day 3, loss of epidermal structures was observed (the stratum spinosum and the granular layer were indistinguishable). After 7 days, hyperplasia was noted. At day 14, epidermal regeneration with extensive hyperplasia was observed (Joseph et al., 2011). In addition, the report from Dorandeu et al. (2011) showed similar H&E data 3 days post-exposure of SKH-1 mice dorsal skin injured with liquid SM. Biopsies were collected at 6 hr, 3, 9 and 30 days post exposure for histological analysis but as mentioned the only H&E data shown in their report was from 3 days post exposure. Erosion of the epidermis, global necrosis of the superior dermis, the deterioration of cell adhesion in the tissue, massive infiltration of neutrophils and separation of epidermis and dermis causing blisters were seen (Dorandeu et al., 2011), similar to our NM exposure model.

2. Effects of NM Injury in the SKH-1 Hairless Mouse on mRNA Levels of Inflammatory Biomarkers IL-6, IL-1B, COX-2 and a Remodeling Phase Biomarker, MMP-9.

In our study, the mRNA expression levels for inflammation biomarkers IL-6, IL-1B and COX-2 and a biomarker of the remodeling phase of wound healing, MMP-9 were altered, also indicating that NM exposure impacted these. NM exposure resulted in upregulation of mRNA levels of IL-6, IL-1B and COX-2 (Figures 11A, 11B and 11C). Up-regulation of IL-6 and IL-1B mRNAs by NM from day 1 to day 10 (Figures 11A and 11B) is similar to that observed in the SKH-1 mouse dorsal skin exposed to SM vapor (Vallet et al., 2011). In this SM exposure study (8 min, ~0.5 cm^2 from 10 μl liquid SM), samples were collected at 6 hr, 1, 2, 3, 4, 7, 14 and 21 days post exposure for analysis. It was found that IL-1B and IL-6 mRNA

levels increased as early as 6 hr (the first time point tested) and remained upregulated for 14 days. The mRNA levels of IL-6 also peaked at 6 hr post exposure. While our study's first measurement was at day 1 post exposure, our data agrees with theirs. Further support of NM causing a similar injury phenotype as SM comes from a weanling pig skin model (exposure with SM vapor, 10 µl of 1.27 g/mL for 15 min). Saborin et al. (2002) found IL-1B and IL-6 mRNA levels increased at 3, 6, 24, 48 and 72 hr post SM exposure, which is also consistent with our findings. Furthermore, we saw a trend in the upregulation of COX-2 mRNA levels from day1 to day 7 before they returned to day 1 levels on day 10 (Figure 11C). This trend is comparable to the immunohistochemistry (IHC) staining of COX-2 protein in SM-exposed dorsal skin in SKH-1 mice (Joseph et al., 2011). It was found that at day 1, COX-2 was expressed by basal keratinocytes. At day 3, increased COX-2 was identified in inflammatory cells at the dermal/epidermal boundary. At day 7, there was increased expression of COX-2 at the dermal/epidermal boundary but at day 14 the expression was reduced (Joseph et al., 2011). A literature search revealed no other publications regarding the analysis of COX-2 mRNA in SM exposed animals.

Finally, our study's upregulation of MMP-9 mRNA at days 7 and 10 after NM exposure (Figure 12B) is similar to all the previously mentioned SM exposure studies (Vallet et al., 2011; Sabourin et al., 2002; Shakarjian et al., 2006). Vallet et al., (2011) found MMP-9 mRNA still upregulated at day 7 in SM-exposed mice dorsal skin. Sabourin et al. (2002) reported that the production of MMP-9 mRNA increased from 24 to 72 hr (the last time point studied) post SM exposure in weanling pig skin. Shakarjian et al. (2006) investigated the expression of MMP-9 mRNA in SM-exposed mouse ear skin and found a 27 fold increase in expression of MMP-9 mRNA at 168 hr (7 days) post SM exposure.

In summary, our data demonstrate that NM produces injury analogous to SM, with significant time-dependent changes in edema and histopathological features, including severe inflammation and separation of the dermis from the epidermis. Both agents cause the prolonged presence of inflammatory cells. IL-1B, IL-6 and MMP-9 are significantly increased from both exposures as determined by qRT-PCR. Both mustards induced significant hyperplasia at day 7 post exposure. Taken together, our data suggests that the lesions on SKH-1 dorsal skin due to NM exposure are comparable to the skin damage reported for SM exposure of both the MVEM and SKH-1 mouse skin models.

3. Effects of NM Exposure on Gap Junction Proteins Cx43, Cx26 and Cx30 in SKH-1 Mouse Skin.

By employing the SKH-1 mouse dorsal skin model to study NM-induced skin injury, we demonstrated that Cx43 mRNA was downregulated by NM exposure (Figure 16A), similar to what normally occurs in nondiabetic incisional and excisional wounds in mice (Mori et al., 2006). This was a surprise since the healing of both NM chemical burn injuries and diabetic wounds are prolonged, but Cx43 is upregulated in a rat diabetic wound model (Wang et al., 2007) opposite of NM injury. In contrast, Cx26 and Cx30 are upregulated in all these wound models, including NM chemical burn injuries (Figures 16B and 16C), incisional/excisional wounds, and diabetic wounds (Brandner et al., 2004; Coutinho et al., 2003; Goliger and Paul, 1995; Mori et al., 2006). Our findings from NM-induced skin injuries are consistent with studies reported in the literature indicating that there is a downregulation of Cx43 and an upregulation of Cx26 and Cx30 in keratinocytes at wound edges after injury in rodents (Brandner et al., 2004, Coutinho et al., 2003, Goliger and Paul, 1995, Mori et al., 2006). The Cx26 and Cx30 are then downregulated to normal levels within the epidermis after wound closure. As for Cx43, its expression returns to normal levels as the epidermis regains its characteristic laminar architecture (Brandner et al., 2004). This

modulation of individual connexins levels appears to be a generalized phenomenon of wound repair in non-diabetic wounds, despite the cause of injury. The alteration in connexins levels may modulate the timing of release of signaling molecules necessary for wound closure. Coutinho et al. (2003) reported that both Cx26 and Cx30 are dramatically upregulated at 1–2 day post wounding and are preferentially in the migrating leading edge. They speculated that this increase of Cx26 and Cx30 might be necessary for the synchronized movement of the leading edge keratinocytes during migration. While the specific signaling molecules mediated by Cx43, Cx26 and Cx30 remain poorly understood, the phenomenon suggests that changes in levels and/or properties of Cx43, Cx26 and Cx30 might be necessary for effective wound closure. The data presented here are consistent with the idea that Cx43, Cx26 and Cx30 play important roles in the wound healing of NM-induced skin injuries. Downregulation of Cx43 in NM-exposed mouse skin was found by both qRT-PCR (Figure 16A) and Western Blot (Figure 17A) analysis.

4. Effects of Cx43 asODN on NM-Induced Skin Injury

Cx43 asODN downregulated the Cx43 mRNA levels (Figure 16A), and facilitated the healing process after NM exposure (Figures 14 and 15), as observed in both diabetic wounds in rats and incisional/excisional wounds in mice treated with Cx43 asODN (Qiu et al., 2003; Mori et al., 2006; Wang et al., 2004). The expression of Cx43 protein was reduced and the healing rate was improved after Cx43 asODN treatment in all wound healing models discussed. Also, we found the mRNA levels of Cx26 and Cx30 were significantly reduced by Cx43 asODN (Figures 16B and 16C), indicating that treatment with Cx43 asODN in some way regulates Cx26 and Cx30 mRNAs, perhaps by base pairing with an area homologous in the three connexin RNAs. A literature search revealed no other publications regarding the analysis of mRNA or protein of Cx26 and Cx30 after the treatment of wounds with Cx43

asODN. Therefore, this is the first report regarding the reduction of the mRNA levels of Cx26 and Cx30 by Cx43 asODN. In addition, the Cx43 asODN we used in the studies is a custom-made material, which has the same sequence as Cx43 asODN used by Qiu et al. (2003). However, the analytical data, particularly the cross reactivity testing of Cx43 asODN with Cx43, Cx26 and Cx30 is not available from the vendor. The Basic Local Alignment Search Tool (BLAST®) is a program provided by the National Center for Biotechnology Information (NCBI) capable of finding regions of local similarity between sequences of nucleotide or protein. A search using this program for regions of sequence similarity between Cx43, Cx26, and Cx30 mRNA was performed. Significant alignment was found in the 5' end of the mRNAs, but no region homologous to the 3' end of Cx43 where the Cx43 asODN binds was found in Cx26 and Cx30 mRNAs. Therefore, it is not likely that base pairing with a homologous area in the three connexins (Cx43, Cx26 and Cx30) play a role in the cross-reactivity of downregulation of Cx26 and Cx30 with the Cx43 asODN. The protein sequences of Cx43, Cx26 and Cx30 were also aligned (Table 4), and the dissimilarity further supported the assertion that the Cx43 asODN does not directly reduce Cx26 and Cx30 levels. With no homology in the 3' end nucleotides nor the carboxyl region amino acids, it can only be concluded that the mechanism(s) for how Cx43 asODN treatment affects levels of Cx26 and Cx30 mRNA is not direct. It is apparently an as yet unidentified effect that occurs downstream of the reduction in Cx26 and Cx30 by the Cx43 asODN.

Table 4. Alignment of Cx43, Cx26 and Cx30 Proteins. The protein sequences of Cx43, Cx26 and Cx30 in the mouse are aligned using the Basic Local Alignment Search Tool (BLAST®). The area corresponding to the antisense Cx43 asODN is shown in blue.

```
CX43     1 MGDWSALGKL LDKVQAYSTA GGKVWLSVLF IFRILLLGTA VESAWGDEQS AFRCNTQQPG
CX26       M DWGTLQSI LGGVNKHSTS IGKIWLTVLF IFRIMILVVA AKEVWGDEQA DFVCNTLQPG
CX30       M DWGTLHTVI GGVNKHSTSI GKVWITVIF IFRVMILVVA AQEVWGDEQE DFVCNTLQPG

CX43    61 CENVCYDKSF PISHVRFWVL QIIFVSVPTL LYLAHVFYVM RKEEKLNKKE EELKVAQTDG
CX26       CKNVCYDHYF PISHIRLWAL QLIMVSTPAL LVAMHVAY-R RHEKKRKFMK GEIKNEFKDI
CS30       CKNVCYDHFF PVSHIRLWAL QLIFVSTPAL LVAMHVAYYR -HETARKFIR GEKRNEFKDL

CX43   121 VNVEMHLKQI EIKKFKYGIE EHGKVKMRGG LL  RTYIISIL FKSVFEVAFL LIQWYIYGFS
CX26       EEIKTQKVRI         EG SLWWTYTTSIF FRVIFEAVFMYVFYIMYNGFF
CX30       EDIKRQKVRI            EGSL       WWTYTSSIF FRIIFEAAFMYVFYFLYNGYH

CX43   181 LSAVYTCKRD PCPHQVDCFL SRPTEKTIFI IFMLVVSLVS LALNIIELFY VFFKGVKDRV
CX26       MQRLVKCNAW PCPNTVDCFI SRPTEKTVFT VFMISVSGIC ILLNITELCY LFIRY
CX30       LPWVLKCG IDPCPNLVDCFI SRPTEKTVFT VFMISASVIC MLLNVAELCY LLLKLCFR

CX43   241 KGRSDPYHAT TGPLSPSKDC GSPKYAYFNG CSSPTAPLSP MSPPGYKLVT GDRNNSSCRN
CX26                          CSGKSKRPV
CX30

CX43   301 YNKQASEQNW ANYSAEQNRM GQAGSTISNS HAQPFDFPDD SQNAKKVAAG HELQPLAIVD
CX26
CX36                                                  QN         EMNEL ISD

CX43   361 QRPSSRASSR ASSRPRPDDL EI
CX26
CX30          SGQNAITSFPS
```

However, Langlois et al. (2007) used RNA-mediated interference knockdown in a rat epidermal keratinocyte cell line to reduce the protein level of Cx43 and observed that when Cx43 expression was knocked down by 50–75% there was a coordinate 55–65% reduction in Cx26 protein level. They concluded that Cx43 and Cx26 collectively co-regulate epidermal differentiation from basal keratinocytes but only play a minimal role in the maintenance of established epidermis (Langlois et al., 2007). Therefore, reduction of Cx26 mRNA level by Cx43 asODN as observed in the current studies could be due to a similar collective co-regulation effect of Cx43 and Cx26 in epidermal differentiation post-NM exposure. In our case, antisense technology was used to reduce Cx43 levels. Since Cx26 and Cx30 are closely homologous (Richard, 2000), it is likely that Cx30 mRNA was reduced by Cx43 asODN through the same mechanism as Cx26 was reduced. Further work is required to understand the interplay between Cx43 asODN treatment and the mRNA levels of Cx26 and Cx30.

Pathways involved in the enhancement of wound healing by down regulation of Cx43 have been discussed for the incisional/excisional and diabetes skin wound models (Mori et al., 2006; Qiu et al., 2003; Bajpai et al., 2009). In brief, treatment of a wound with Cx43 asODN resulted in decreasing macrophage and neutrophil infiltration, decreasing inflammatory markers (CCL-2 and TNF-α), increasing the rate of re-epithelialization, increasing growth factor production, increasing keratinocyte proliferation and increasing wound repair molecule (TGF-β1) and collagen I α1 (Bajpai et al., 2009). Since the mRNA levels of Cx26 and Cx30 were reduced toward their basal levels with Cx43 asODN treatment as observed in our studies, theoretically, these reductions may enhance wound healing as well. The reason for the upregulation of Cx26 and Cx30 mRNA levels during the initial wound healing response remains unclear. However, studies suggest that Cx26 and Cx30 may control wound healing by regulating keratinocyte proliferation, differentiation and/or migration in mice (Coutinho

et.al., 2003). Based on our data, the further downegulation of Cx43 by Cx43 asODN resulted in the reduction of inflammation after NM exposure and is likely associated with the reduction of inflammatory cells infiltration. Indeed, Cx43 is expressed by most immunocompetent cells, including neutrophils, mast cells, macrophages, and lymphocytes. Increased expression of Cx43 has been reported to be associated with increased levels of various inflammatory and immunomodulatory molecules like IL-1 and IL-6 in co-cultured endothelial cells and smooth muscle cells in humans (Bajpai et al., 2009). In the inflammation phase of wound healing, production of various cytokines is required. Cytokines can affect gap junctional intercellular communication in various cells and tissues. It is likely that these cytokines may also influence connexins in cutaneous wound healing in humans (Brandner et al., 2004). Cx43 was found expressed on the surface of activated immune cells that mediate the inflammatory response (Oviedo-Orta and Howard, 2004) and in rabbits on blood vessels that carry inflammatory cells to wound sites (Chaytor et al., 1998). Coutinho et al. (2003) reported that in mice, the downregulation of Cx43 might result in the reduction of the vascular response to injury, which in turn alters the number and distribution of inflammatory cells reaching the wound and accelerating wound closure. The aforementioned literature provides possible venues by which connexins affect the inflammation that we observed in NM-induced injuries.

As previously mentioned, Mori et al. and Qiu et al. reported that the immediate downregulation of Cx43 in epidermis and dermis with a single topical Cx43 asODN treatment resulted in accelerated wound healing in both incisional, excisional and burn skin wounds in mice (Mori et al., 2006, Qiu et al., 2003). A similar Cx43 asODN effect was seen in STZ (streptozotocin)-induced diabetic wounds in rats (Wang et al., 2007). However, after NM injury we observed a significant reduction of the level of Cx43 mRNA by Cx43 asODN treatment after 7 days, not at 1 day after treatment (Figure D2 of Appendix D, Figure 16A).

Qiu et al. reported that a single topical application of Cx43 asODN in a gel delivery system resulted in a transient downregulation of Cx43 protein levels in and around the wound within 2 hr and that the levels recovered after 24 hr (Qiu et al., 2003). Similarly, Mori et al. found that a significant reduction of Cx43 expression occurred 1 day after the treatment of excisional wounds with Cx43 asODN (Mori et al., 2006). In this report, the expression levels of Cx43 at day 7 were similar between the treated and untreated groups. After an excisional wound was made in STZ- induced diabetic rats, Cx43 protein levels dramatically increased in the cells of the epidermal leading edge. This may be one of the reasons for delayed healing of the diabetic wounds (Wang et al., 2007). However, a single topical application of Cx43 asODN gel resulted in a transient downregulation of Cx43 protein levels and improved the healing process to near normal skin (Wang et al., 2007, Brandner et al., 2004). In our study, a rapid effect from Cx43 asODN treatment on Cx43 mRNA on day 1 after NM exposure was not observed. However, significant downregulation of Cx43 was found at day 3 and day 7. This observation of reduction of Cx43 mRNA at day 7 suggests that, with Cx43 asODN treatment of NM-induced wounds, the onset of the effect of Cx43 asODN maybe delayed and the duration of the effect of Cx43 asODN could be longer. This delay in reduction of Cx43 at days 3 and 7 by Cx43 asODN could be due to the delayed onset of the injury (latency period) from NM exposure when compared to incisional and excisional skin wounds. Thus, the healing process and/or the time course for the treatment of NM injury with Cx43 asODN may not exactly follow the healing of incisional/excisional wounds treated with Cx43 asODN.

The patent for Pluronic F-127 (Poloxamer 407, PF-127) gel was approved in 1973. The adoption of the pluronic gel formulation is essential to enhance the delivery of Cx43 asODN to wounded tissue. Cx43 asODN is rapidly broken down (half-life 20–30 minutes) when it contacts cells or sera, so it can only act locally. Pluronic gel in the wound site provides a slow-release reservoir that can maintain delivery of active Cx43 asODN for

several hours (Becker et al., 1999). In addition, use of pluronic gel as a vehicle is deemed acceptable for delivery wound therapy (Becker et al., 1999). A sensitization of the skin with it has not been reported in the literature.

In our current pioneer trial using NM-exposed SKH-1 hairless mice, Cx43 asODN was applied once after the dorsal skin exposure. The application of multiple doses of Cx43 asODN and the application of combined Cx43 asODN, Cx26 asODN (when available) and Cx30 asODN (when available) may be beneficial for future work. In addition, though the opening or closure of gap junctional channels is controlled by gating mechanisms, including calcium ion concentration, pH, transjunctional membrane potential (voltage dependence), and protein phosphorylation, which can modulate channel permeability, the exact mechanism of how they regulate gap junctions remains not clear (Bajpai et al., 2009, Hervé and Derangeon, 2013). Therefore, it would be beneficial to conduct additional studies regarding the effects of Cx43 asODN in NM-exposed SKH-1 mice as suggested in the "Future Study" section.

The Cx43 asODN which we used in the current study has been registered as NEXAGON® by CoDa Therapeutics Inc., San Diego, California. As of September 12, 2013, a clinical Phase 2 study to investigate the safety and clinical effects of Nexagon® as a topical treatment for subjects suffering from diabetic foot ulcers (DUNE) is in progress. CoDa Therapeutics Inc. announced positive results from the Phase 2b clinical trial of Nexagon in patients with chronic venous leg ulcers in January 8, 2013. The study was conducted at the University of North Carolina Limb Salvage/Wound Healing Center. The company is preparing a manuscript for publication of the data in a peer-reviewed journal. The company also maintains that these results are sufficient to support advancing Nexagon into Phase 3 trials. These encouraging results support the idea that Cx43 asODN will be effective clinically for patients suffering from dermal SM injury. Our animal studies with positive

effects from the treatment of NM-exposed mice with Cx43 asODN are a step toward verifying Nexagon's efficacy for this indication.

In summary, our qRT-PCR data showed Cx43, Cx26, and Cx30 play roles during the healing of NM cutaneous injuries in our model similar to that reported for the incisional/excisional wound model. After injury, Cx43 is downregulared while Cx26 and Cx30 are upregulated. In addition, post exposure treatment with Cx43 asODN leads to attenuation of the mRNA for Cx43, Cx26, and Cx30. Together these connexins facilitate wound repair as demonstrated by the macroscopic and the histologic appearance of mice skin from the current studies.

5. The Role of Cellular Gap Junction Proteins and Communication in NM Injury and Wound Healing

Gap junctional intercellular communication is actively involved in almost the entire cellular life cycle of organism, from cell growth to cell death. Gap junction communication is the quickest and most direct intercellular communication pathway (Lampe et al., 2004; Sohl et al., 2005; Oyamada et al., 2005). Connexins in gap junctions play an essential role in tissue and organ homeostasis and in keratinocyte growth and differentiation (Di et al., 2001; Langlois et al., 2007). Thus, local cell-cell communication plays a significant regulatory role in wound repairs (Mori et al., 2006). Local injury causes a complex response for the healing of injured tissues, and cellular regeneration. The initiation, maintenance, and resolution of those responses require this cellular communication through gap junctions (Chanson et al., 2005). Therefore, it is rational that antisense Cx43 asODN plays important roles in the healing of injuries in NM-induced SKH-1 mice dorsal skin through affecting Cx43, Cx26, Cx30 levels.

The hundreds of gap junctions between cells provide a vast number of intercellular channels which play a crucial role in excitable cell contraction, embryonic development,

apoptosis, metabolic transport and morphogenesis in multicellular organisms (Oyamada et al., 2005; Cooper et al., 2002; Cameron et al., 2003; Burra et al., 2011; Wong et al., 2006). Apoptosis is involved in the regulation of wound healing (Greenhalgh, 1998) and is the most suitable method of down-regulating the cell number without causing tissue damage or inflammatory responses. Based on the literature, gap junctions are implicated in the maintenance and regulation of apoptosis. Therefore, gap junction proteins (connexins) might be able to transfer apoptotic signals to healthy cells and cause their death after NM exposure. On the other hand, since the application of Cx43 asODN facilitates wound healing, it is possible that connexins could transport cell survival molecules to dying cells. Currently, it is poorly understood what cell death or survival signaling molecules pass through gap junctions or are released via hemichannels. However, Ca^{2+}, pH and phosphorylation of Cx43 may be involved in this signaling. Ca^{2+} ions are likely to be involved in cell death because, in general, an increased calcium ion concentration and decreased pH result in closure of gap junction channels (Decrock et al., 2011). In diabetic wounds, the upregulation and opening of Cx43 gap junctional channels allows various apoptotic and inflammatory signals to pass through channels between cells and result in increased endothelial cell apoptosis and delayed wound contraction (Bajpai et al., 2009). Furthermore, decreased expression and phosphorylation of Cx43 by protein kinase C may inhibit the formation of gap junctions between cells, thereby blocking the passage of various inflammatory and apoptotic signals. This could lead to early healing of diabetic wounds (Bajpai et al., 2009). Thus, Ca^{2+}, pH, and phosphorylation of Cx43 are likely to play important roles in healing of NM-exposed mouse skin.

The histologic examination of tissue sections and macroscopic appearance of mouse skin indicated that Cx43 asODN reduced inflammatory cell infiltration, hyperplasia, thickening of the stratum corneum. This seemed to result in a faster rate of re-epithelization (Figures 14 and 15). It is known that neutrophils can produce and secret the pro-

inflammatory cytokine IL-1B (Matsukawa and Yoshinaga, 1999, Becker, 2009). The fact that hyperplasia was reduced after a single application of Cx43 asODN indicates that Cx43 plays a role in epithelial over-proliferation. The reduction in numbers and/or properties of Cx43, Cx26 and Cx30 by Cx43 asODN may reduce the transport of proliferation signals, thereby reducing the hyperplasia. Hyperplasia is a normal physiological response to injury. In normal wound healing, cell proliferation increases but it is still controlled by the regulatory mechanisms that prevent tumor formation (Kumar et al., 2007). Hyperplasia can be induced after the loss of large portions of the epidermis (Smith et al., 1997). In addition, it has been postulated that hyperplasia observed after exposure to SM might be due to inflammatory cytokines (e.g. IL-1B and IL-6) produced and secreted by keratinocytes (Arroyo et al., 2000; Vallet et al., 2011; Sidell and Hurst, 1997). Therefore, the reduction of inflammatory cell numbers (neutrophils) and the lessened hyperplasia observed in our studies correlates well with the attenuation of injury seen at days 1, 3, 7 and 10 in NM exposed skin treated with Cx43 asODN. Furthermore, the observation of the significant effects of Cx43 asODN treatment on the reduction of the pro-inflammatory cytokine IL-1B (day 1, Study 1, Appendix D, Figure D5), the increase of the anti-inflammatory cytokine, IL-10 (day 3 and day 7, Study 1, Appendix D, Figure D6) and the reduction of COX-2, the rate determining enzyme for the production of PGE-2 (day 1, Study 2, Figure 18D) further support the notion that Cx43 asODN treatment improves wound healing when used as a therapy after NM exposure.

Based on our data, the reduction of the mRNA levels of Cx43 and Cx26 at day 3 and day 7 and the reduction of Cx30 mRNA at day 3 after Cx43 asODN treatment is associated with the increase of anti-inflammatory cytokine IL-10 mRNA expression at day 3 and day 7 (Figures 16A, 16B, 16C, and Appendix D, Figures D2-D4, D6). In addition, the reduction of Cx26 and Cx30 mRNA at day 1 is associated with the reduction of COX-2 mRNA at day 1

(Figures 16B, 16C,18D and Appendix D, Figures D3-D4). The aforementioned data suggests that Cx43 asODN successfully reduced the protein level of Cx43, and the mRNA levels of Cx26 and Cx30. The resulting reductions in Cx43, Cx26 and Cx30 protein appear to improve healing of NM-induced injuries. Because the levels of Cx26 and Cx30 are extremely low in the unwounded epidermis but are elevated after wounding (Coutinho et.al., 2003), the reduction of Cx26 and Cx30 by Cx43 asODN toward normal levels likely also enhance the wound healing (Brandner et al., 2004, Coutinho et.al., 2003). Finally, since Cx26 and Cx30 were still highly upregulated on day 10 after exposure with NM, it is possible that a longer time may be needed for Cx26 and Cx30 to return to the unwounded low level after NM exposure, possibly explaining the phenomenon of delayed wound healing of mustard injuries. Therefore, in addition to connexin 43, connexins 26 and 30 may potentially be used as biomarkers for prolonged wound healing after NM exposure if a study time of 14 to 21 days is used to obtain their long term RNA level profile.

6. The Potential Reasons for Discrepancies in the qRT-PCR Analysis of Inflammatory and Remodeling Phase Biomarkers in Skin Biopsies

Data acquired from qRT-PCR analysis of mRNA of biomarkers were normalized to GAPDH expression and expressed as mRNA fold change relative to naïve (unexposed control) or vehicle controls (exposed to methylene chloride and treated with 30% Pluronic F-127 in PBS for Study 1) and (exposed to acetone and treated with 30% Pluronic F-127 in PBS for Study 2). In study 1, we found conspicuous differences in mRNA fold change between vehicle control and naïve control (mRNA fold change =1) in the analysis of Cx43, IL-10 and MMP-12 (Appendix A, Tables A1, A10 and A16). The mRNA fold change of vehicle control ranged 0.6 to 1.2 for Cx43, 0.7 to 2.3 for IL-10 and 0.8 to 1.8 for MMP-12 from day 1 to day 10. In Study 2, substantial differences between vehicle control and naïve control in the qRT-PCR analyses of Cx43, IL-10 and MMP-12 were still observed, in

addition to those of PGES-2, MMP-2 and MMP-9 in Study 2 (Appendix A, Tables A2, A11, A13-A15 and A17). The mRNA fold change of vehicle control ranged 1.1 to 1.9 for PGES-2, 1.4 to 1.7 for MMP-2 and 1.1 to 2.2 for MMP-9 from day 1 to day 10. Since both methylene chloride and acetone solvents showed a vehicle effect, it could be beneficial to consider trying other solvents (eg. DMSO) in any follow-up studies. In addition, although GAPDH is one of the most suitable reference genes, consideration of trying other reference genes (eg. a triplet of house keeping genes (peptidylprolyl isomerase (Ppia), ribosomal protein, large, P0 (Rplp0), and TATA-box binding protein (Tbp)) used by Vellet et al. (2011) might be helpful. Furthermore, many biological samples, particularly the solid tissue biopsies, may contain inhibitors or interfering factors for qRT-PCR analysis (Bustin et al. 2005). This may contribute to the discrepancy of qRT-PCR data acquired for IL-1B and IL-10 between Study 1 and Study 2. The high variation observed in the histology analysis might be due to the variation from the biopsy samples since both NM and Cx43 asODN were applied topically to the dorsal skin and the application might not have been perfectly uniform.

The aforementioned vehicle effect on qRT-PCR analysis of MMP-2 may account for the discrepancy between our data and the published literature. Our data show mRNA of MMP-2 was upregulated significantly at day 7 and day 10 compared to vehicle control (Figure 12A). However, the data published by Vallet et al., 2011, Sabourin et al., 2002, and Shakarjian et al., 2006 showed MMP-2 mRNA levels basically remained unchanged by SM exposure over the time period studied. Whether this is a vehicle effect could be addressed in the future. The other possibility leading to the discrepancy is that NM is less potent than SM, though histological data showed similar injuries to the skin; the degree of injury could be milder with NM exposure. Therefore, more MMP-2 could be produced in viable skin keratinocytes and secreted by epidermal cells at day 7 and day 10 (Nagase et al., 2006). The lower than vehicle control mRNA levels of MMP-2 and MMP-9 at day 1 and day 3 post NM

exposure observed in the current study could be due to the delayed inflammatory skin response by exposure with NM. A similar lower than control mRNA level of MMP-9 was observed 1 day after SM exposure in SKH-1 hairless mice skin (Vellet et al., 2011) and 3 and 6 hr post SM exposure in weanling pig skin (Sabourin et al., 2002).

Conclusion

In conclusion, the results of our studies indicate that NM-induced injury of mouse dorsal skin is comparable to sulfur mustard exposure of the previously established mouse dorsal skin model. In addition, our data reveal that Cx43, Cx26, and Cx30 play important roles in the healing of mustard injuries in mouse dorsal skin, similar to healing of incisional/excisional wounds. Finally, post exposure treatment with Cx43 asODN leads to reduction of Cx43, Cx26, and Cx30 and facilitates wound repair after NM-exposure.

Future Work

Perform Cx43, Cx26 and Cx30 IF (Immunofluorescence) histology to determine the location of these connexins in NM-exposed and Cx43 asODN treated mice skin.

Investigate the effect of Gap27, a potent, specific and reversible inhibitor of Cx43, to NM-exposed injuries in SKH-1 mice and compare to the data acquired from Cx43 asODN treatment studies. In addition, the model and method established from the current studies can be used to screen all other potential Cx43, Cx26 and Cx30 inhibitors.

Evaluate a better vehicle to minimize the potential vehicle effect, which may result in interference to qRT-PCR analysis of Cx43, IL-10, MMP2 and MMP-12 in mice skin biopsies found from our studies.

Investigate the effects of multiple doses of Cx43 asODN and compare to current single dose application for a better therapeutic regime.

Evaluate the optimal time interval between the exposure with NM and the application of Cx43 asODN to obtain the optimal efficacy.

Add more time points (eg. 12 hr, 14 days) to obtain a more complete concentration (level)-time profiles of Cx43, Cx26, Cx30 and other biomarkers involved in NM injuries.

Investigate the effects of Cx26 asODN and Cx30 asODN and the combinations of Cx43 asODN, Cx26 asODN and Cx30 asODN for the treatment of NM injuries. The combined therapy may enhance the healing rate by comparing to the single Cx43 asODN treatment.

Investigate the roles of Ca^{2+}, pH, and phosphorylation of Cx43 in healing of NM-exposed mouse skin.

References

Anumolu, S. S., Menjoge, A. R., Deshmukh, M., Gerecke, D., Stein, S., Laskin, J., Sinko, P. J. (2011). Doxycycline hydrogels with reversible disulfide crosslinks for dermal wound healing of mustard injuries. Biomaterials. 32 (4):1204-1217.

Anwar, A., Gu, M., Brady, S., Qamar, L., Behbakht, K., Shellman, Y. G., Agarwal, R., Norris, D. A., Horwitz, L. D., Fujita. M. (2008). Photoprotective effects of bucillamine against UV-induced damage in an SKH-1 hairless mouse model. Photochem. Photobiol. 84: 477-483.

Arroyo, C.M., Schafer, R. J., Kurt, E. M., Broomfield, C. A., Carmichael, A. J. (2000). Response of normal human keratinocytes to sulfur mustard: Cytokine release. J. Appl. Toxicol. 20:S63–S72.

Bajpai, S., Shukla, V. K., Tripathi, K., Srikrishna, S., Singh, R.K. (2009). Targeting connexin 43 in diabetic wound healing: Future perspectives. J Postgrad Med. 55(2):143-9.

Balali-Mood, M., Hefazi, M. (2005). The pharmacology, toxicology, and medical treatment of sulphur mustard poisoning. Fundam. Clin. Pharmacol. 19:297–315.

Balali-Mood, M., Hefazi, M. (2006). Comparison of early and late toxic effects of sulfur mustard in Iranian veterans. Basic Clin. Pharmacol. Toxicol. 99(4):273–282.

Becker, D. L., McGonnell, I., Makarenkova, H. P., Patel, K., Tickle, C., Lorimer, J., Green, C. R. (1999). Roles for alpha 1 connexin in morphogenesis of chick embryos revealed using a novel antisense approach. Dev. Genet. 24:33-42.

Becker, D. L. (2009). Accelerating wound repair by targeting connexin43 expression. European Dermatology. Touching briefings. 79-81.

Black, A.T., Joseph L.B., Casillas, R.P., Heck, D.E., Gerecke, D.R., Sinko, P.J., Laskin, D.L., Laskin, J.D. (2010). Role of MAP kinases in regulating expression of antioxidants and inflammatory mediators in mouse keratinocytes following exposure to the half mustard, 2-chloroethyl ethyl sulfide. Toxicology and Applied Pharmacology. 245:352–360.

Black, A.T., Hayden, P.J., Casillas, R.P., Heck, D.E., Gerecke, D.R., Sinko, P.J., Laskin, D.L., Laskin, J.D. (2010). Expression of proliferative and inflammatory markers in a full-thickness human skin equivalent following exposure to the model sulfur mustard vesicant, 2-chloroethyl ethyl sulfide. Toxicology and Applied Pharmacology. 249(2):178-187.

Blaha, M., Bowers, W. Jr., Kohl,J., DuBose, D., Walker, J., Alkhyyat, A., Wong, G. (2000). Effects of CEES on inflammatory mediators, Heat Shock Protein 70A, H J. Appl. Toxicol. 20: S101–S108.

Bradner, J.M, Houdek, P., Hu, S. B., Kaiser, C., Moll, I. (2004). Connexins 26, 30, and 43: Differences among spontaneous, chronic, and accelerated human wound healing. J Invest Dermatol. 122:1310-1320.

Brinkley, F. B., Mershon, M. M., Yaverbaum, S., Doxzon, B. F., and Wade, J. V. (1989). The mouse ear model as an in vivo bioassay for the assessment of topical mustard (HD) injury. In 1989 Medical Defense Bioscience Review, 15–17 August 1989, Aberdeen Proving Ground, MD, 595–602.

Burra, S., Jiang, J. X. (2011). Regulation of cellular function by connexin hemichannels. Int J Biochem Mol Biol. 2(2):119-128.

Bustin, S.A., Benes1, V., Nolan, T., Pfaffl, M.W. (2005). Quantitative real-time RT-PCR – a perspective. Journal of Molecular Endocrinology. 34:597–601.

Cameron, S.J., Malik S, Akaike M, Lerner-Marmarosh N, Yan C, Lee JD, Abe J, Yang J. (2003). Regulation of epidermal growth factor-induced connexin 43 gap junction communication by big mitogen-activated protein kinase 1/ERK5 but not ERK1/2 kinase activation. J. Biol. Chem. 278(20):18682-8.

Casillas, R. P., Mitcheltree, L. W., and Stemler, F. W. (1997). The mouse ear model of cutaneous sulfur mustard injury. Toxicol. Methods. 7:381–397.

Chanson, M., Derouette, J-P., Roth, I., Foglia, B., Scerri, I., Dudez, T., Kwak, B. R. (2005). Gap junctional communication in tissueinflammation and repair. Biochimica et Biophysica Acta. 1711:197–207.

Chaytor, A. T., Evans, W. H., Griffith, T. M. (1998). Central role of heterocellular gap junctional communication in endothelium-dependent relaxations of rabbit arteries. J. Physiol. 508:561-573.

Choung, Y-H., Park, K., Kang, S-O., Raynov, A.M., Kim, C.H., Choung, P-H. (2006). Expression of the gap junction proteins connexin 26 and connexin 43 in human middle ear cholesteatoma. Acta Otolaryngol. 126(2):138-43.

Cooper, C.D., Lampe, P.D. (2002). Casein kinase 1 regulates connexin-43 gap junction assembly. J. Biol. Chem. 277(47):44962-8.

Coulombe, P. A., Kerns, M. L., and Fuchs, E. (2009). Epidermolysis bullosa simplex: a paradigm for disorders of tissue fragility. J. Clin. Invest. 119:1784-1793.

Coutinho, P., Qiu, C., Frank, S., Tamber, K., Becker, D. (2003). Dynamic changes in connexin expression correlate with key events in the wound healing process. Cell Biology International. 27:525–541.

Crooke, S.T. (2000). Progress in antisense technology: the end of the beginning. Methods Enzymol. 313:3-45.

Dachir, S., Cohen, M., Fishbeine, E., Sahar, R., Brandies, R., Horwitz, V. (2010). Characterization of acute and long-term sulfur mustardinduced skin injuries in hairless guinea-pigs using non-invasive methods. Skin Res Technol. 6:114–124.

Dbouk, H.A., Mroue, R. M., El-Sabban, M. E., Talhouk, R. S. (2009). Connexins: a myriad of functions extending beyond assembly of gap junction channels. Cell Communication and Signaling. 7: 4.

Decrock, E., Vinken, M., Bol, M., D'Herde, K., Rogiers, V., Vandenabeele, P., Krysko, D. V., Bultynck, G., Leybaert, L. (2011). Calcium and connexin-based intercellular communication, a deadly catch? Cell Calcium. 50(3):310-21.

Di, W.L., Rugg, E.L., Leigh, I.M., Kelsell, D.P. (2001). Multiple epidermal connexins are expressed in different keratinocyte subpopulations including connexin 31. J Invest Dermatol. 117:958–64.

Dorandeu, F., Taysse, L, Boudry, I., Foquin, A., Hérodin, F., Mathieu, J. et al. (2011). Cutaneous challenge with chemical warfare agents in the SKH-1 hairless mouse. (I) Development of a model for screening studies in skin decontamination and protection. Hum Exp Toxicol. 30:470–490.

Enk, A. H., Katz, S. I. (1992). Identification and induction of keratinocyte-derived IL-10. J. Immunol. 149:92–95.

Ganesan, K., Raza, S. K., Vijayaraghavan, R. J. (2010). Chemical warfare agents. J Pharm Bioallied Sci. 2(3):166–178.

Ghabili, K., Agutter, P.S., Ghanei, M., Ansarin, K., Panahi, Y., Shoja, M.M. (2011). Sulfur mustard toxicity: History, chemistry, pharmacokinetics, and pharmacodynamics. Critical Reviews in Toxicology. 41(5): 384–403.

Goliger, J.A., Paul, D.L. (1995). Wounding alters epidermal connexin expression and gap junction-mediated intercellular communication. Mol Biol Cell. 6:1491-1501.

Goodenough, D., Paul, D.L. (2003). Beyond the gap: functions of unpaired connexon channels. Nature Reviews Molecular Cell Biology 4: 285-295.

Goodenough, D., Paul, D.L. (2009). Gap junctions. Cold Spring Harb Perspect Biol. 1:a002576.

Gordon, M.K., Desantis, A., Deshmukh, M. et al. (2010). Doxycycline hydrogels as a potential therapy for ocular vesicant injury. J. Ocul Pharmaco Ther. 26(5):407-19.

Grahama, J.S., Stevenson, R.S., Mitcheltree, L.W., Hamilton, T.A., Deckert, R.R., Lee, R. B., Schiavetta, A.M. (2009). Medical management of cutaneous sulfur mustard injuries. Toxicology. 263:47–58.

Greenhalgh, D.G. (1998). The role of apoptosis in wound healing. Int J Biochem cell Biol. 30(9):1019-30.

Hervé, J.C., Derangeon, M. (2013). Gap-junction-mediated cell-to-cell communication. Cell Tissue Res. 352:21-31.

Husøy, T., Helle, K. Knutsen, V._eronique Cruciani, Hege B. Ølstørn, Svein-Ole Mikalsen, Else Marit Løberg , Jan Alexander. (2005). Connexin43 is overexpressed in ApcMin/1-mice adenomas and colocalises with COX-2 in myofibroblasts. Int. J. Cancer, 116:351–358.

Ivarsson, U., Nilsson, H., Santesson, J. (1992). A FOA briefing book on chemical weapons: Threat, Effects, and Protection. Umeå: National Defence Research Establishment.

Joseph, L.B., Gerecke, D.R., Heck, D.E., Black, A.T., Sinko, P.J., Cervelli, J.A., Casillas, R.P., Babin, M.C., Laskin, D.L., Laskin, J.D. (2011). Structural changes in the skin of hairless mice following exposure to sulfur mustard correlate with inflammation and DNA damage. Exp Mol Pathol. 91(2):515-27.

Kehe, K., Balszuweit, F., Steinritz, D., Thiermann, H. (2009). Molecular toxicology of sulfur mustard-induced cutaneous inflammation and blistering. Toxicology. 263:12–19.

Kimura, K., Nishida, T. (2010). Role of the ubiquitin-proteasome pathway in downregulation of the gap-junction protein connexin43 by TNF-a in human corneal fibroblasts. Investigative Ophthalmology & Visual Science. 51:1943-1947.

Kretz, M., Euwens, C., Hombach, S., Eckardt, D., Teubner, B., Traub, O., Willecke, K., Ott, T. (2003). Altered connexin expression and wound healing in the epidermis of connexin-deficient mice. J. Cell. Sci. 116:3443– 3452.

Kuma, V., Abbas, A. K., Fausto, N., Mitchell, R., Eds. (2007). Robbins Basic pathology, 8th Ed. Chapter 1: Cell Injury, Cell Death and Adaptations. p. 4.

Laird, D. W. (2006). Life cycle of connexins in health and disease. Biochem. J. 394:527–543.

Lampe, P. D., Lau, A. F. (2004). The effects of connexin phosphorylation on gap junctional communication. Int. J. Biochem. Cell Biol. 36:1171–1186.

Langlois, S., Maher, A., Manias, J. L., Shao, Q., Kidder, G. M., Laird, D.W. (2007). Connexin levels regulate keratinocyte differentiation in the epidermis. J Biol Chem. 282(41):30171-80.

Lee, W. Y., Lockniskar, M. F., Fischer, S. M. (1994). Interleukin-1 alpha mediates phorbol ester-induced inflammation and epidermal hyperplasia. FASEB J. 8(13):1081-7.

Lindsay, C. D., Hambrook, J. L., Brown, R. F., Platt, J. C., Knight, R., and Rice, P. (2004). Examination of changes in connective tissue macromolecular components of large white pig skin following application of Lewisite vapour. J. Appl. Toxicol. 24:37–46.

Liu, X., Das, A.M., Seideman, J., Griswold, D., Afuh, C.N., Kobayashi, T., Abe, S., Fang, Q., Hashimoto, M., Kim, H., Wang, X., Shen, L., Kawasaki, S., and Rennard, S.I. (2007). The CC chemokine Ligand 2 (CCL2) mediates fibroblast survival through IL-6. Am J Respir Cell Mol Biol. 37:121–128.

Liu, Y., Min, D., Bolton, T., Nub'e, V., Twigg, S., Yue, D.K., Mclennan, S.V. (2009). Increased matrix metalloproteinase-9 predicts poor wound healing in diabetic foot ulcers. Diabetes Care. 32:117–119.

Marrs, T.C., Maynard, R.L., Sidell, F.R.. (1996). Chemical warfare agents: toxicology and treatment. John Wiley and Sons, Chichester, UK.

Matsukawa, A., Yoshinaga, M. (1999). Neutrophils as a source of cytokines in inflammation. (1999). Histol Histopathol. 14:511-516.

Matsuo, Y., Nomata, K., Eguchi, J., Aoki, D., Hayashi, T., Hishikawa, Y., Kanetake, H., Shibata, Y., Koji, T. (2007). Immunohistochemical analysis of connexin43 expression in infertile human testes. Acta Histochem. Cytochem. 40(3):69–75.

Matsushima, H., Ogawa, Y., Miyazaki, T., Tanaka, H., Nishibu, A., Takashima, A. (2010). Intravital imaging of IL-1b production in skin, Journal of Investigative Dermatology. 130:1571–1580.

Mendoza-Naranjo, A, Cormie, P., Serrano, A.E., Hu, R., O'Neill, S., et al. (2012). Targeting Cx43 and N-cadherin, which are abnormally upregulated in venous leg ulcers, influences migration, adhesion and activation of Rho GTPases. PLoS ONE 7(5): e37374. doi:10.1371/journal.pone.0037374

Meşe, G., Richard, G.,White, T. W. (2007). Gap Junctions: Basic Structure and Function. Journal of Investigative Dermatology. 127:2516–2524.

Monteiro-Riviere, N. A., Inman, A. O., Babin, M. C., Casillas, R. P. (1999). Immunohistochemical characterization of the basement membrane epitopes in bis(2-chloroethyl) sulfide-induced toxicity in mouse ear skin. J Appl Toxicol. 19(5):313-28.

Mori, R., Power, K. T., Wang, C. M., Martin, P., Becker, D. L. (2006). Acute downregulation of connexin43 at wound sites leads to a reduced inflammatory response, enhanced keratinocyte proliferation and wound fibroblast migration. J Cell Sci. 119:5193-5203.

Nagase, H., Visse, R., Murphy, G. (2006). Structure and function of matrix metalloproteinases and TIMPs. Cardiovascular Research. 69:562–573.

Nicholson, B.J. (2003). Gap junctions – from cell to molecule. J. Cell Sci. 116(22):479-81.

Nyska, A., Lomnitski, L., Maronpot, R., Moomaw, C., Brodsky, B., Sintov, A., Wormser, U. (2001). Effects of iodine on inducible nitric oxide synthase and cyclooxygenase-2 expression in sulfur mustard-induced skin. Arch. Toxicol. 74:768–774.

Ouyang, W., Rutz, S., Crellin, N. K., Valdez, P. A., Hymowitz, S. G. (2011). Regulation and functions of IL-10 family cytokines in inflammation and diseases. Ann. Rev. Immunol. 29: 71–109.

Oviedo-Orta, E., Howard, E. W. (2004). Gap junctions and connexin mediated communication in the immune system. Biochim Biophys Acta. 662:102-12.

Oyamada, M., Oyamada, Y., Takamatsu, T. (2005). Regulation of connexin expression. Biochimica et Biophysica Acta. 1719:6–23.

Qiu, C., Coutinho, P., Frank, S., Franke, S., Law, L-Y, Martin, P., Green, C. R., Becker, D. L. (2003). Targeting connexin 43 expression accelerates the rate of wound repair. Current Bioloy. 13:1697-1703.

Rapaport, E., Isiura, K., Agrawal, S., Zamecnik, P. (1992). Antimalarial activities of oligodeoxynucleotide phosphorothioates in chloroquine-resistant Plasmodium falciparum. PNAS. 89(18):8577-8580.

Reilly, D. M., Parslew, R., Sharpe, G. R., Powell, S., Green, M. R. (2000). Inflammatory mediators in normal, sensitive and diseased skin types. Acta Derm Venereol. 80:171-174.

Ricciotti, E., Garret, A., Fitz, G. (2011). Prostaglandins and Inflammation. Arterioscler Thromb Vasc Biol. 31:986-1000.

Richard G. (2000). Connexins: a connection with the skin. Exp Dermatol. 9:77–96.

Richard, G. (2005). Connexin disorders of the skin. Clin Dermatol. 23:23–32.

Richards, T.S. et al. (2004). Protein kinase C spatially and temporally regulates gap junctional communication duringhumanwoundrepair via phosphorylation of connexin43 on serine368. J. Cell Biol. 167:555–562.

Rikimaru, T., Nakamura, M., Yano, T., Beck, G., Habicht, G. S., Rennie, L. L., Widra, M., Hirshman, C. A., Boulay, M. G., Spannhake, E. W., et al. (1991). Mediators, initiating the inflammatory response, released in organ culture by full-thickness human skin explants exposed to the irritant, sulfur mustard. J. Invest. Dermatol. 96:888–897.

Sabourin, C. L. K., Danne, M. M., Buxton, K. L., Casillas, R. P., and Schlager, J. J. (2002). Cytokine, chemokine, and matrix metalloproteinase response after sulfur mustard injury to weanling pig skin. J. Biochem. Mol. Toxicol. 16:263–272.

Salmela, M.T., Pender, S., Reunala, T., MacDonald, T., Saarialho-Kere, U. (2001). Parallel expression of macrophage metalloelastase (MMP-12) in duodenal and skin lesions of patients with dermatitis herpetiformis. Gut. 48:496–502.

Salomon, D., Masgrau, E., Vischer, S., Ullrich, S., Dupont, E., Sappino, P. et al. (1994). Topography of mammalian connexins in human skin. J Invest Dermatol. 103:240–7.

Samuelsson, B., Morgenstern, R., Jakobsson, P-J. (2007). Membrane prostaglandin E synthase-1: A novel therapeutic target. Pharmacol Rev. 59(3):207-224.

Saonere, J.A. (2011). Antisense therapy, a magic bullet for the treatment of various diseases: Present and future prospects. Journal of Medical Genetics and Genomics. 3(5):77–83.

Scott, C. A., Tattersall, D., O'Toole, O. E., Kelsell, D. P. (2012). Connexins in epidermal homeostasis and skin disease. Biochimica et Biophysica Acta. 1818:1952–1961.

Shakarjian, M. P., Bhatt, P., Gordon, M. K., Chang, Y. C., Casbohm, S. L., Rudge, T. L., Kiser, R. C., Sabourin, C. L., Casillas, R. P., Ohman-Strickland, P., Riley, D. J., Gerecke, D.R. (2006). Preferential expression of matrix metalloproteinase-9 in mouse skin after sulfur mustard exposure. J Appl Toxicol. 26(3):239-46.

Shakarjian, M.P., Heck, D.E., Gray, J.P,, Sinko, P.J., Gordon, M.K., Casillas, R.P., et al. (2010). Mechanisms mediating the vesicant actions of sulfur mustard after cutaneous exposure. Toxicol Sci. 114(1):5–19.

Sharma, M., Vijayaraghavan, R., Ganesan, K. (2008). Comparison of toxicity of selected mustard agents by percutaneous and subcutaneous routes. Indian J. Exp. Biol. 46:822–830.

Sidell, F. R., Hurst, C. G. (1997). Long-term health effects of nerve agents and mustard. In Textbook of Military Medicine—Medical Aspects of Chemical and Biological Warfare (R. Zaitchuk and R. F. Bellamy, Eds.), pp. 229–246. Office of the Surgeon General, Department of the Army, Washington, DC.

Siller-Jackson, A.J., Burra, S., Gu, S., Xia, X., Bonewald, L. F., Sprague,E., Jean, X. (2008). Adaptation of connexin 43-hemichannel prostaglandin release to mechanical loading. J Biol Chem. 283(39):26374–26382.

Smith, K. J., Casillas, R., Graham, J., Skelton, H. G., Stemler, F., Hackley, B. E., Jr. (1997). Histopathologic features seen with different animal models following cutaneous sulfur mustard exposure. J. Dermatol. Sci. 14;126–135.

Smith, W. J., Dunn, M. A. (1991). Medical defense against blistering chemical warfare agents. Arch Dermatol. 127(8):1207-13.

Sohl, G., Willecke, K. (2003). An update on connexin genes and their nomenclature in mouse and man, Cell Commun. Adhes. 10:173–180.

Sohl, G., Maxeiner, S., Willecke, K. (2005). Expression and functions of neuronal gap junctions. Nat. Rev. Neurosci. 6(3):191-200.

Solberg, Y., Alcalay, M., Belkin, M. (1997). Ocular injury by mustard gas. Surv Ophthalmol. 41(6):461-6.

Stramer, B.M., Mori, R., Martin, P. (2007). The inflammation-fibrosis link ? A jekyll and hyde role for blood cells during wound repair. J. Investigative Dermatology.127:1009-1017

Tacheau, C., Laboureau, J., Mauviel, A., Verrecchia, F. (2008). TNF-alpha represses connexin43 expression in Hacat keratinocytes via activation of JNK signaling. J. Cell. Physiol. 216:438–444.

Tang, C., Tsai, C. (2012). CCL2 increases MMP-9 expression and cell motility in human chondrosarcoma cells via the Ras/Raf/MEK/ERK/NF-kB signaling pathway. Biochemical Pharmacology. 83:335–344.

Tewari-Singh, N., Rana, S., Gu, M., Pal, A., Orlicky, D. J., White, C. W., Agarwal, R. (2009). Inflammatory biomarkers of sulfur mustard analog 2-chloroethyl ethyl sulfide-induced skin injury in SKH-1 hairless mice. Toxicol. Sci. 108:194–206.

Uitto, J., Pulkkinen, L. (2001). Molecular genetics of heritable blistering disorders. Arch. Dermatol. 137:1458–1461.

Vaalamo, M., Kariniemi, A-L., Shapiro, S. D., Saarialho-Kere, U. (1999). Enhanced expression of human metalloelastase (MMP-12) in cutaneous granulomas and macrophage migration. Journal of Investigative Dermatology. 112:499–505.

Vallet, V., Poyot, T., Cléry-Barraud, C., Coulon,D., Sentenac, C., Peinnequin, A., Boudry, I. (2011). Acute and long-term transcriptional responses in sulfur mustard-exposed SKH-1 hairless mouse skin. Cutaneous and Ocular Toxicology. 1–10.

Wagner, C. (2008). Function of connexins in the renal circulation. Kidney International. 73: 547–555.

Wang, C. M., Lincoln, J., Cook, J.E., Becker, D.L. (2007). Abnormal connexin expression underlies delayed wound healing in diabetic skin. Diabetes. 56:2809–2817.

Werner, S., Grose, R. (2003). Regulation of wound healing by growth factors and cytokines. Physiol Rev. 83:835–870.

Wong, R.C., Dottori, M., Koh, K.L., Nguyen, L.T., Pera, M.F., Pebay, A. (2006). Gap junctions modulate apoptosis and colony growth of human embryonic stem cells maintained in a serum-free system. Biochem Biophys Res Commun. 344 (1):181-8.

Wormser, U., Langenbach, R., Peddada, S., Sintov, A., Brodsky, B., Nyska, A. (2004). Reduced sulfur mustard-induced skin toxicity in cyclooxygenase-2 knockout and celecoxib-treated mice. Toxicol. Appl. Pharmacol. 200:40–47.

Xue, S.-N., Lei, J., Yang, C., Lin, D-Z., Yan, L. (2012). The biological behaviors of rat dermal fibroblasts can be inhibited by high levels of MMP9. Experimental Diabetes Research. Volume 2012, Article ID 494579, 7 pages.

Zhang, Z., Peters, B. P., Monteiro-Riviere, N. A. (1995). Assessment of sulfur mustard interaction with basement membrane components. Cell Biol Toxicol. 11(2):89-101.

Appendix A

qRT-PCR analysis of Cx43, Cx26, Cx30 and Selected Inflammation and Remodeling Biomarkers from Study 1 and Study 2. Fold changes in mRNA at each time point were compared to unexposed naïve control.

Table A1. Mean fold changes versus days from qRT-PCR analysis of Cx43 (Study 1)

Mean Fold Changes (rQ = Cx43/GapDH fold change) vs. Days

Day	Naïve	MG	NM	sC	As
1	1	1.23795	0.52519	0.74342	0.40590^{*+}
3	1	0.97376	1.05305	0.63292	0.45647$^{+\#\wedge}$
7	1	0.59062	0.53137	0.30863	0.27764$^{*+\#}$
10	1	0.55695	0.43806	0.34528	0.33415^{*+}

MG-Vehicle control (Methylene Chloride/pluronic gel)
NM-Nitorgen mustard alone
sC-NM with sense control
As-NM with antisense
Naïve: Time 0

* As vs. Naïve (p< 0.05)
+ As vs. MG (p< 0.05)
# As vs. NM (p< 0.05)
^ As vs. sC (p< 0.05)

Figure A1: Mean fold changes versus days from qRT-PCR analysis of Cx43 (Study 1)

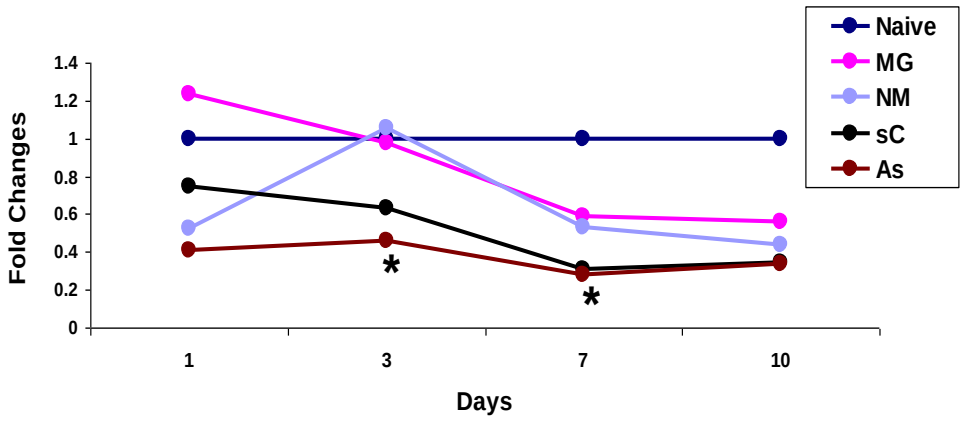

*** As vs. NM (p< 0.05)**

Table A2. Mean fold changes versus days from qRT-PCR analysis of Cx43 (Study 2)

Mean Fold Changes (rQ = Cx43/GapDH fold change) vs. Days

Day	Naïve	AG	NM	sC	As
1	1	1.49538	0.65324	0.80669	0.68425^{*+}
3	1	1.31103	0.91586	0.65685	0.59295$^{*+\#}$
7	1	1.14582	0.77328	0.98376	0.49600$^{*+\#\wedge}$
10	1	1.29435	1.11831	1.06007	0.89297^{+}

AG-Vehicle control (Acetone/pluronic gel)
NM-Nitorgen mustard alone
sC-NM with sense control
As-NM with antisense
Naïve: Time 0

* As vs. Naïve ($p< 0.05$)
$^{+}$ As vs. AG ($p< 0.05$)
$^{\#}$ As vs. NM ($p< 0.05$)
$^{\wedge}$ As vs. sC ($p< 0.05$)

Figure A2: Mean fold changes versus days from qRT-PCR analysis of Cx43 (Study 2)

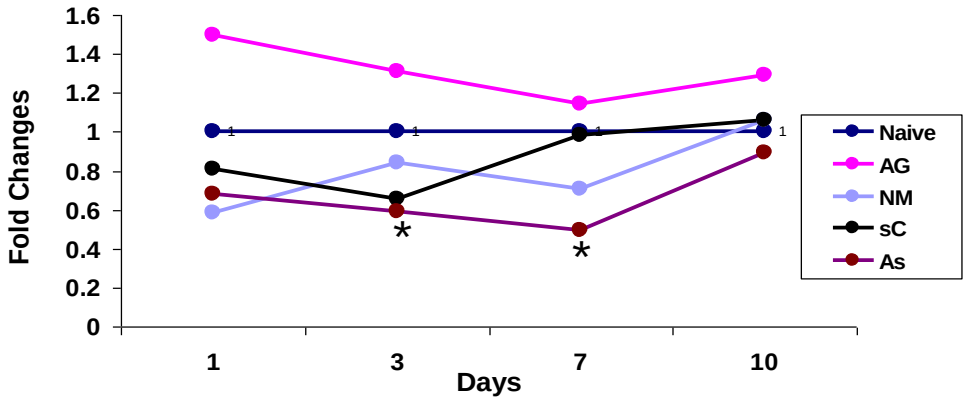

*** As vs. NM ($p< 0.05$)**

Table A3. Mean fold changes versus days from qRT-PCR analysis of Cx26 (Study 1)

Mean Fold Changes (rQ = Cx26/GapDH fold change) vs. Days

Day	Naïve	MG	NM	sC	As
1	1	1.35768	2.57260	1.80337	0.99802
3	1	0.93121	4.96457	4.68286	1.70769$^{\#\,\wedge}$
7	1	0.62969	4.08079	2.05418	1.52863$^{+\,\#}$
10	1	0.70744	5.79770	3.11430	2.62103^{+}

MG-Vehicle control (Methylene Chloride/pluronic gel)
NM-Nitorgen mustard alone
sC-NM with sense control
As-NM with antisense
Naïve: Time 0

* As vs. Naïve (p< 0.05)
+ As vs. MG (p< 0.05)
# As vs. NM (p< 0.05)
^ As vs. sC (p< 0.05)

Figure A3: Mean fold changes versus days from qRT-PCR analysis of Cx26 (Study 1)

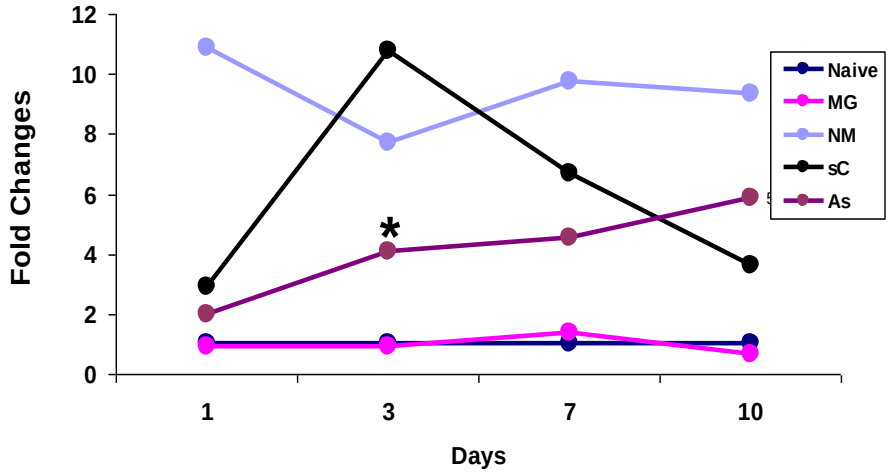

*** As vs. NM (p< 0.05)**

Table A4. Mean fold changes versus days from qRT-PCR analysis of Cx26 (Study 2)

Mean Fold Changes (rQ = Cx26/GapDH fold change) vs. Days

Mean Fold Changes vs. Days

Day	Naïve	AG	NM	sC	As
1	1	1.549902	3.07079	3.109867	2.043497*#^
3	1	1.433495	8.27025	7.228919	5.091554*+#
7	1	1.003496	7.114075	5.486151	4.186652
10	1	1.229961	7.391644	9.074712	5.592165*+

AG-Vehicle control (Acetone/pluronic gel)
NM-Nitorgen mustard alone
sC-NM with sense control
As-NM with antisense
Naïve: Time 0

* As vs. Naïve (p< 0.05)
+ As vs. AG (p< 0.05)
# As vs. NM (p< 0.05)
^ As vs. sC (p< 0.05)

Figure A4: Mean fold changes versus days from qRT-PCR analysis of Cx26 (Study 2)

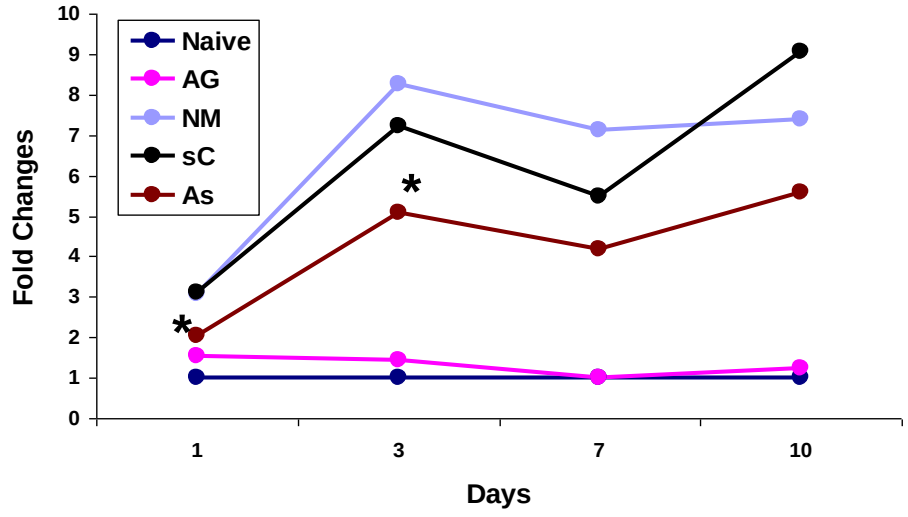

*** As vs. NM (p< 0.05)**

Table A5. Mean fold changes versus days from qRT-PCR analysis of Cx30 (Study 1)

Mean Fold Changes (rQ = Cx30/GapDH fold change) vs. Days

Day	Naïve	MG	NM	sC	As
1	1	0.91943	10.85653	2.90308	1.99841
3	1	0.91204	7.73403	10.77226	4.09980^
7	1	1.39161	9.75520	6.69989	4.55983+ #
10	1	0.67178	9.34038	3.63399	5.87930+

MG-Vehicle control (Methylene Chloride/pluronic gel)
NM-Nitorgen mustard alone
sC-NM with sense control
As-NM with antisense
Naïve: Time 0

* As vs. Naïve (p< 0.05)
+ As vs. MG (p< 0.05)
# As vs. NM (p< 0.05)
^ As vs. sC (p< 0.05)

Figure A5. Mean fold changes versus days from qRT-PCR analysis of Cx30 (Study 1)

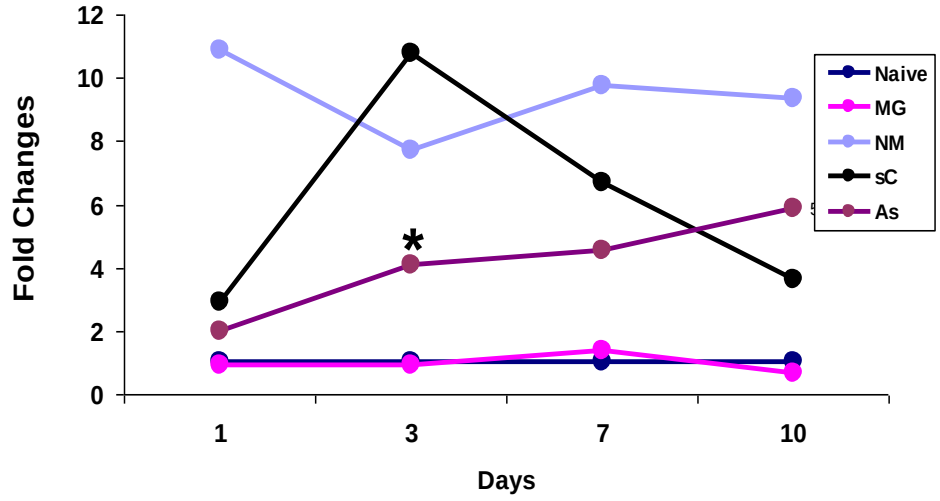

*** As vs. NM (p< 0.05)**

Table A6. Mean fold changes versus days from qRT-PCR analysis of Cx30 (Study 2)

Mean Fold Changes (rQ = Cx30/GapDH fold change) vs. Days

Day	Naïve	AG	NM	sC	As
1	1	1.57525	7.63212	5.80446	3.23436 * + # ^
3	1	1.70672	17.84530	19.85821	13.52566 * +
7	1	1.19754	17.94529	31.67895	10.60271 ^
10	1	1.73758	16.42055	18.44534	10.90409 * + ^

AG-Vehicle control (Acetone/pluronic gel)
NM-Nitorgen mustard alone
sC-NM with sense control
As-NM with antisense
Naïve: Time 0

* As vs. Naïve ($p < 0.05$)
+ As vs. AG ($p < 0.05$)
# As vs. NM ($p < 0.05$)
^ As vs. sC ($p < 0.05$)

Figure A6: Mean fold changes versus days from qRT-PCR analysis of Cx30 (Study 2)

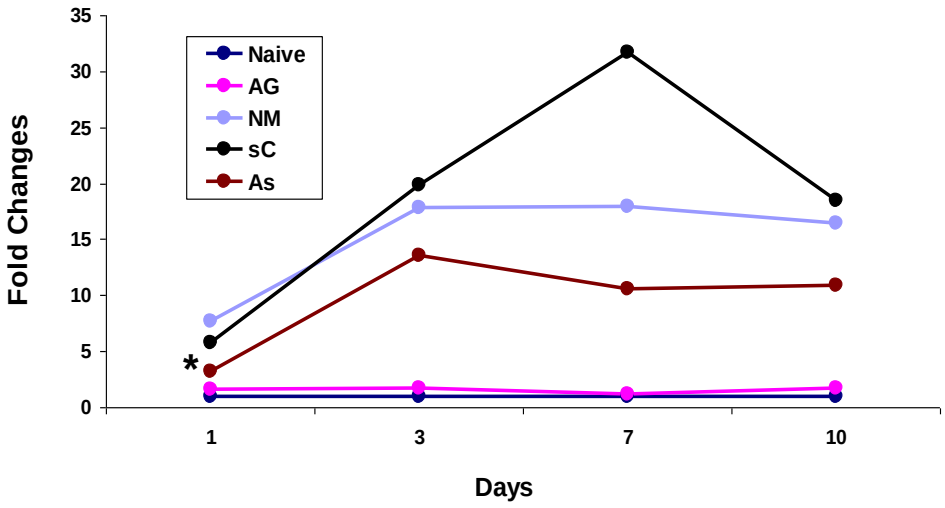

*** As vs. NM ($p < 0.05$)**

Table A7. Mean fold changes versus days from qRT-PCR analysis of IL-1B (Study 1)

Mean Fold Changes (rQ = IL-1B/GapDH fold change) vs. Days

Day	Naïve	MG	NM	sC	As
1	1	0.57519	47.70820	14.18657	12.84044[#]
3	1	0.22131	1.60197	14.30071	24.93663
7	1	2.01695	16.83274	30.93550	47.99541[* + #]
10	1	1.18681	5.27947	37.40038	15.80982[+]

MG-Vehicle control (Methylene Chloride/pluronic gel)
NM-Nitorgen mustard alone
sC-NM with sense control
As-NM with antisense
Naïve: Time 0

* As vs. Naïve (p< 0.05)
+ As vs. MG (p< 0.05)
# As vs. NM (p< 0.05)
^ As vs. sC (p< 0.05)

Figure A7: Mean fold changes versus days from qRT-PCR analysis of IL-1B (Study 1)

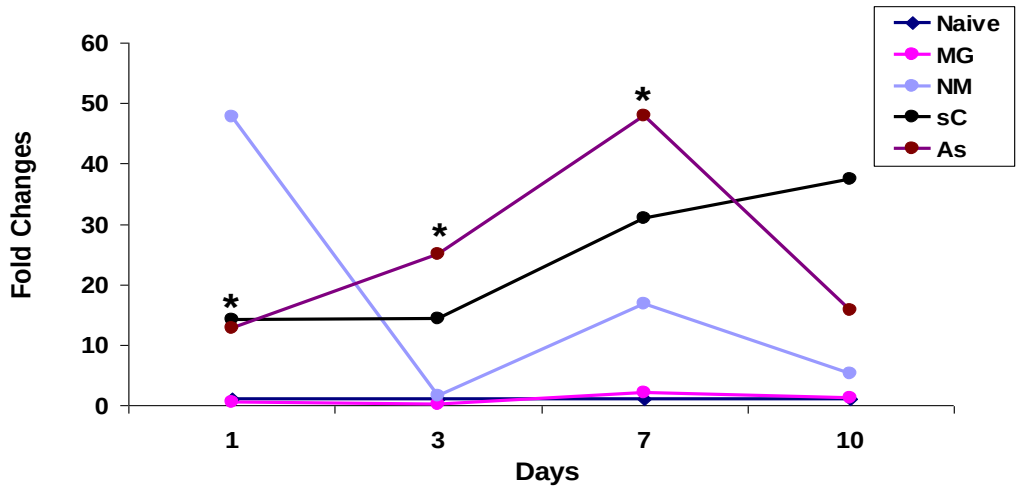

*** As vs. NM (p< 0.05)**

Table A8. Mean fold changes versus days from qRT-PCR analysis of IL-1B (Study 2)

Mean Fold Changes (rQ = IL-1B/GapDH fold change) vs. Days

Day	Naïve	AG	NM	sC	As
1	1	0.30589	42.22903	81.58760	36.25563* +
3	1	0.39056	3.33756	149.62420	159.08768* + #
7	1	0.53390	21.47714	41.44561	138.63835* + #
10	1	0.69415	6.23089	24.85600	33.83459* + #

AG-Vehicle control (Acetone/pluronic gel)
NM-Nitorgen mustard alone
sC-NM with sense control
As-NM with antisense
Naïve: Time 0

* As vs. Naïve (p< 0.05)
+ As vs. AG (p< 0.05)
# As vs. NM (p< 0.05)
^ As vs. sC (p< 0.05)

Table A9. Mean fold changes versus days from qRT-PCR analysis of IL-6 (Study 2)

Mean Fold Changes (rQ = IL-6/GapDH fold change) vs. Days

Day	**Naïve**	**AG**	**NM**	**sC**	**As**
1	**1**	**0.83349**	**25.82225**	**44.07677**	**19.29030*** + ^
3	**1**	**0.77398**	**15.21648**	**48.70752**	**24.05259*** +
7	**1**	**0.44677**	**2.06464**	**11.18659**	**11.45325**+ #
10	**1**	**0.38933**	**0.62418**	**2.64118**	**3.02972**

AG-Vehicle control (Acetone/pluronic gel)
NM-Nitorgen mustard alone
sC-NM with sense control
As-NM with antisense
Naïve: Time 0

*** As vs. Naïve (p< 0.05)**
+ As vs. AG (p< 0.05)
 # As vs. NM (p< 0.05)
^ As vs. sC (p< 0.05)

Table A10. Mean fold changes versus days from qRT-PCR analysis of IL-10 (Study 1)

Mean Fold Changes (rQ = IL-10/GapDH fold change) vs. Days

Day	Naïve	MG	NM	sC	As
1	1	2.319448	0.650180	1.043093	0.821441
3	1	1.072612	0.392499	0.577101	1.099028#
7	1	1.568012	0.605662	0.914073	1.043568#
10	1	0.694163	0.990971	1.232672	0.822716^

MG-Vehicle control (Methylene Chloride/pluronic gel)
NM-Nitorgen mustard alone
sC-NM with sense control
As-NM with antisense
Naïve: Time 0

***** As vs. Naïve (p< 0.05)
\+ As vs. MG (p< 0.05)
\# As vs. NM (p< 0.05)
^ As vs. sC (p< 0.05)

Figure A10. Mean fold changes versus days from qRT-PCR analysis of IL-10 (Study 1)

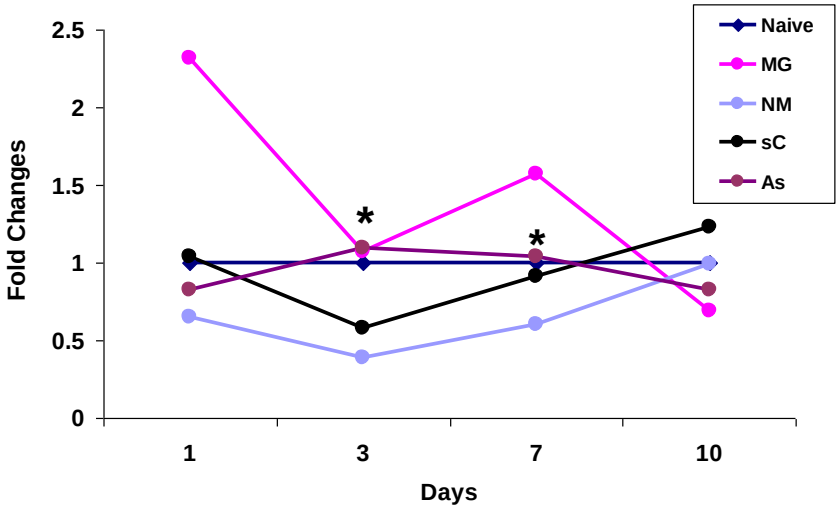

*** As vs. NM (p< 0.05)**

Table A11. Mean fold changes versus days from qRT-PCR analysis of IL-10 (Study 2)

Mean Fold Changes (rQ = IL-10/GapDH fold change) vs. Days

Day	Naïve	AG	NM	sC	As
1	1	7.264835	1.333566	1.836791	1.135756[+]
3	1	2.454861	1.848352	1.82919	1.779616[*]
7	1	2.443484	2.369271	22.61715	1.840453[*^]
10	1	12.52354	8.578954	5.013429	7.120733[*]

AG-Vehicle control (Acetone/pluronic gel)
NM-Nitorgen mustard alone
sC-NM with sense control
As-NM with antisense
Naïve: Time 0

[*] As vs. Naïve ($p < 0.05$)
[+] As vs. AG ($p < 0.05$)
[#] As vs. NM ($p < 0.05$)
[^] As vs. sC ($p < 0.05$)

Figure A11. Mean fold changes versus days from qRT-PCR analysis of IL-10 (Study 2)

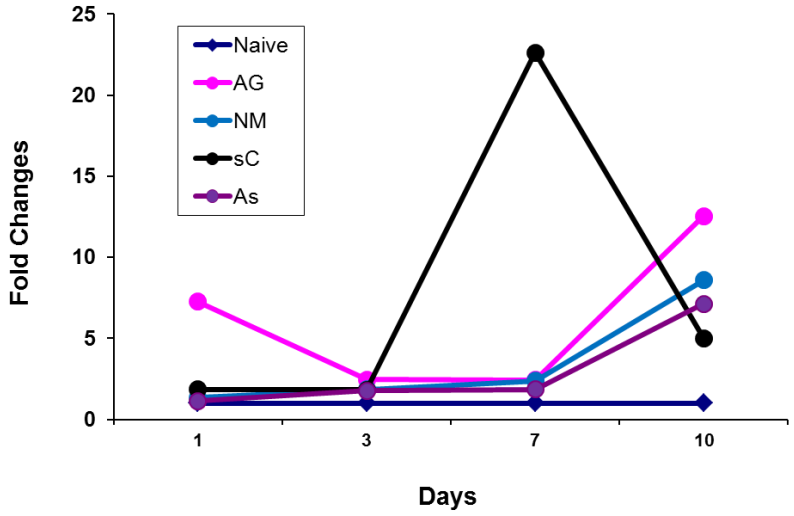

Table A12. Mean fold changes versus days from qRT-PCR analysis of COX-2 (Study 2)

Mean Fold Changes (rQ = COX-2/GapDH fold change) vs. Days

Day	Naïve	AG	NM	sC	As
1	1	2.205891	23.89593	27.55787	14.81151*+ # ^
3	1	1.373399	24.23281	120.1537	194.6694* + #
7	1	1.209478	37.99707	124.0611	60.10299* +
10	1	1.289329	12.54931	25.54332	24.35206* +

AG-Vehicle control (Acetone/pluronic gel)
NM-Nitorgen mustard alone
sC-NM with sense control
As-NM with antisense
Naïve: Time 0

* As vs. Naïve (p< 0.05)
+ As vs. AG (p< 0.05)
# As vs. NM (p< 0.05)
^ As vs. sC (p< 0.05)

Figure A12. Mean fold changes versus days from qRT-PCR analysis of COX-2 (Study 2)

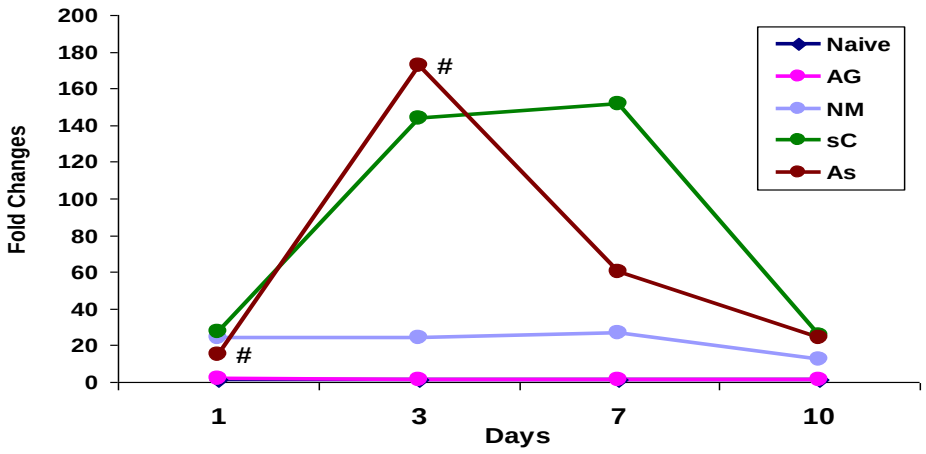

*** As vs. NM (p< 0.05)**

Table A13. Mean fold changes versus days from qRT-PCR analysis of PGES-2 (Study 2)

Mean Fold Changes (rQ = PGES-2/GapDH fold change) vs. Days

Day	Naïve	AG	NM	sC	As
1	1	1.60791	0.70283	0.93157	0.74991*+
3	1	1.50380	0.67859	0.65634	0.55714*+
7	1	1.13161	0.74473	1.78554	0.67338*+^
10	1	1.87124	1.13519	0.97132	1.08936+

AG-Vehicle control (Acetone/pluronic gel)
NM-Nitorgen mustard alone
sC-NM with sense control
As-NM with antisense
Naïve: Time 0

* As vs. Naïve ($p < 0.05$)
+ As vs. AG ($p < 0.05$)
# As vs. NM ($p < 0.05$)
^ As vs. sC ($p < 0.05$)

Table A14. Mean fold changes versus days from qRT-PCR analysis of MMP-2 (Study 2)

Mean Fold Changes (rQ = MMP-2/GapDH fold change) vs. Days

Day	Naïve	AG	NM	sC	As
1	1	1.69322	0.20008	0.43808	0.19443*+
3	1	1.70964	0.26642	0.41012	0.21050*+
7	1	1.42895	10.23482	3.25172	11.55290*+^
10	1	1.51655	7.39558	6.14529	10.13038*+

AG-Vehicle control (Acetone/pluronic gel)
NM-Nitorgen mustard alone
sC-NM with sense control
As-NM with antisense
Naïve: Time 0

* As vs. Naïve ($p < 0.05$)
+ As vs. AG ($p < 0.05$)
# As vs. NM ($p < 0.05$)
^ As vs. sC ($p < 0.05$)

Table A15. Mean fold changes versus days from qRT-PCR analysis of MMP-9 (Study 2)

Mean Fold Changes (rQ = MMP-9/GapDH fold change) vs. Days

Day	Naïve	AG	NM	sC	As
1	1	1.37040	0.48258	0.82407	0.68501
3	1	1.84763	0.81648	1.73441	1.40267
7	1	1.13487	3.99794	1.82137	8.10566*+ ^
10	1	2.21367	3.71783	4.35976	4.25857*+

AG-Vehicle control (Acetone/pluronic gel)
NM-Nitorgen mustard alone
sC-NM with sense control
As-NM with antisense
Naïve: Time 0

* As vs. Naïve (p< 0.05)
+ As vs. AG (p< 0.05)
# As vs. NM (p< 0.05)
^ As vs. sC (p< 0.05)

Table A16. Mean fold changes versus days from qRT-PCR analysis of MMP-12 (Study 1)

Mean Fold Changes (rQ = MMP-12/GapDH fold change) vs. Days

Day	Naïve	MG	NM	sC	As
1	1	1.75198	0.38462	0.24572	0.30741*
3	1	0.77310	0.11522	0.32605	0.18505*
7	1	1.78380	2.80005	1.08168	1.49222
10	1	1.49910	2.16218	1.64881	1.50235

MG-Vehicle control (Methylene Chloride/pluronic gel)
NM-Nitorgen mustard alone
sC-NM with sense control
As-NM with antisense
Naïve: Time 0

* As vs. Naïve (p< 0.05)
+ As vs. MG (p< 0.05)
# As vs. NM (p< 0.05)
^ As vs. sC (p< 0.05)

Table A17. Mean fold changes versus days from qRT-PCR analysis of MMP-12 (Study 2)

Mean Fold Changes (rQ = MMP-12/GapDH fold change) vs. Days

Day	Naïve	AG	NM	sC	As
1	1	1.63978	0.25594	0.42045	0.41770*+
3	1	1.81530	0.14757	0.38494	0.19734*+
7	1	1.45896	1.37878	2.23367	2.18944*
10	1	2.64904	3.01369	3.08487	3.45009*

AG-Vehicle control (Acetone/pluronic gel)
NM-Nitorgen mustard alone
sC-NM with sense control
As-NM with antisense
Naïve: Time 0

* As vs. Naïve ($p < 0.05$)
+ As vs. AG ($p < 0.05$)
# As vs. NM ($p < 0.05$)
^ As vs. sC ($p < 0.05$)

Appendix B

Body Weights and Biopsy Weights

Figure B1. Body weight changes 10 days post exposure with NM from Study 1 and Study 2.

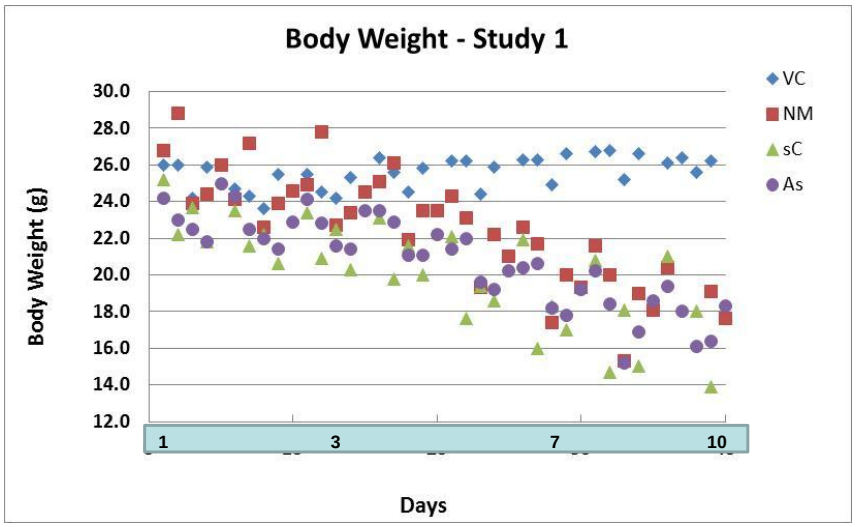

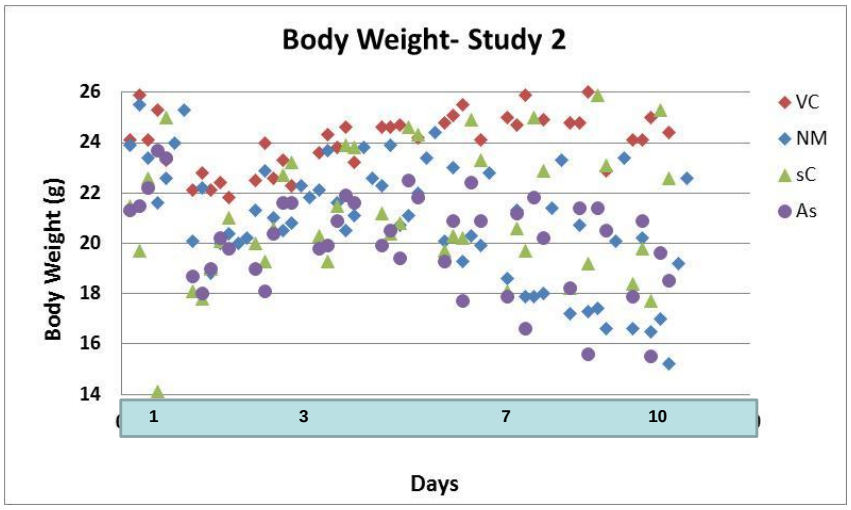

Figure B2. Biopsy weight changes 10 days post exposure with NM from Study 1 and Study 2.

Study 1- 12 mm punch weight (g)

Day	VC (g)	NM (g)	Relative skin weight (%)	NM+sC (g)	Relative skin weight (%)	NM+As (g)	Relative skin weight (%)
1	0.0992	0.3152	217.7	0.3200	222.6	0.2967	199.1
3	0.0853	0.2223	160.5	0.2216	159.7	0.2207	158.6
7	0.0931	0.1315	41.2	0.1751	88.1	0.1613	73.2
10	0.0832	0.0895	7.5	0.1155	38.8	0.1169	40.4

VC: Vehicle Control (Methylene Chloride); NM: NM-exposed; NM+Sc: NM-exposed treated with Cx43 scODN; NM+As: NM-exposed treated with Cx43 asODN.

Example of relative skin weight calculation:
Relative skin weight (%) = 100 x [NM-exposed biopsy weight - vehicle control biopsy weight]/[vehicle control biopsy weight]

Study 2- 12 mm punch weight (g)

Day	VC (g)	NM (g)	Relative skin weight (%)	NM+sC (g)	Relative skin weight (%)	NM+As (g)	Relative skin weight (%)
1	0.0676	0.2542	276.1	0.2441	261.2	0.2621	287.8
3	0.0769	0.1671	117.4	0.1575	104.9	0.1663	116.3
7	0.0659	0.1337	102.8	0.1463	121.9	0.1602	143.1
10	0.0674	0.1139	68.9	0.1530	126.9	0.1323	96.3

VC: Vehicle Control (Acetone); NM: NM-exposed; NM+Sc: NM-exposed treated with Cx43 scODN; NM+As: NM-exposed treated with Cx43 asODN.

Example of relative skin weight calculation:
Relative skin weight (%) = 100 x [NM-exposed biopsy weight - vehicle control biopsy weight]/[vehicle control biopsy weight]

Appendix C

Macroscopic Appearance and H&E Histology from All Individual Mice (Study 2)

Figure C1. Macroscopic appearance from unexposed control (naïve) group

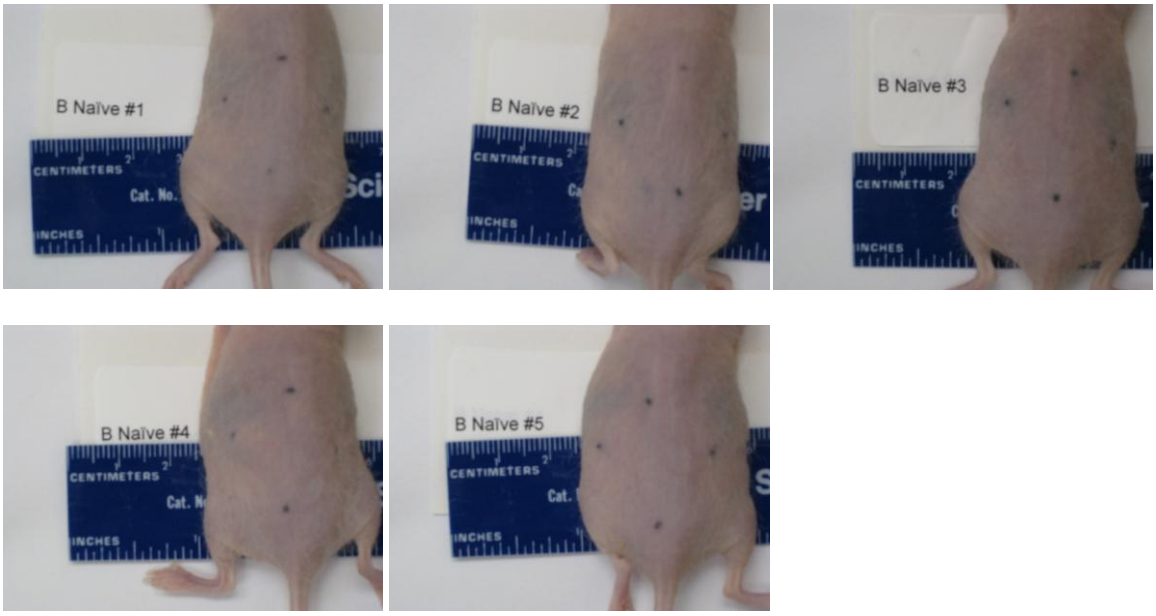

Figure C2. H&E histology from unexposed control (naïve) group (Bar=200 µm)

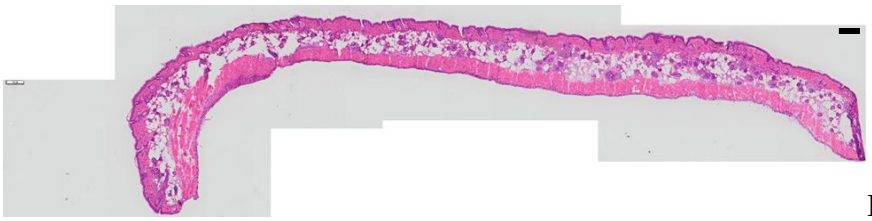

Mouse #1

Mouse #2

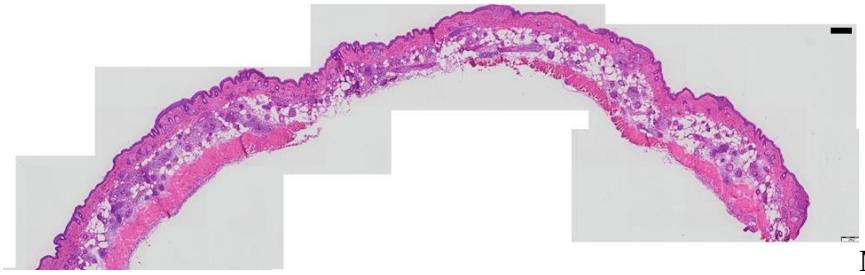

Mouse #3

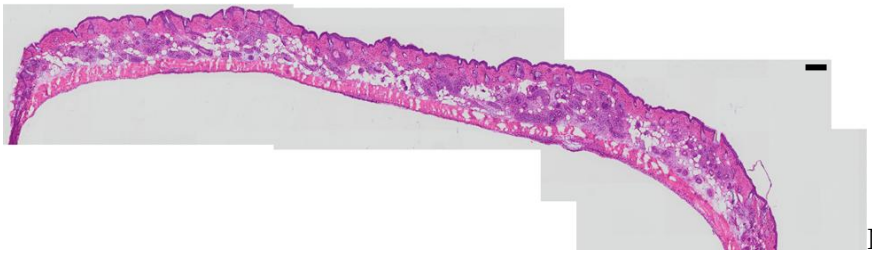

Mouse #4

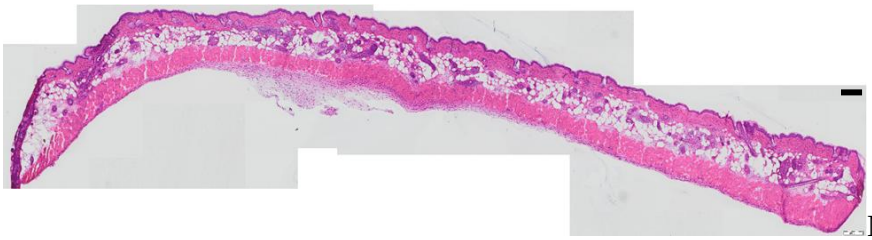

Mouse #5

Figure C3. Macroscopic appearance from vehicle (acetone) control group (Day 1)

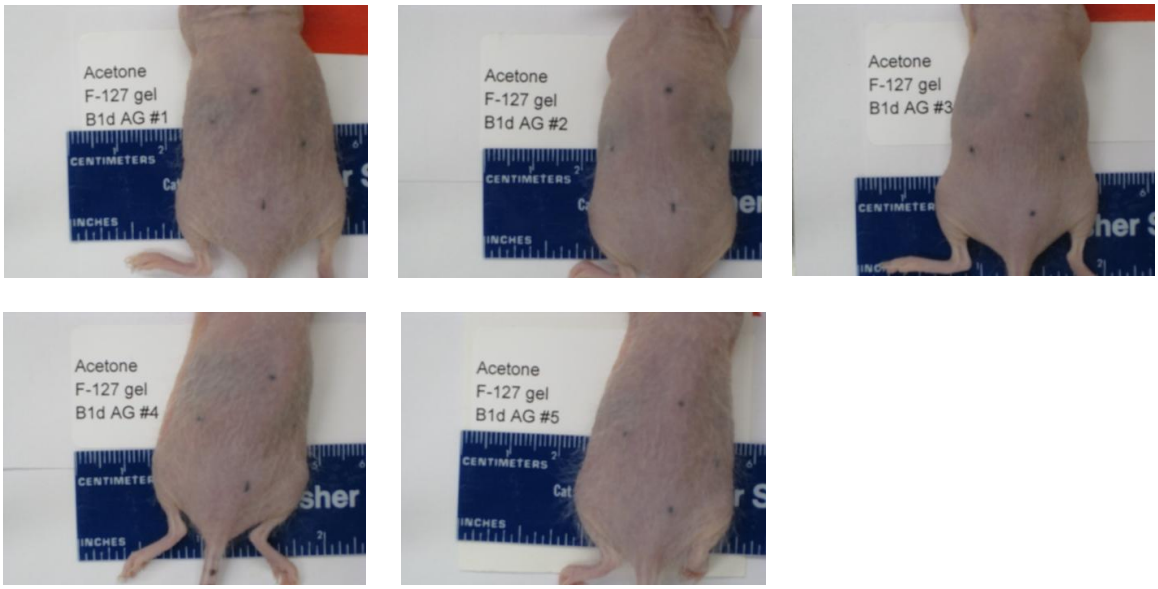

Figure C4. H&E histology from vehicle (acetone) control group (Day 1) (Bar=200 µm)

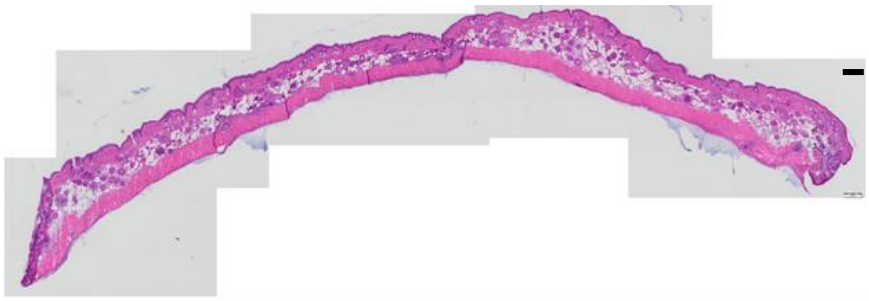

Mouse #1

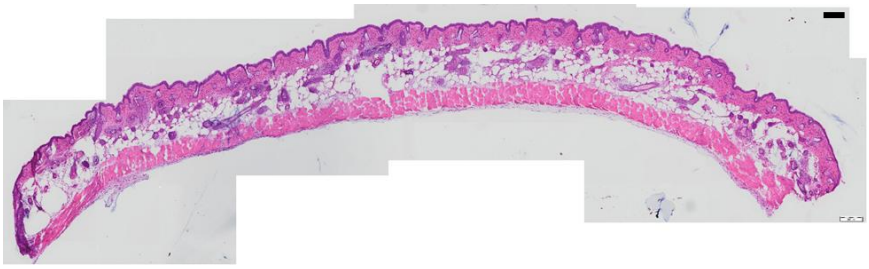

Mouse #2

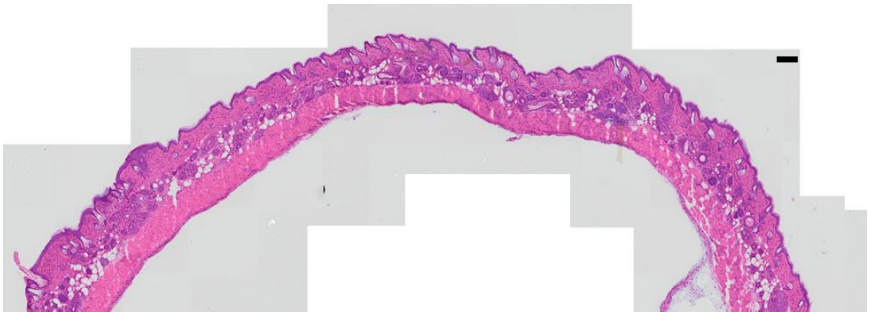

Mouse #3

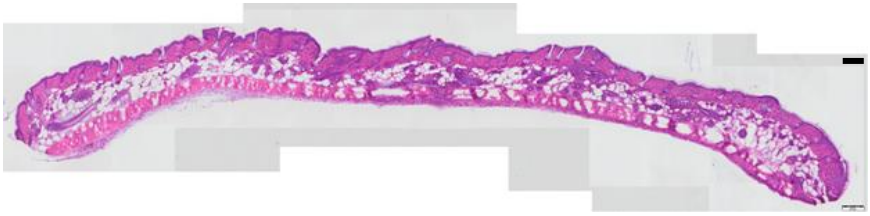

Mouse #4

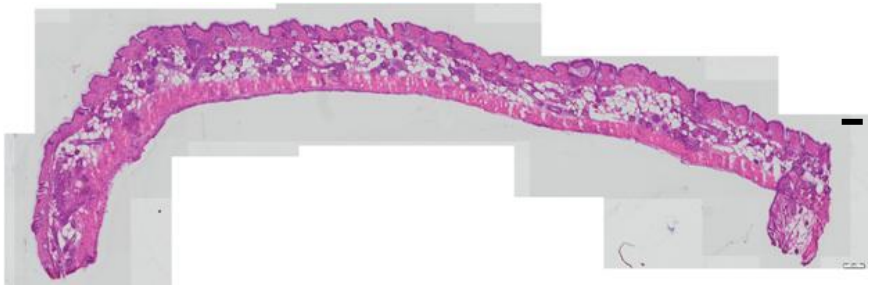

Mouse #5

Figure C5. Macroscopic appearance from NM exposed group (Day 1)

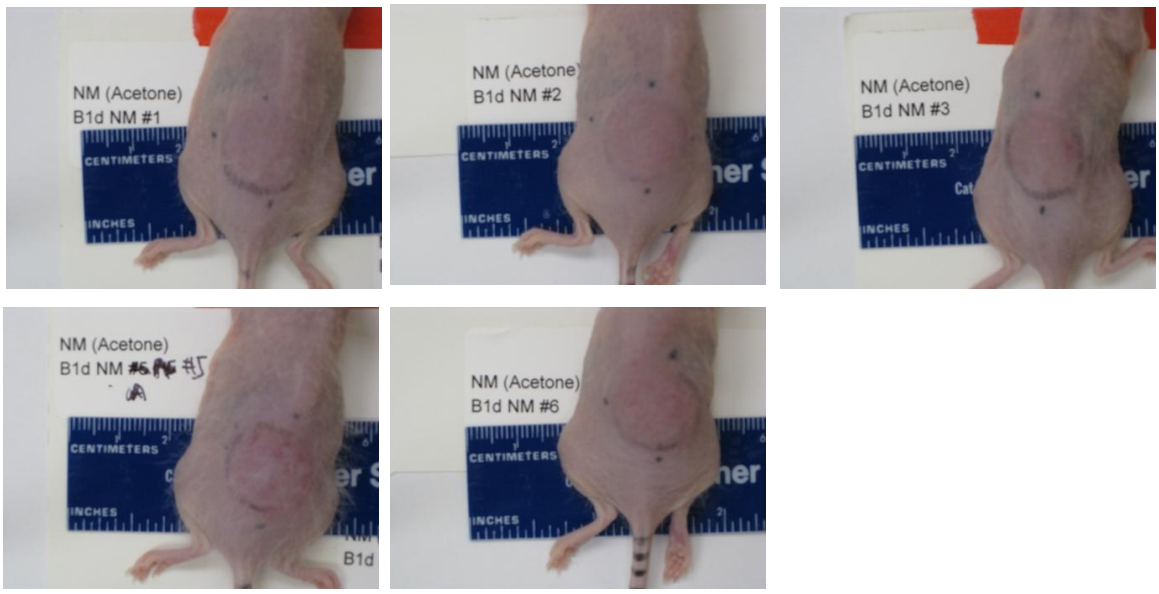

Figure C6. H&E histology from NM exposed group (Day 1) (Bar=200 µm)

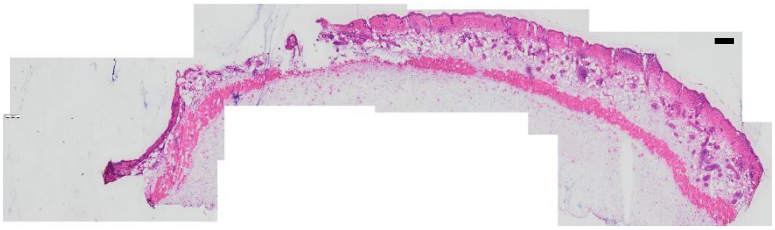
Mouse #1

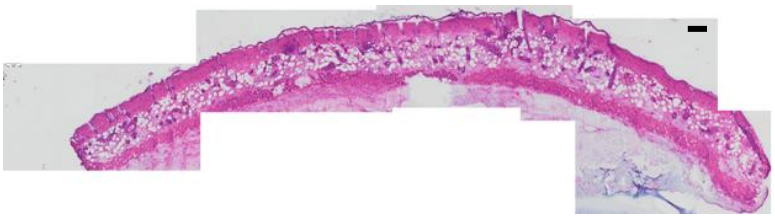
Mouse #2

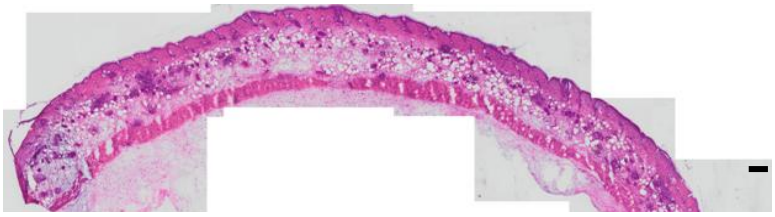
Mouse #3

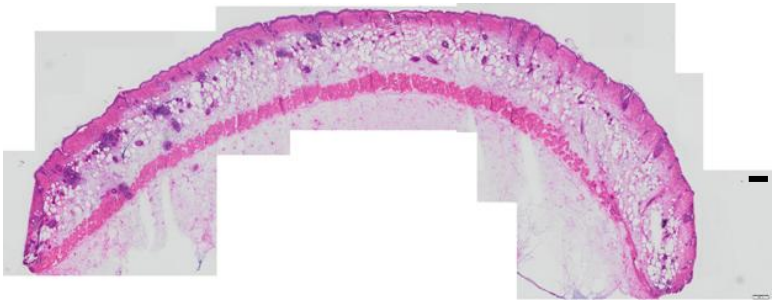
Mouse #4

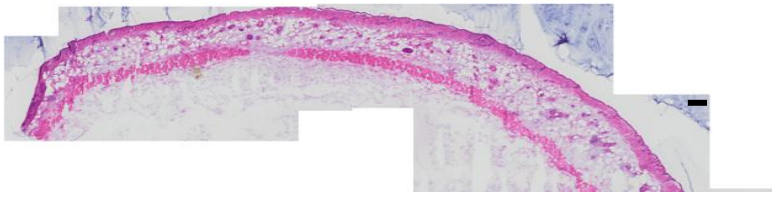
Mouse #5

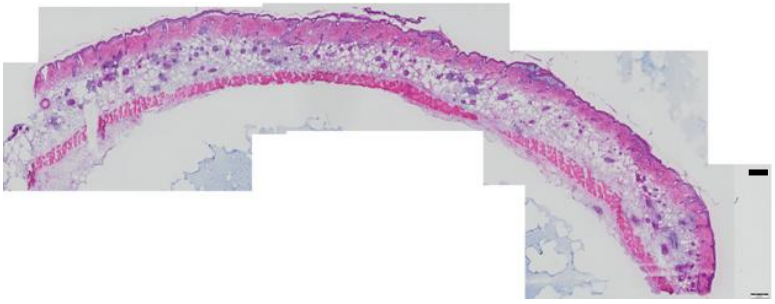
Mouse #6

Figure C7. Macroscopic appearance from NM exposed treated with Cx43 scODN group (Day 1)

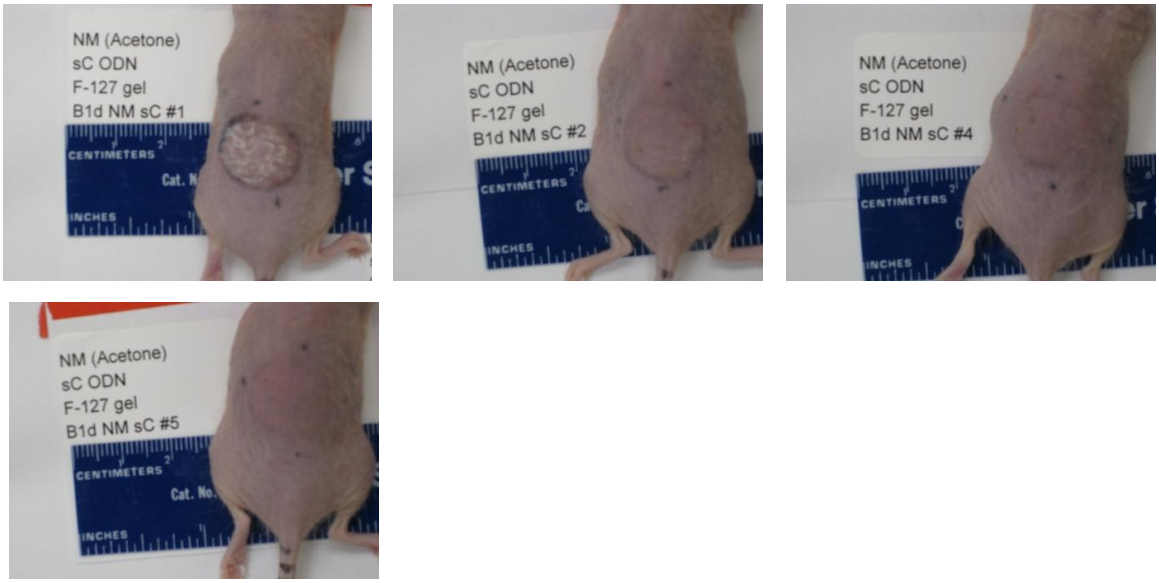

Figure C8. H&E histology from NM exposed treated with Cx43 scODN group (Day 1) (Bar=200 µm)

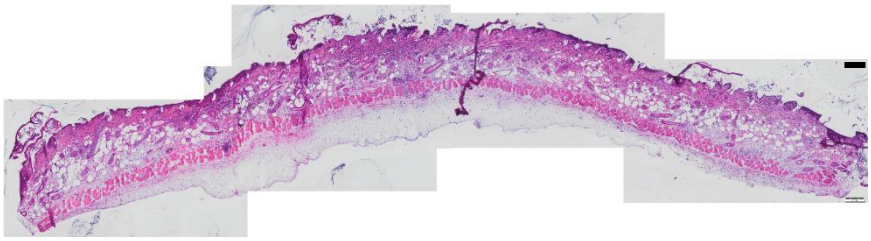

Mouse #1

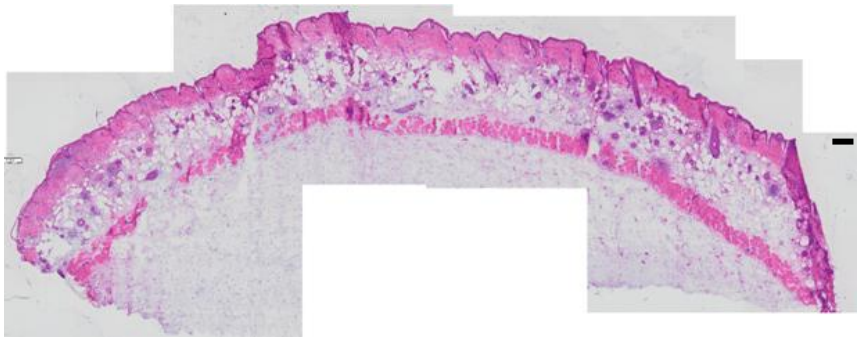

Mouse #2

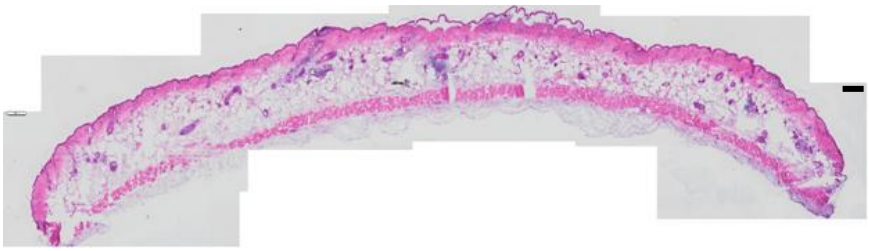

Mouse #3

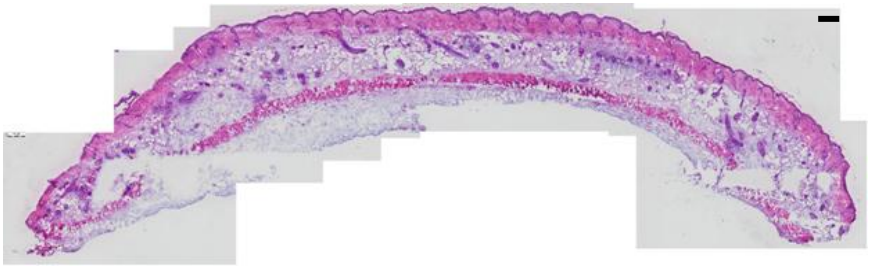

Mouse #4

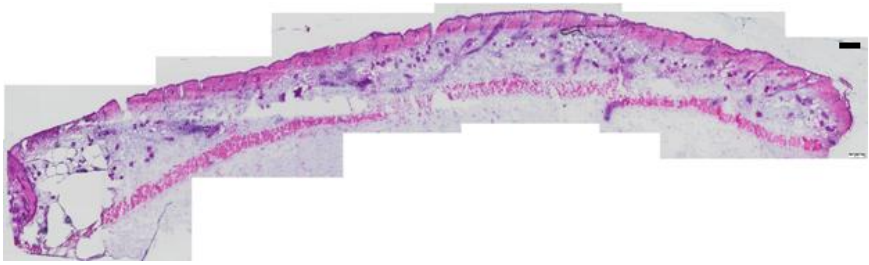

Mouse #5

Figure C9. Macroscopic appearance from NM exposed treated with Cx43 asODN group (Day 1)

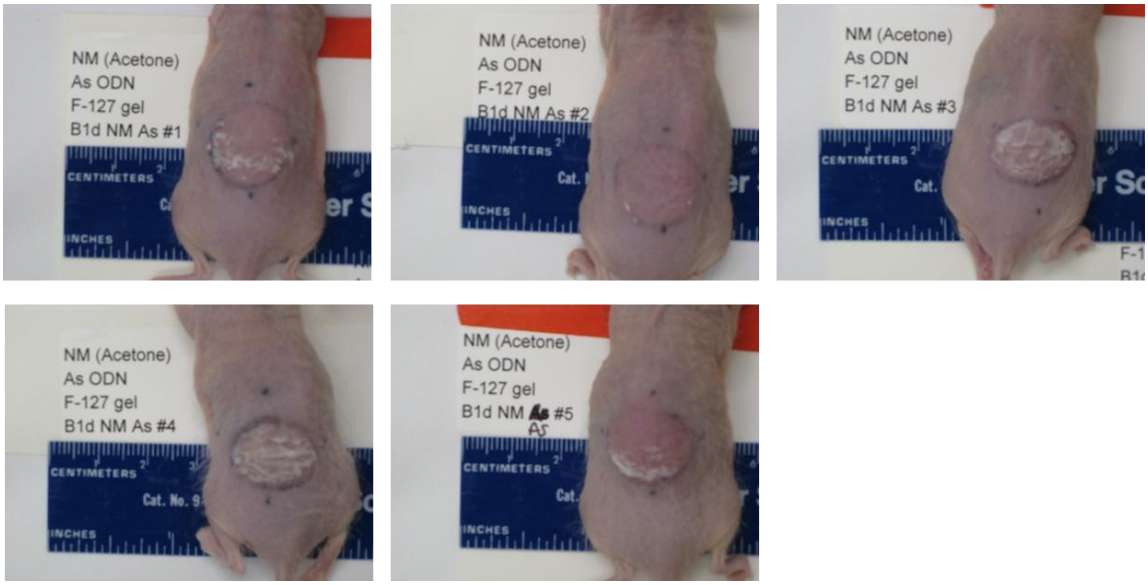

Figure C10. H&E histology from NM exposed treated with Cx43 asODN group (Day 1) (Bar=200 µm)

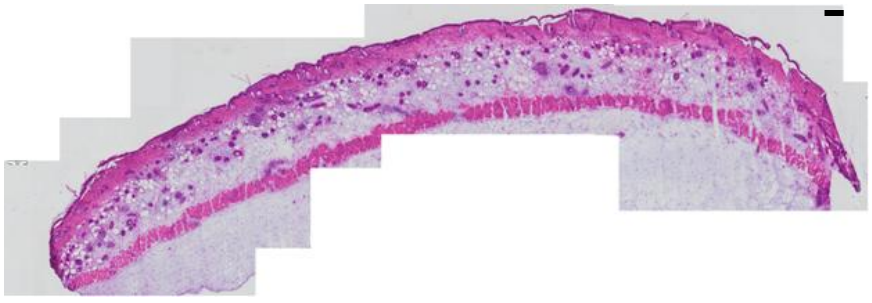

Mouse #1

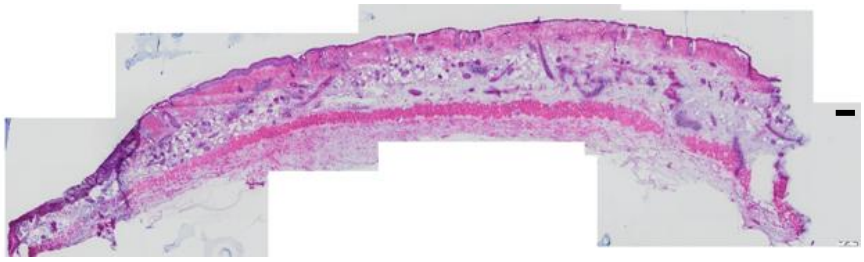

Mouse #2

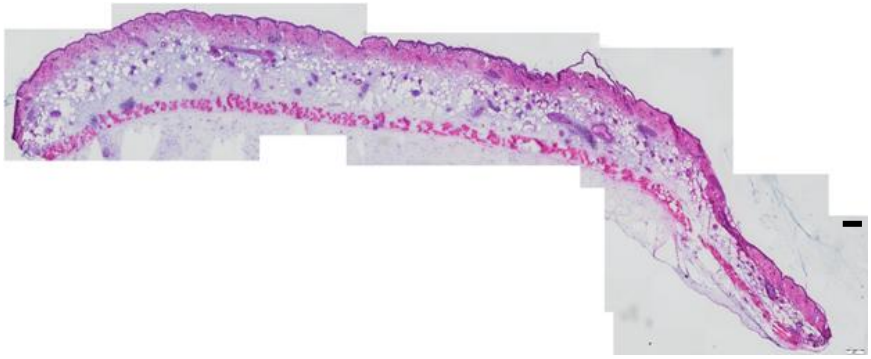

Mouse #3

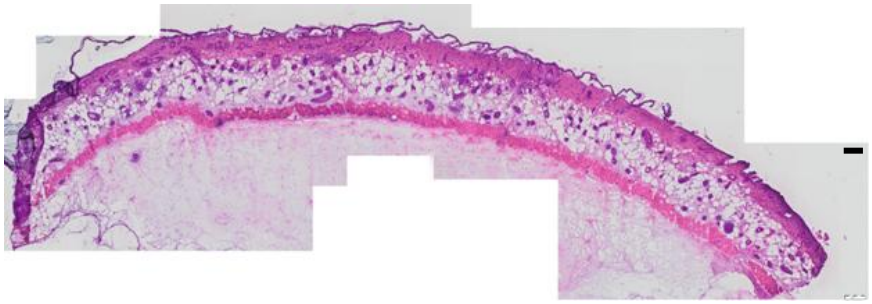

Mouse #4

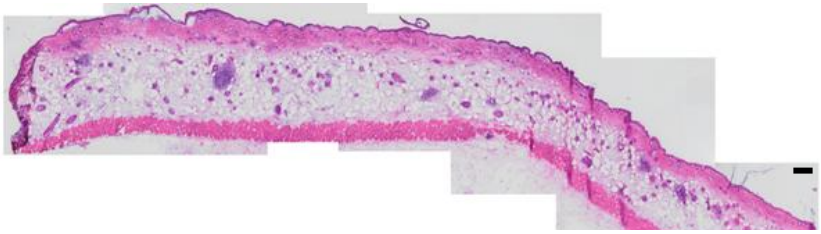

Mouse #5

Figure C11. Macroscopic appearance from vehicle (acetone) control group (Day 3)

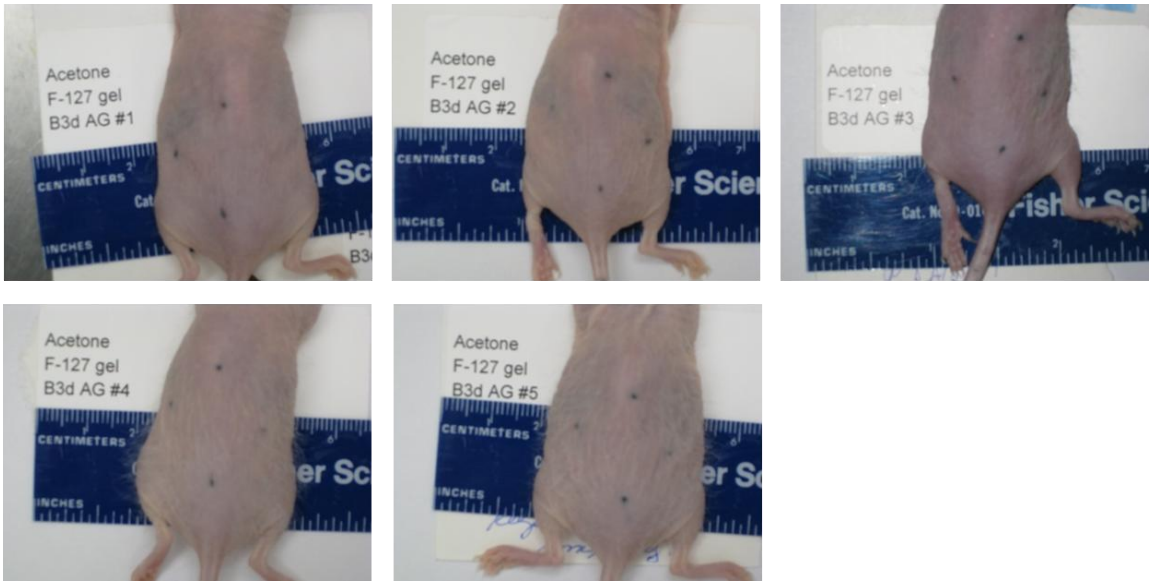

Figure C12. H&E histology from vehicle (acetone) control group (Day 3) (Bar=200 µm)

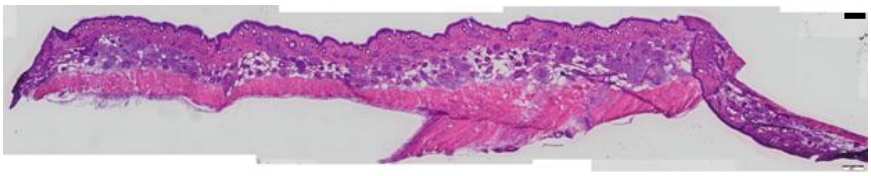

Mouse #1

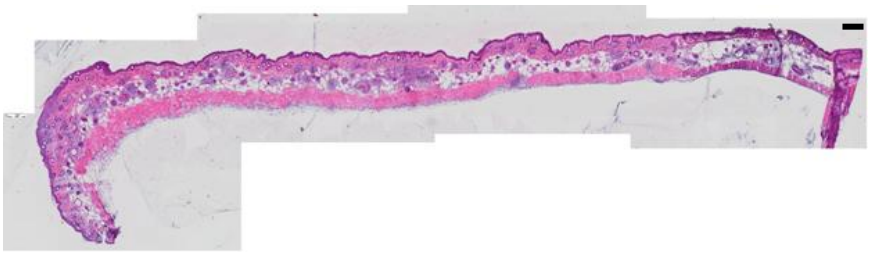

Mouse #2

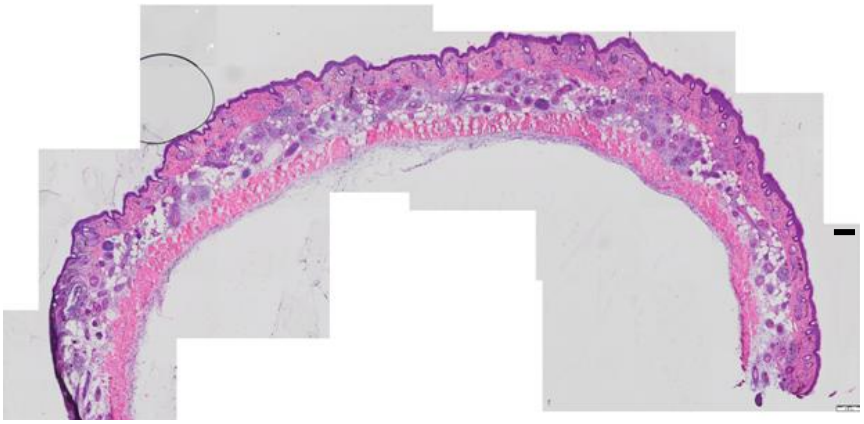

Mouse #3

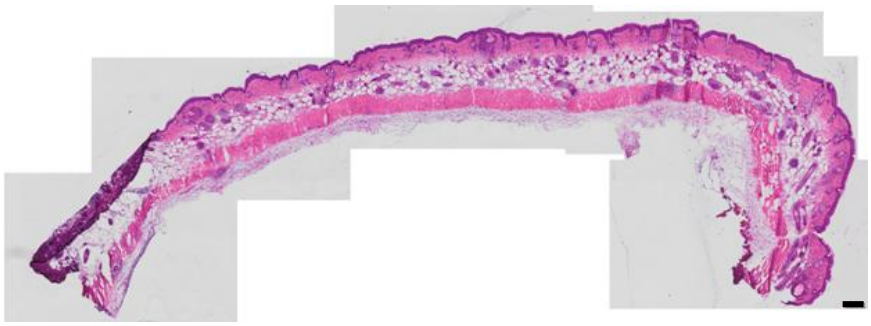

Mouse #4

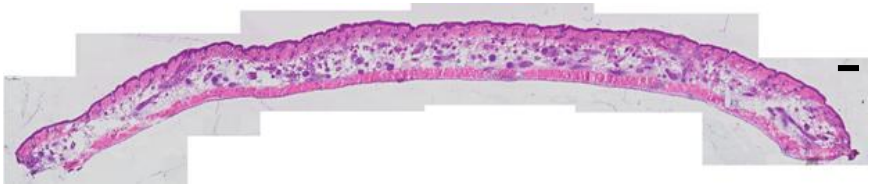

Mouse #5

Figure C13. Macroscopic appearance from NM exposed group (Day 3)

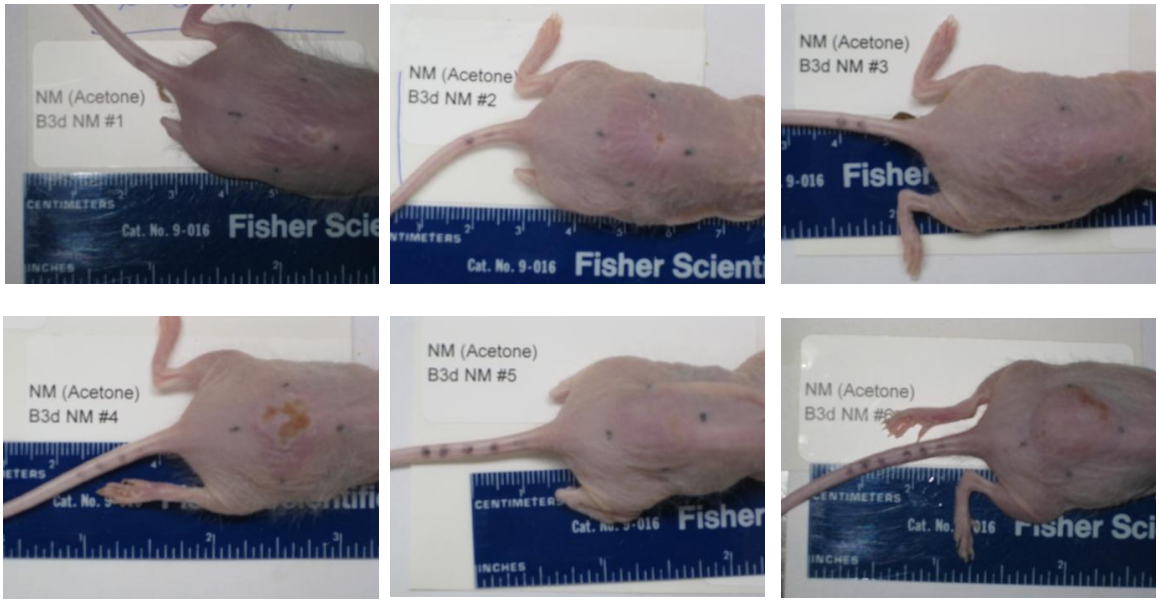

Figure C14. H&E histology from NM exposed group (Day 3) (Bar=200 µm)

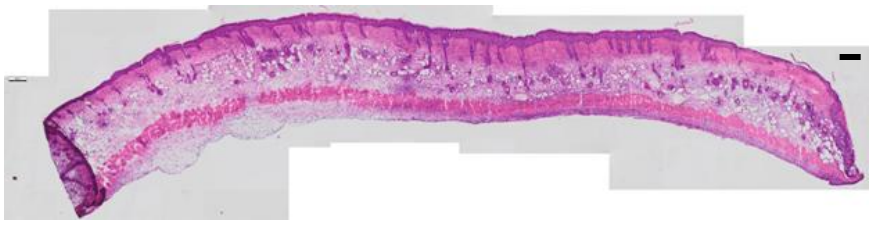

Mouse #1

Mouse #2

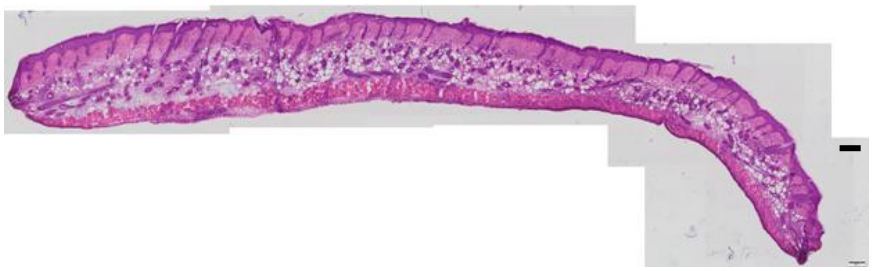

Mouse #3

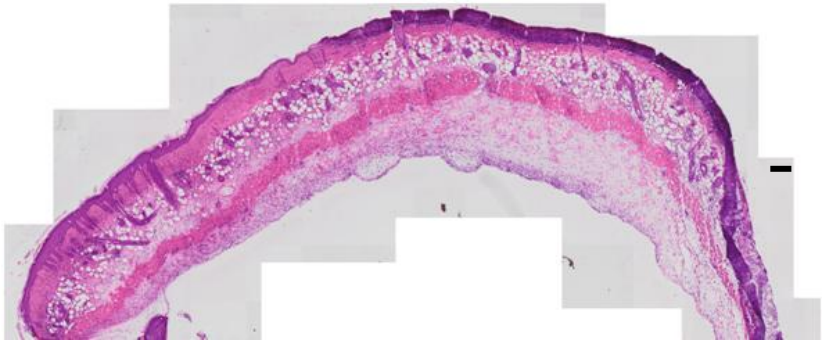

Mouse #4

Mouse #5

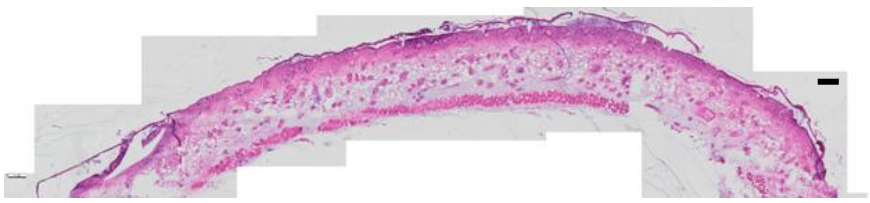

Mouse #6

Figure C15. Macroscopic appearance from NM exposed treated with Cx43 scODN group (Day 3)

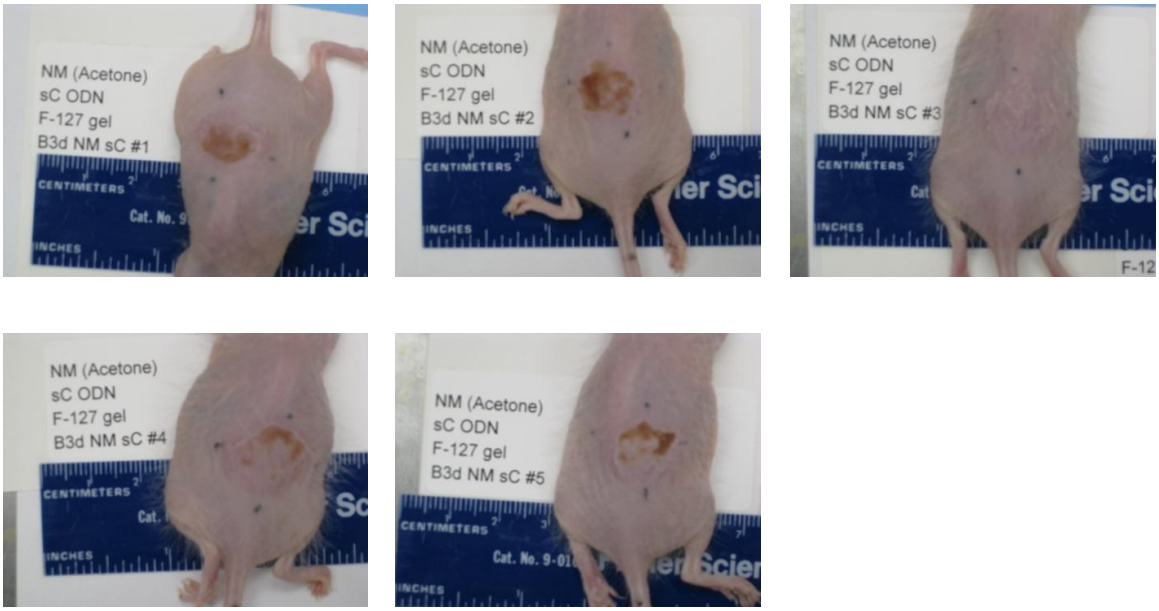

Figure C16. H&E histology from NM exposed treated with Cx43 scODN group (Day 3) (Bar=200 µm)

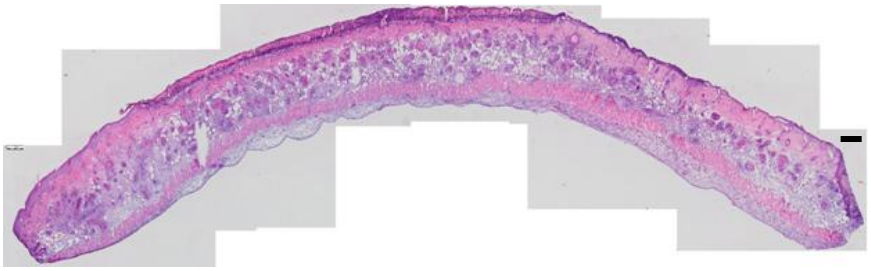

Mouse #1

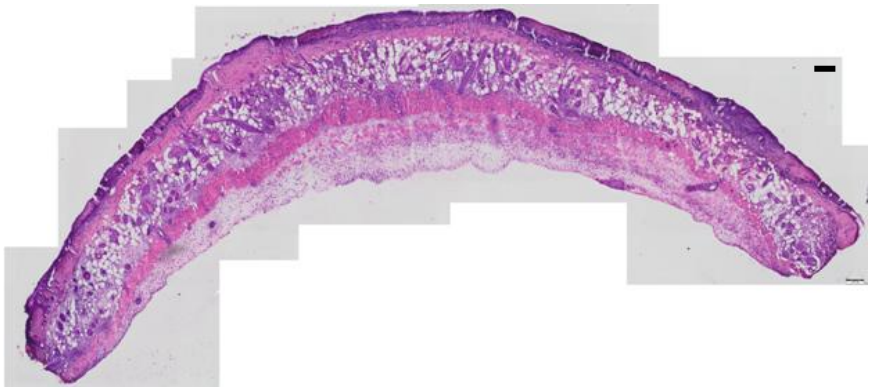

Mouse #2

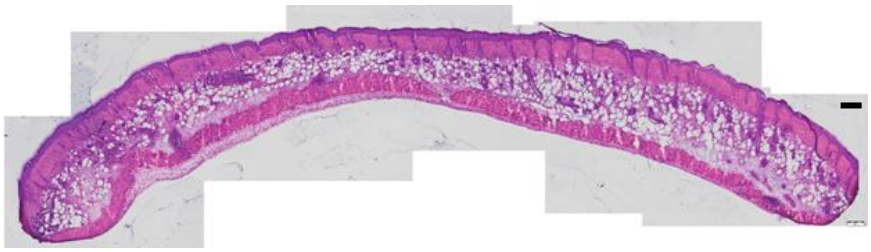

Mouse #3

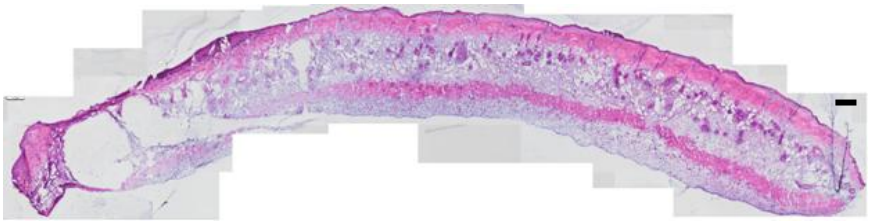

Mouse #4

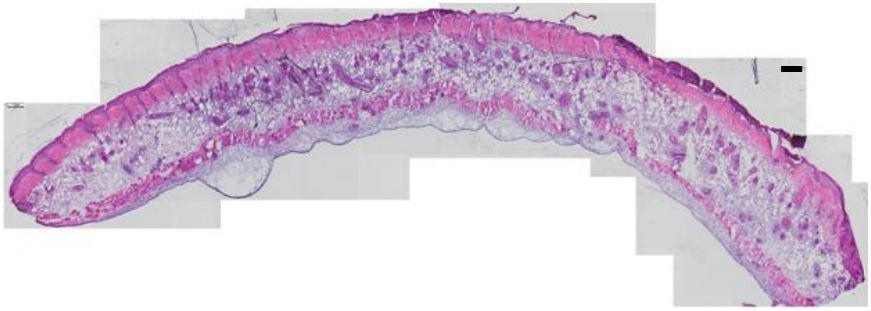

Mouse #5

Figure C17. Macroscopic appearance from NM exposed treated with Cx43 asODN group (Day 3)

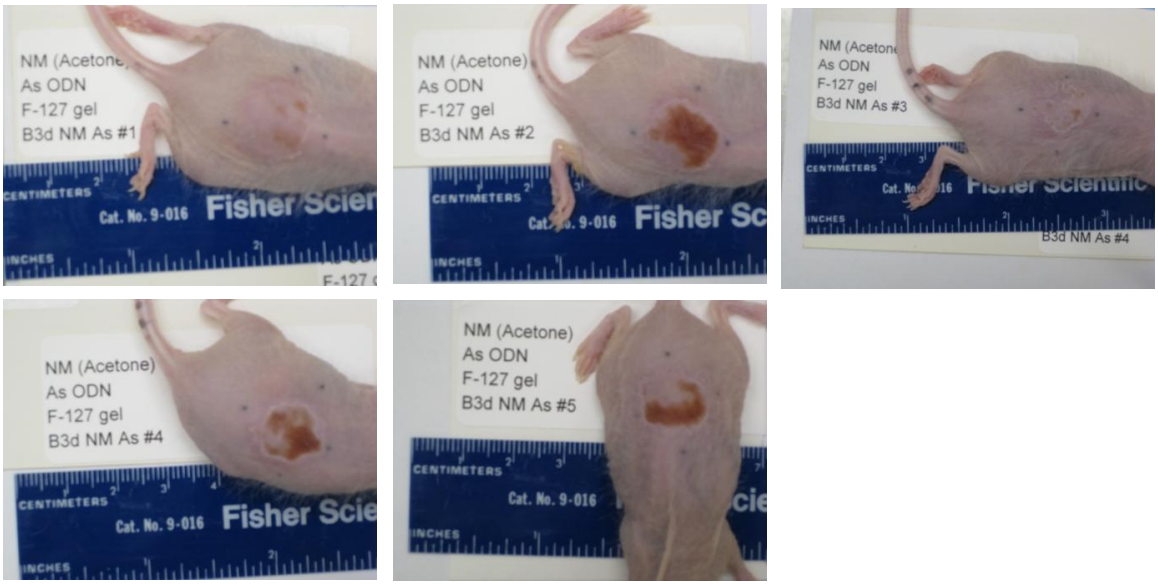

Figure C18. H&E histology from NM exposed treated with Cx43 asODN group (Day 3) (Bar=200 μm)

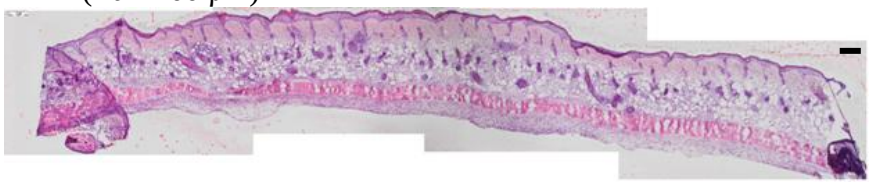

Mouse #1

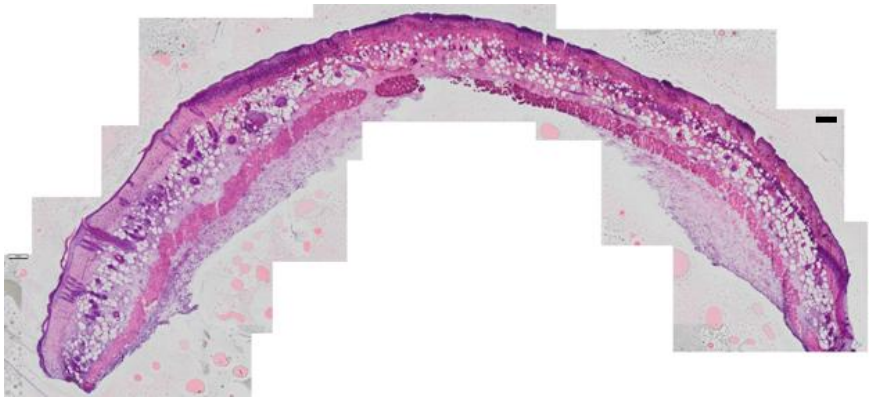

Mouse #2

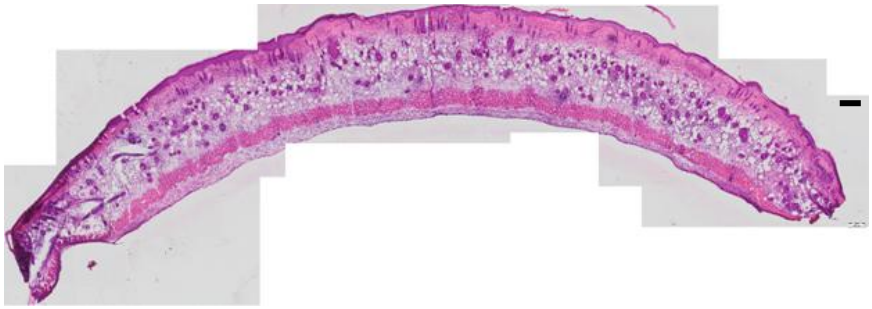

Mouse #3

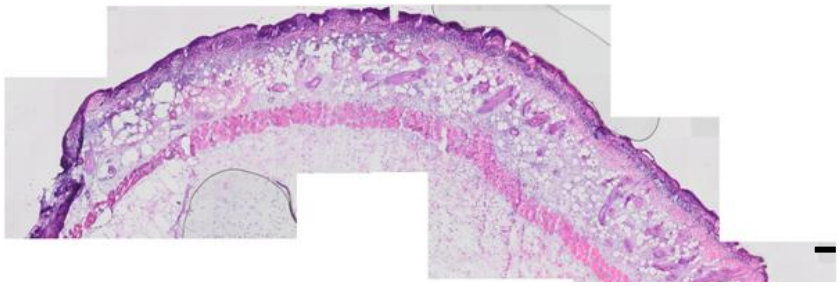

Mouse #4

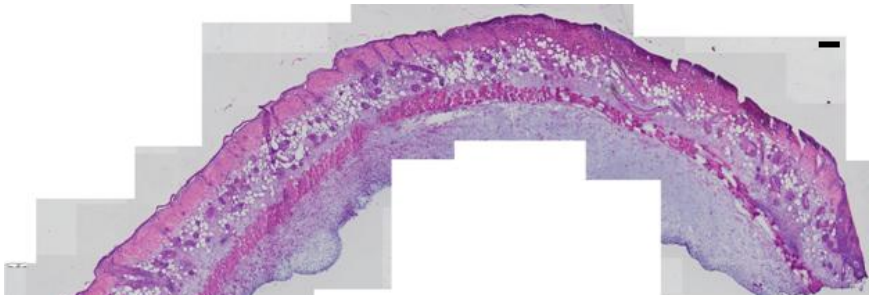

Mouse #5

Figure C19. Macroscopic appearance from vehicle (acetone) control group (Day 7)

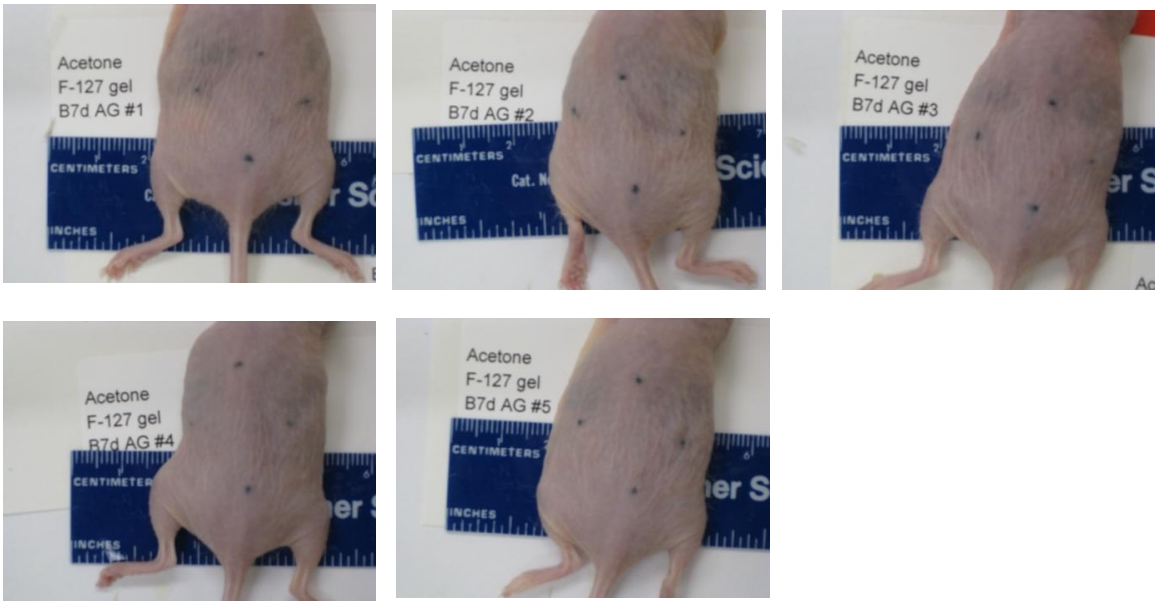

Figure C20. H&E histology from vehicle (acetone) control group (Day 7) (Bar=200 µm)

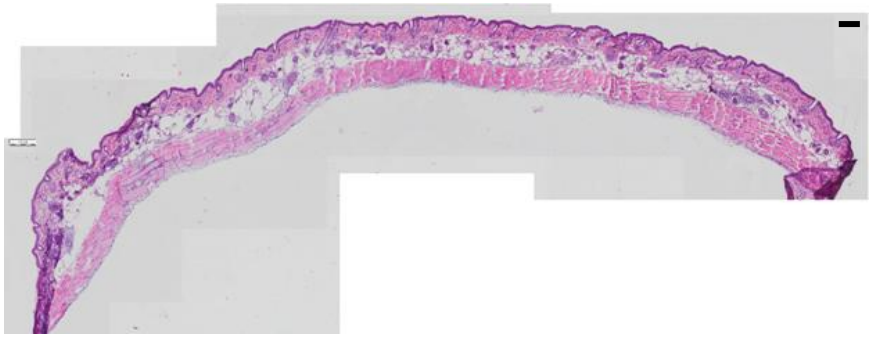

Mouse #1

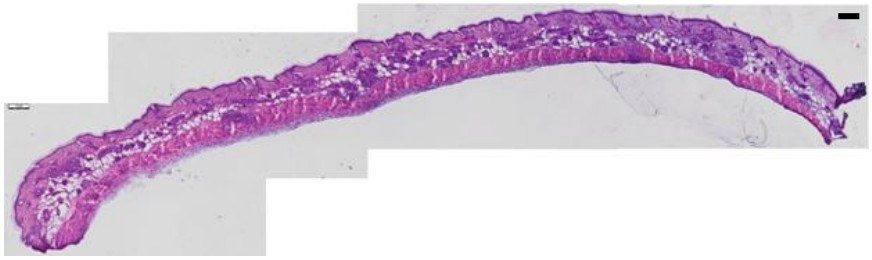

Mouse #2

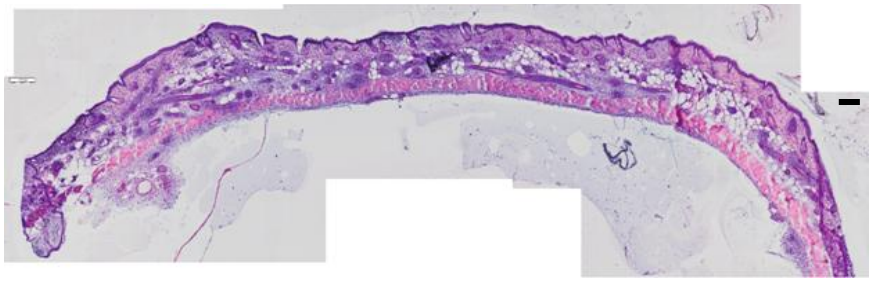

Mouse #3

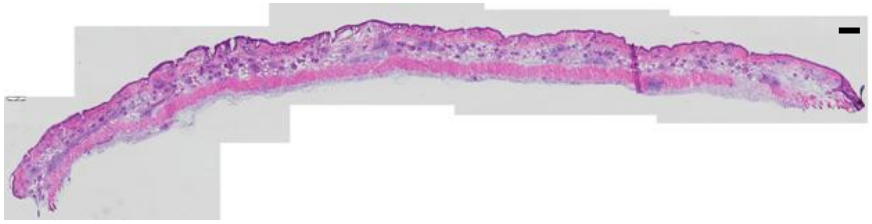

Mouse #4

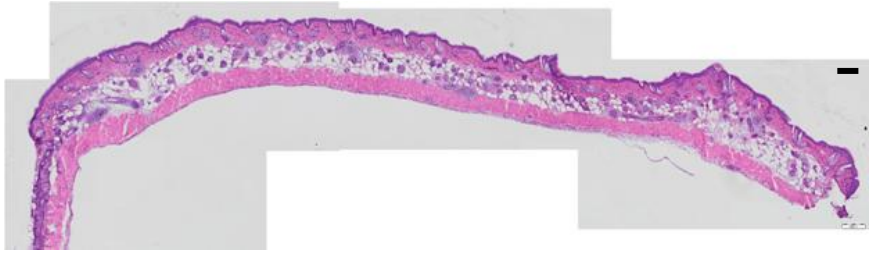

Mouse #5

Figure C21. Macroscopic appearance from NM exposed group (Day 7)

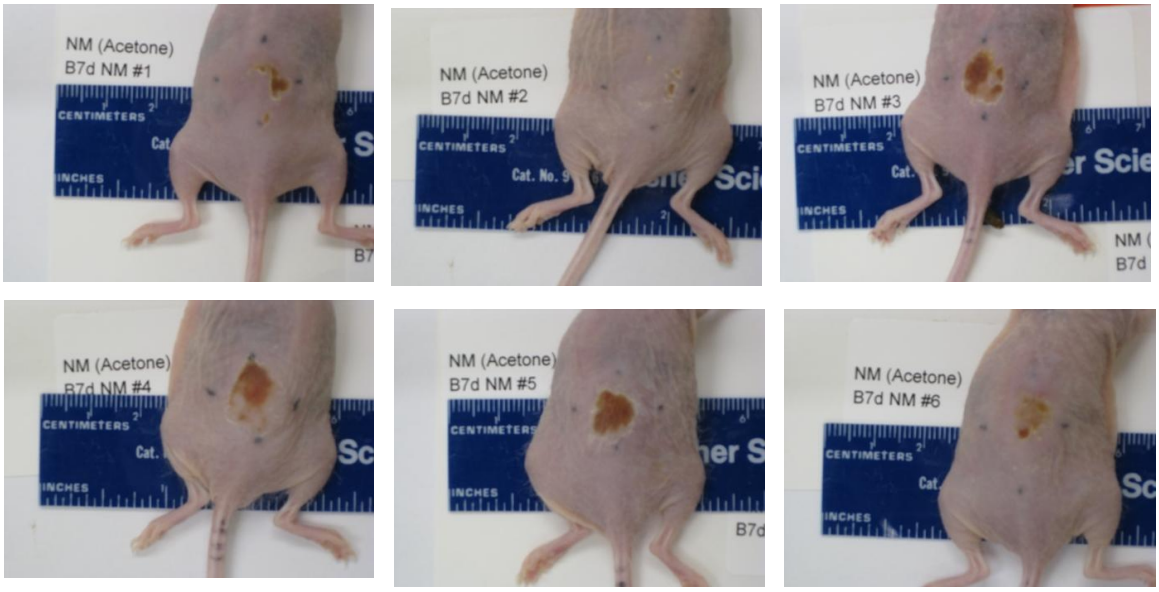

Figure C22. H&E histology from NM exposed group (Day 7) (Bar=200 µm)

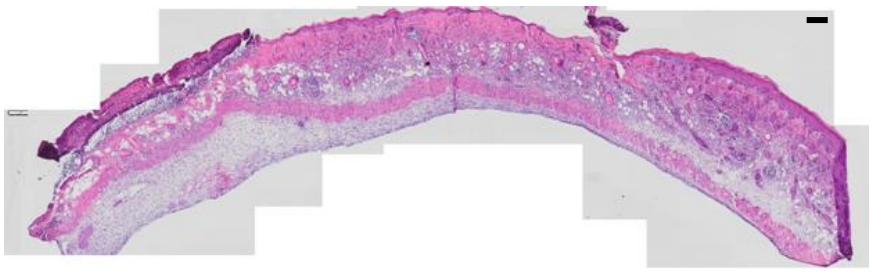
Mouse #1

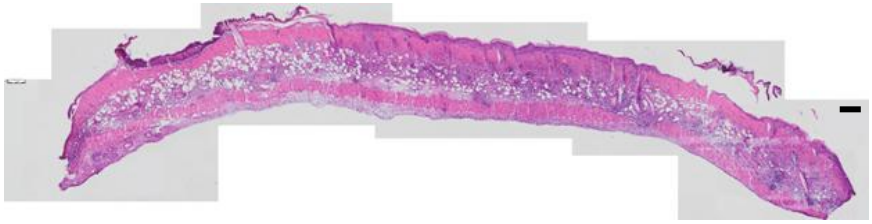
Mouse #2

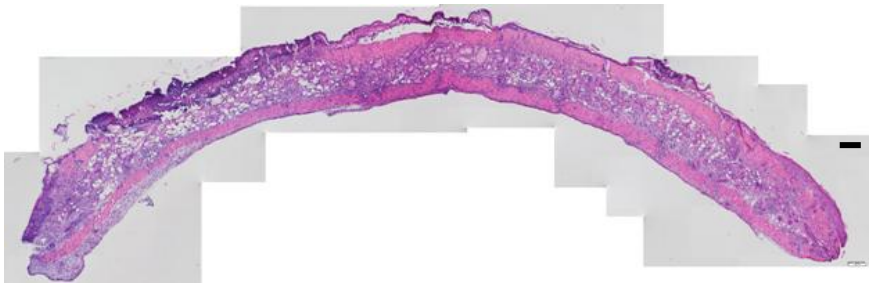
Mouse #3

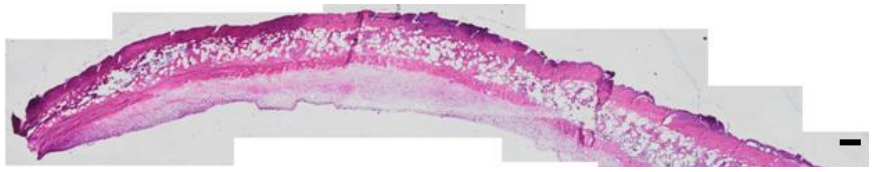
Mouse #4

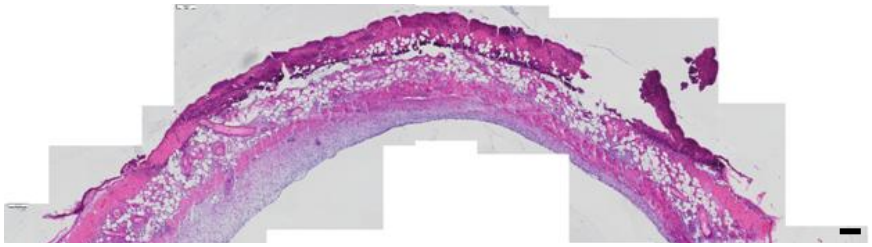
Mouse #5

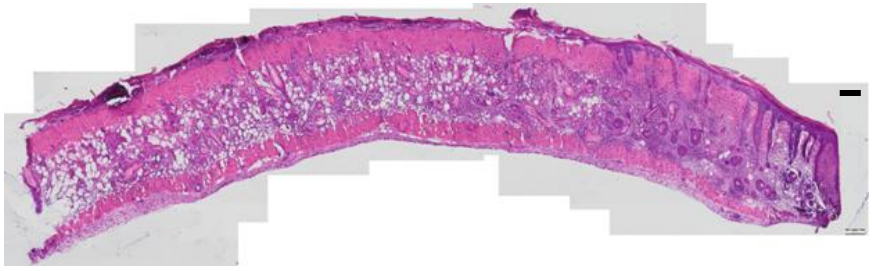
Mouse #6

Figure C23. Macroscopic appearance from NM exposed treated with Cx43 scODN group (Day 7)

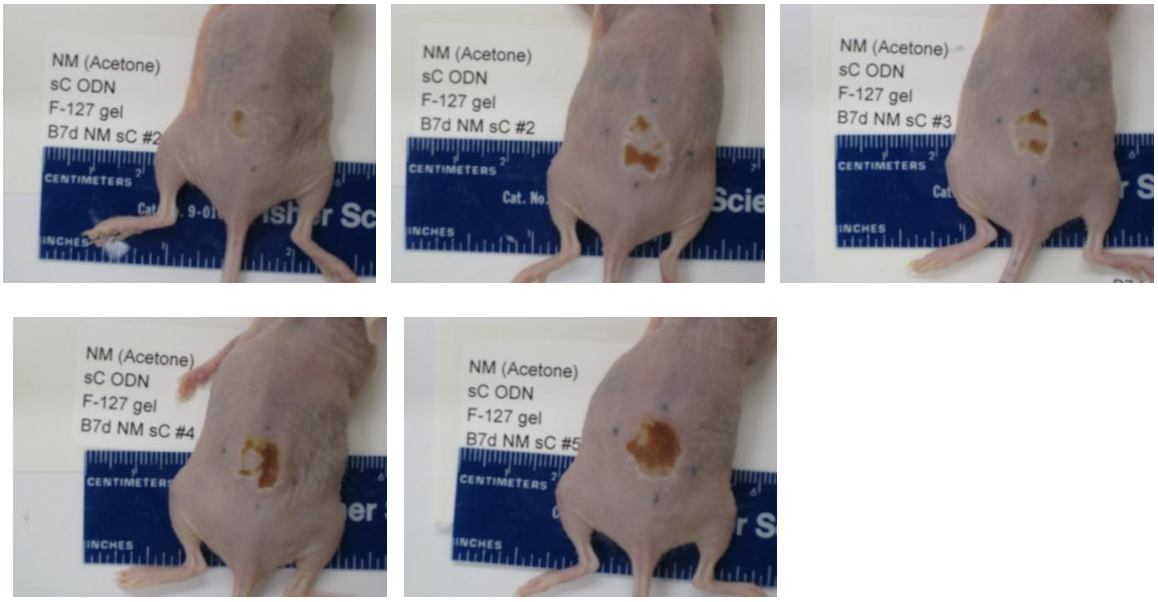

Figure C24. H&E histology from NM exposed treated with Cx43 scODN group (Day 7) (Bar=200 µm)

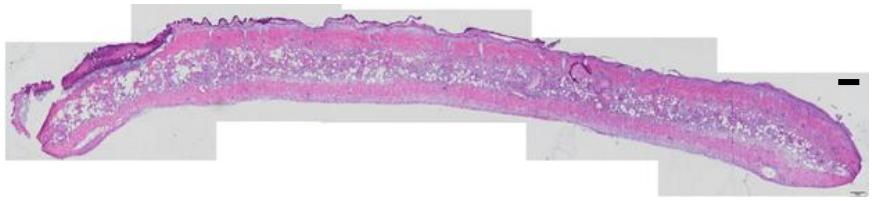

Mouse #1

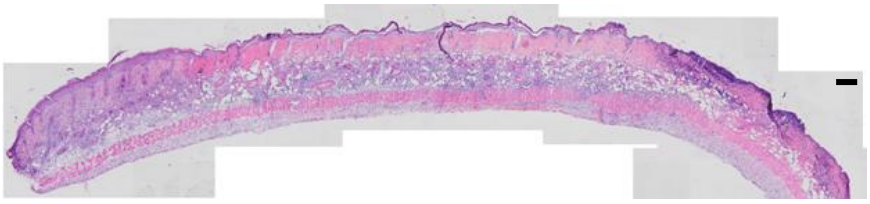

Mouse #2

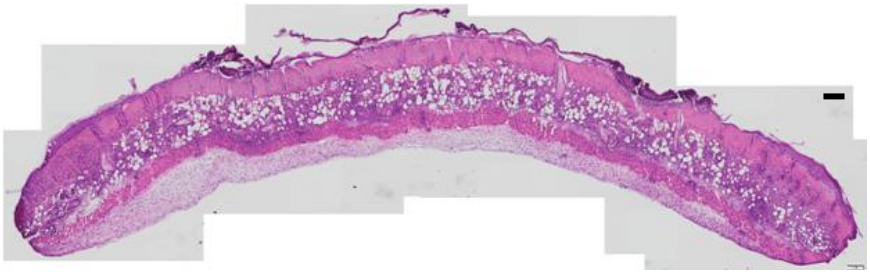

Mouse #3

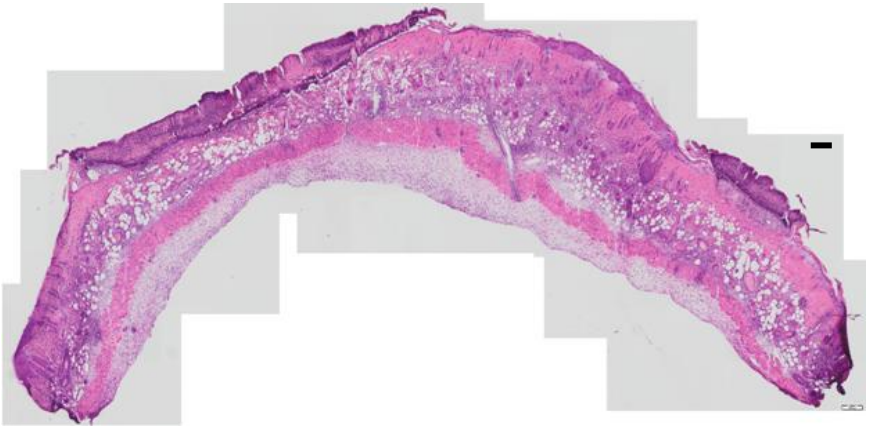

Mouse #4

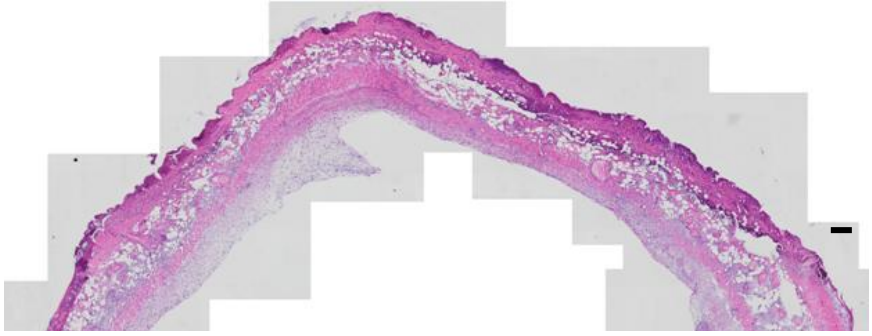

Mouse #5

Figure C25. Macroscopic appearance from NM exposed treated with Cx43 asODN group (Day 7)

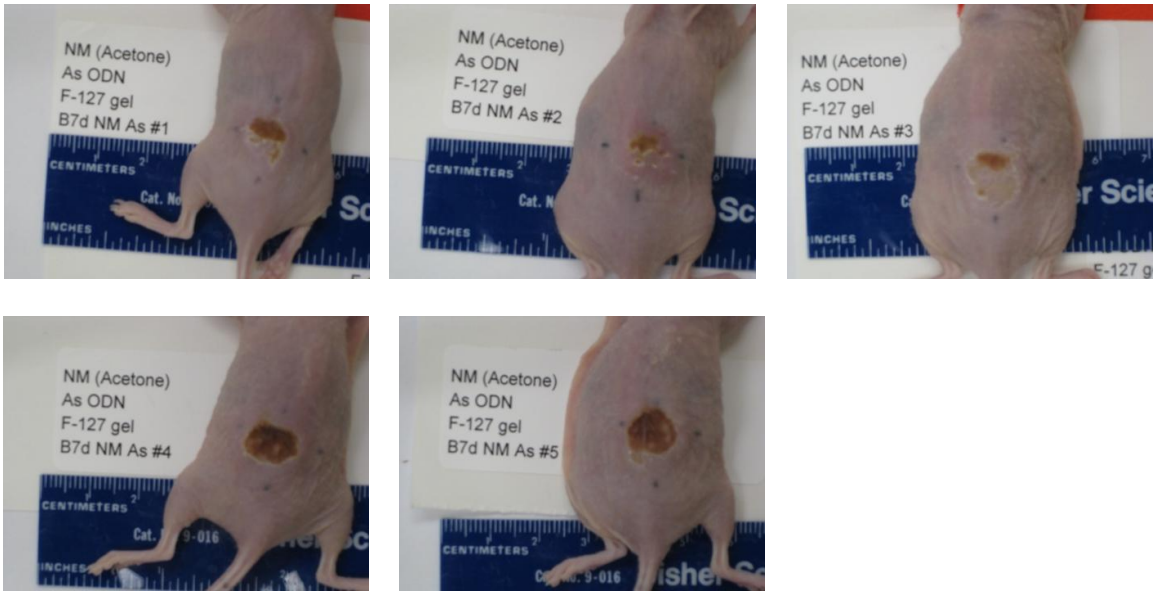

Figure C26. H&E histology from NM exposed treated with Cx43 asODN group (Day 7)

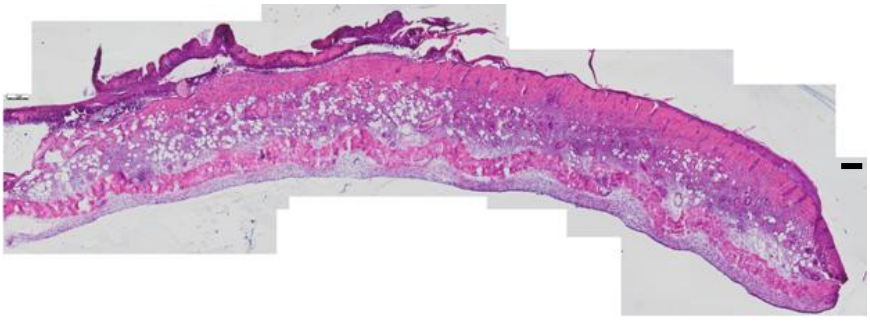

Mouse #1

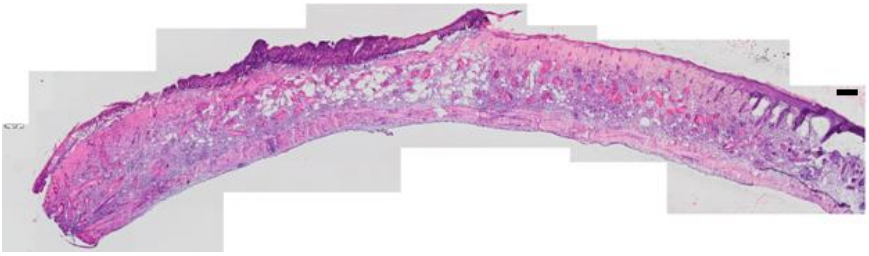

Mouse #2

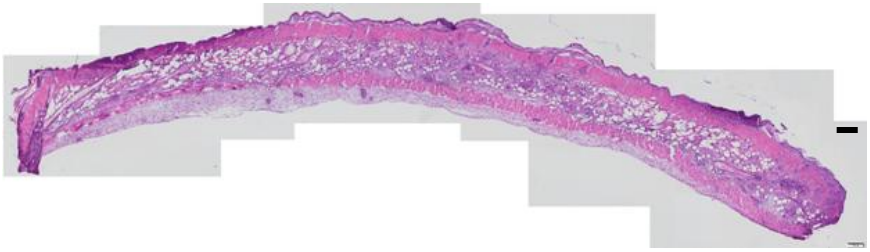

Mouse #3

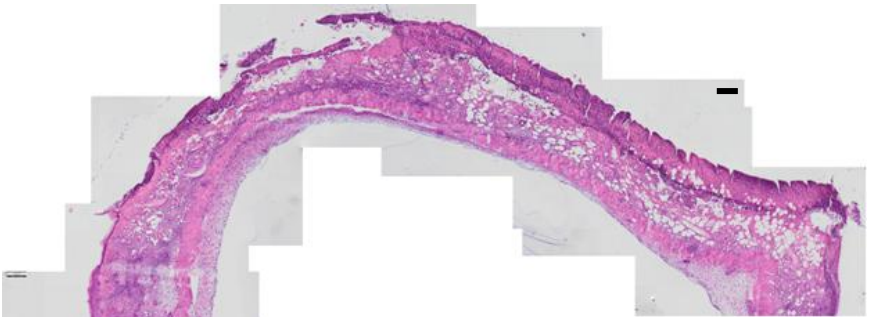

Mouse #4

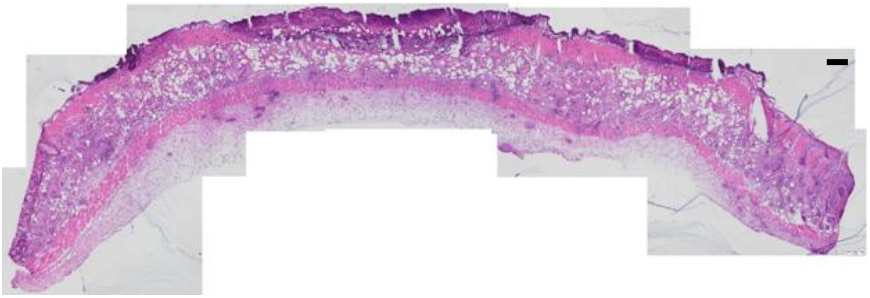

Mouse #5

Figure C27. Macroscopic appearance from vehicle (acetone) control group (Day 10)

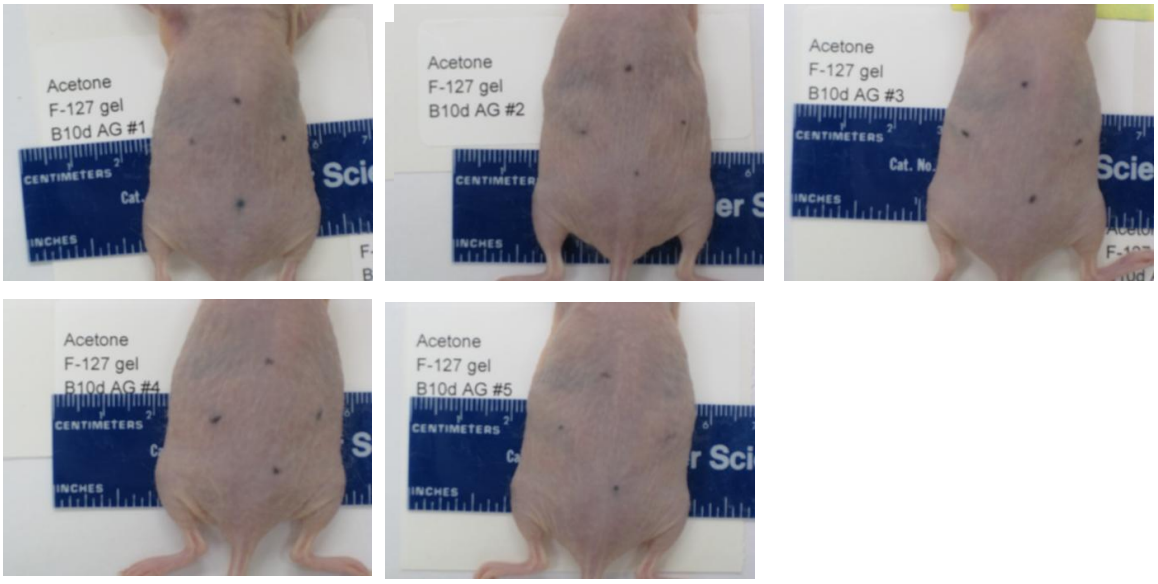

Figure C28. H&E histology from vehicle (acetone) control group (Day 10) (Bar=200 µm)

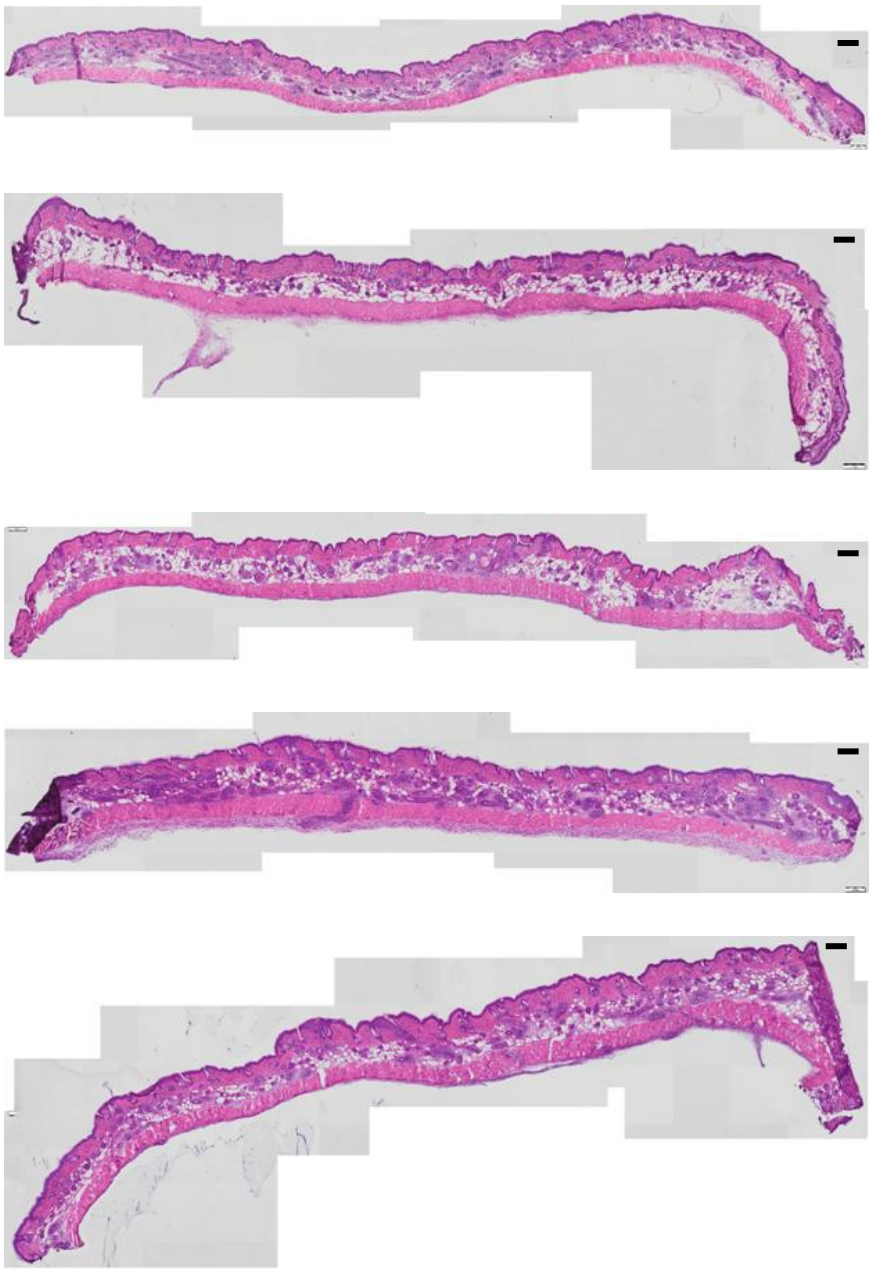

Figure C29. Macroscopic appearance from NM exposed group (Day 10)

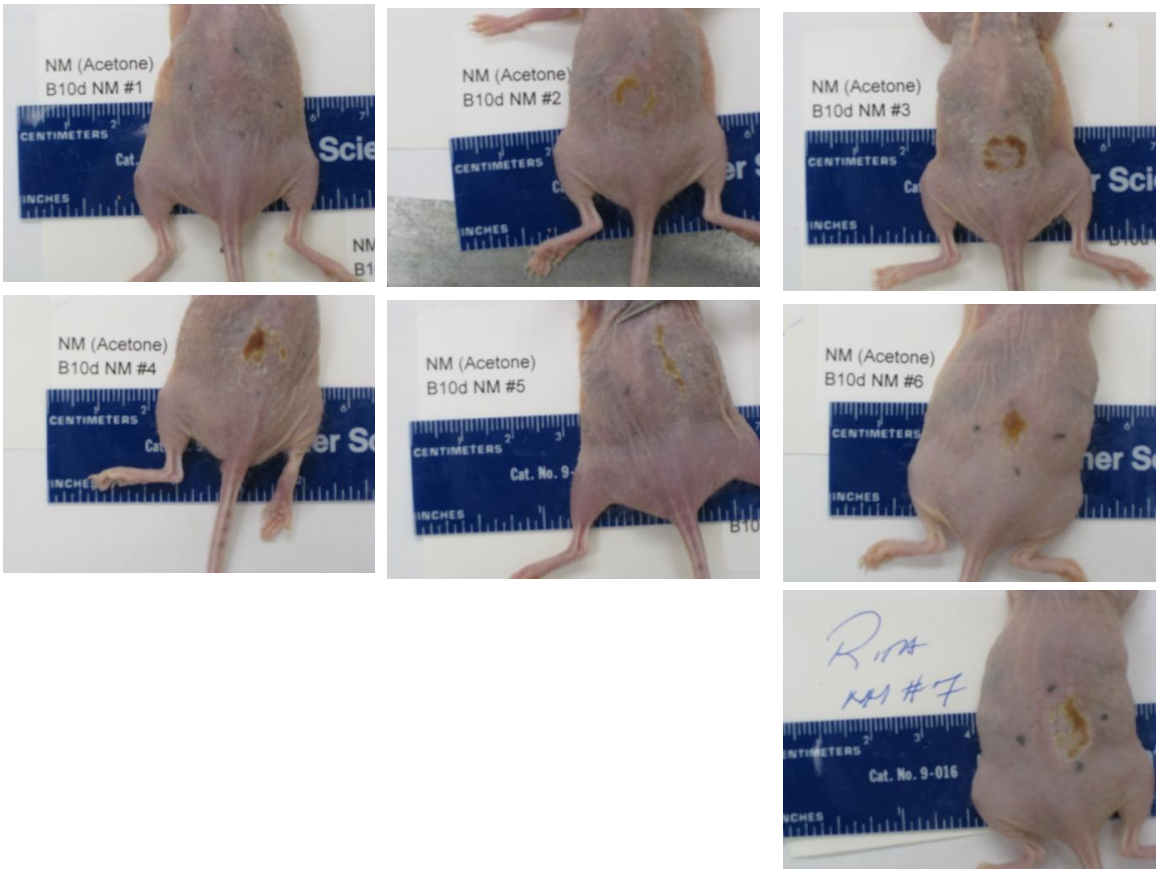

Figure C30. H&E histology from NM exposed group (Day 10) (Bar=200 μm)

Mouse #1

Mouse #2

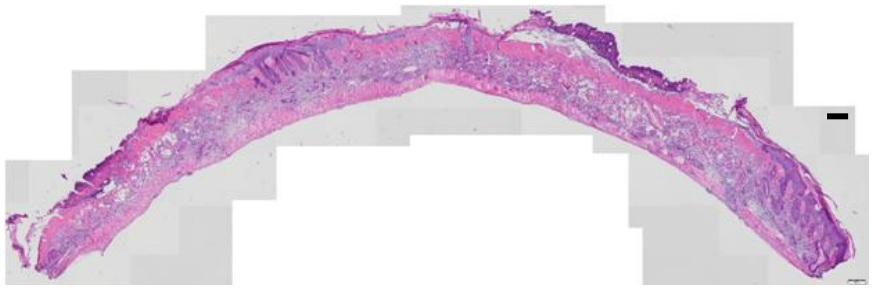

Mouse #3

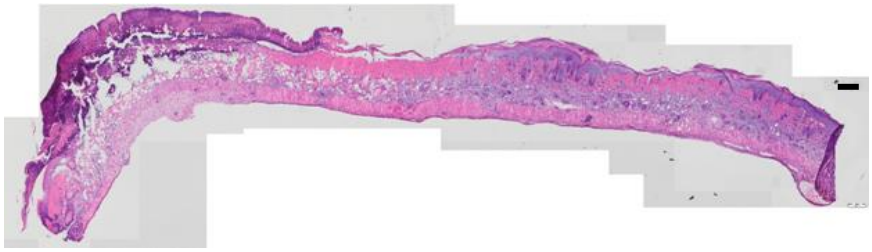

Mouse #4

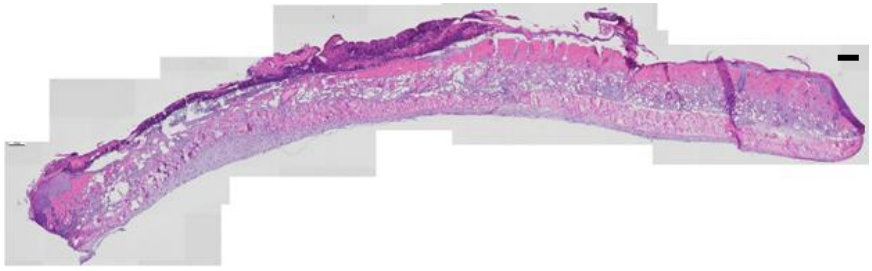

Mouse #6

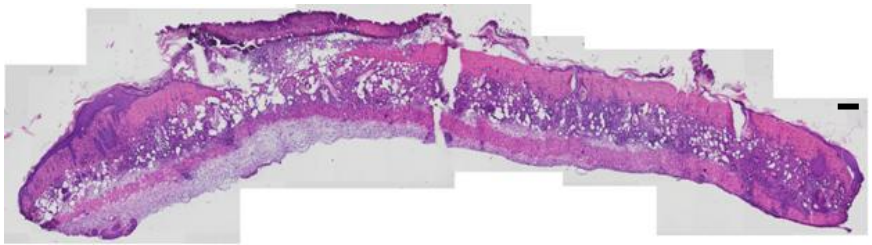

Mouse #7

Figure C31. Macroscopic appearance from NM exposed treated with Cx43 scODN group (Day 10)

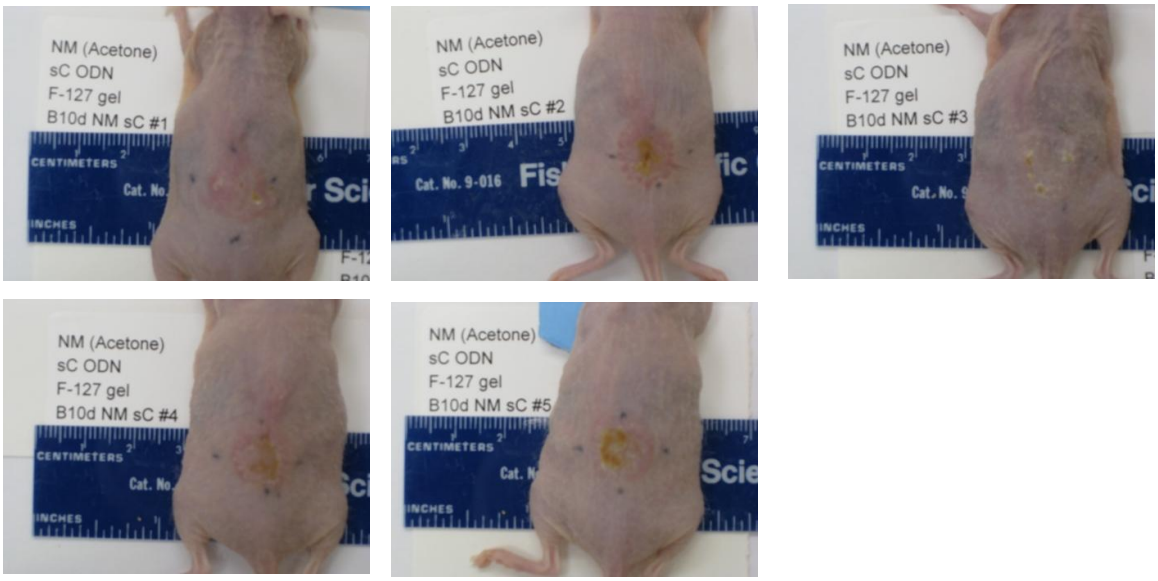

Figure C32. H&E histology from NM exposed treated with Cx43 scODN group (Day 10) (Bar=200 µm)

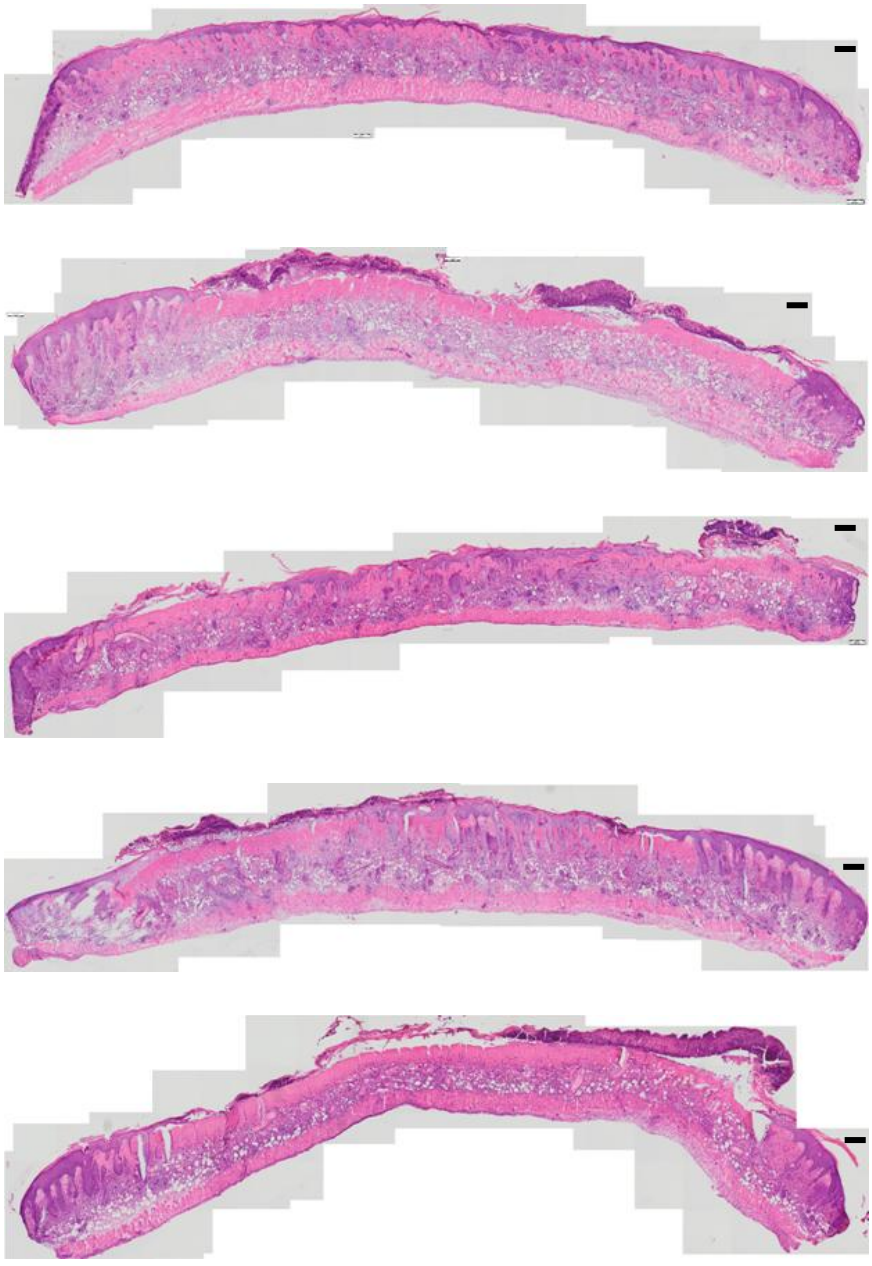

Mouse #1

Mouse #2

Mouse #3

Mouse #4

Mouse #5

Figure C33. Macroscopic appearance from NM exposed treated with Cx43 asODN group (Day 10)

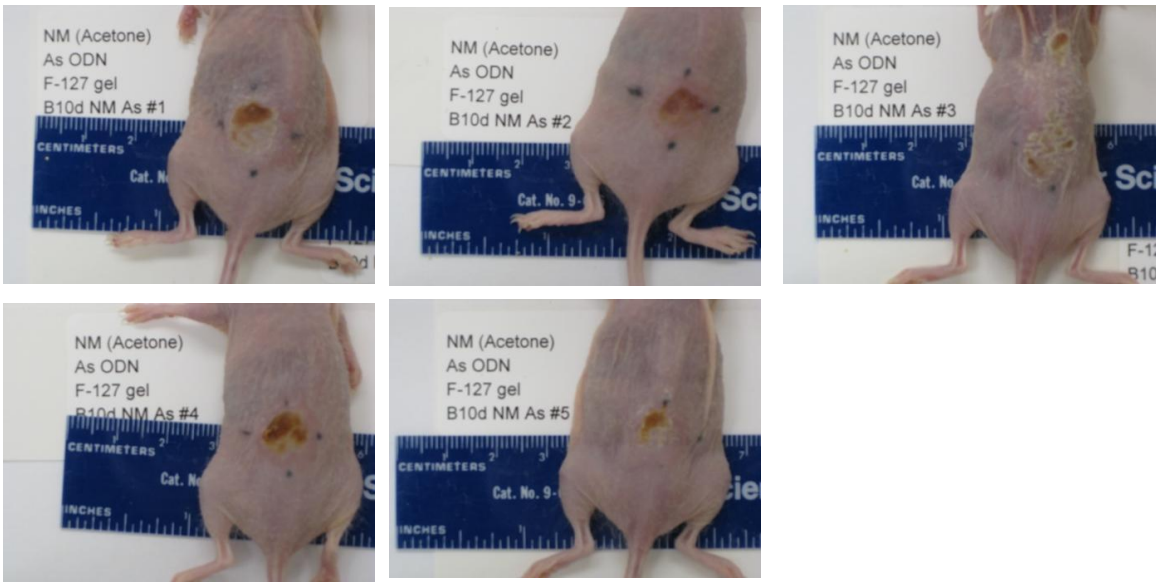

Figure C34. H&E histology from NM exposed treated with Cx43 asODN group (Day 10) (Bar=200 µm)

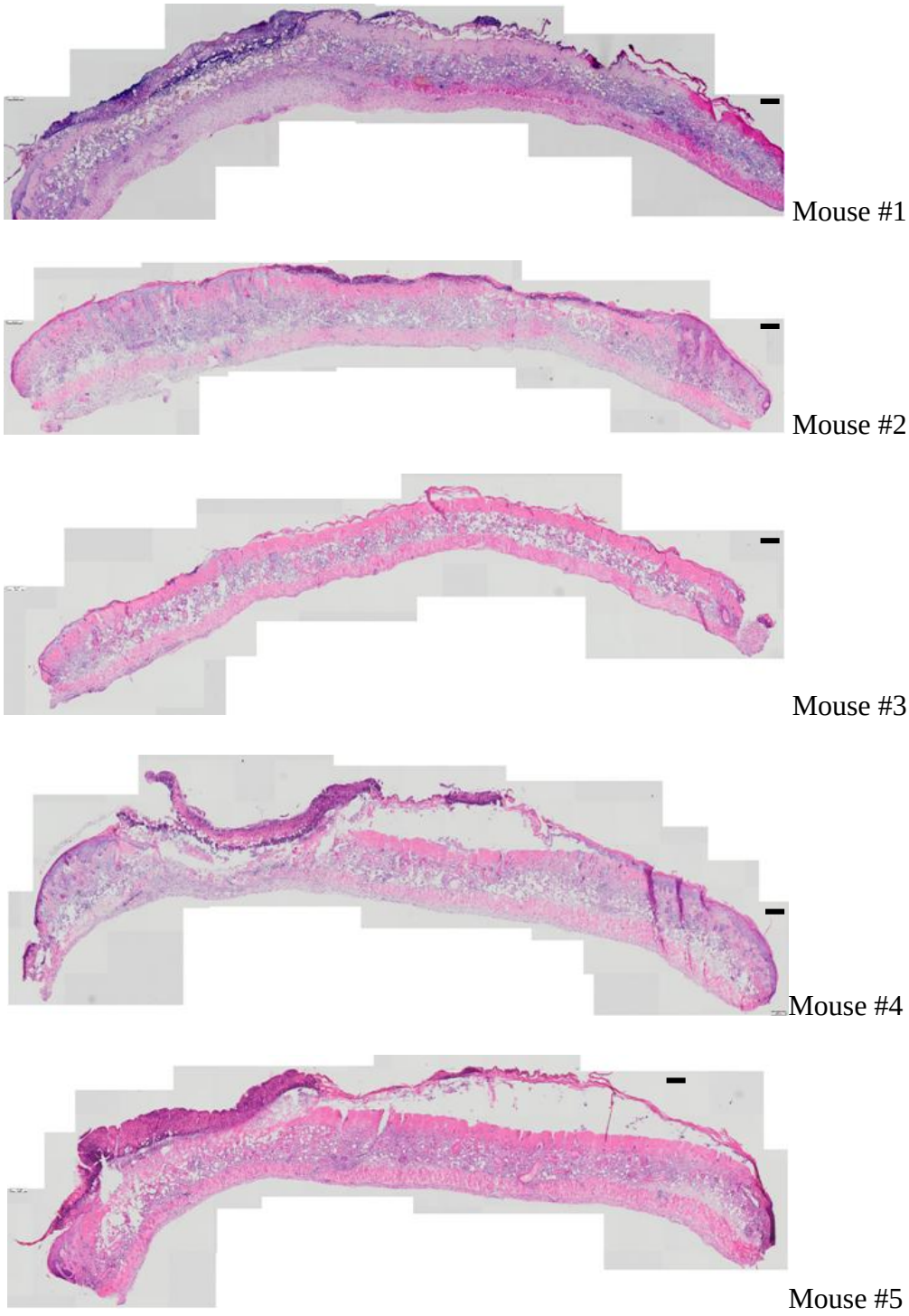

Appendix D

Results of Macroscopic Appearance, Histology, qRT-PCR, Western Blot and Densitometry from Study 1

1. Macroscopic Appearance and Histology

The lesions to the dorsal skin were observed in NM-exposed mice for days 1, 7 and 10. Histological examination of tissue sections of the mouse skin demonstrated hyperplasia and thickening of the stratum corneum (Figure D1, B left panel). Post-exposure treatment with Cx43 asODN reduced hyperplasia and thickening of the stratum corneum for days 1, 7 and 10 (Figure D1, B right panel) when compared to NM-exposed groups. The macroscopic appearance at day 10 also showed Cx43 asODN reduced lesions in the dorsal skin (Figure D1, C).

2. qRT-PCR Analysis of Cx43 - Study 1

qRT-PCR analysis showed that except for NM-exposed mice at 3 days after exposure, Cx43 was down-regulated in NM-exposed and in NM-exposed treated with Cx43 asODN groups (Figure D2).

qRT-PCR analysis showed a statistically significant ($P<0.05$) reduction of Cx43 in the Cx43 asODN group for day 3 (a 57% reduction) and day 7 (a 48% reduction) (Figure D2). Cx43 level was reduced after the treatment with Cx43 asODN on day 1 but the difference was not significant. The results indicated that Cx43 asODN downregulated Cx43.

3. qRT-PCR Analysis of Cx26 - Study 1

Cx26 was upregulated in NM-exposed groups for days 1, 3, 7 and 10 (Figure D3). qRT-PCR analysis showed a statistically significant ($P<0.05$) reduction of Cx26 by Cx43 asODN treatment for day 3 (a 66% reduction) and day 7 (a 63% reduction) when compared to NM-exposed groups (Figure D3). Due to high inter-subject variability, the reduction of

Cx26 by Cx43 asODN treatment at day 10 was not significant. The data suggests that Cx26 mRNA was reduced by Cx43 asODN treatment.

4. qRT-PCR Analysis of Cx30 - Study 1

Cx30 was upregulated in NM-exposed groups for days 1, 3, 7 and 10 (Figure D4). qRT-PCR analysis showed a statistically significant ($P<0.05$) reduction of Cx30 by Cx43 asODN treatment for day 3 (a 53% reduction) when compared NM-exposed treated with Cx43 asODN groups to NM-exposed groups (Figure D4). The reduction of Cx30 by Cx43 asODN at day 1, 7 and 10 were not statistically significant. The data suggest that Cx43 asODN also downregulates Cx30.

5. qRT-PCR Analysis of IL-1B - Study 1

IL-1B was upregulated in the NM-exposed group for days 1, 3, 7 and 10 and the peak was at day 1 as shown in qRT-PCR analysis (Figure D5). A statistically significant ($P<0.05$) reduction of IL-1B by Cx43 asODN treatment for day 1 (a 73% reduction) when compared NM-exposed treated with Cx43 asODN group to NM-exposed group was observed. IL-1B, the proinflammatory cytokine is four times less in the NM-exposed treated with Cx43 asODN group when compared to NM-exposed group on Day 1. The data suggests that Cx43 asODN downregulated IL-1B on day 1. IL1-B was 16 ($P<0.05$), 3 ($P<0.05$) and 3 fold higher in NM-exposed treated with Cx43 asODN groups when compared to NM-exposed groups on days 3, 7 and 10, respectively .

6. qRT-PCR Analysis of IL-10 - Study 1

Except at day 10, IL-10 was downregulated in the NM-exposed group (Figure D6). qRT-PCR analysis showed a statistically significant ($P<0.05$) increase of IL-10 for day 3 (a 64% increase) and day 7 (a 42% increase) by Cx43 asODN treatment when compared NM-exposed treated with Cx43 asODN groups to NM-exposed groups (Figure D6). IL10, the

antinflammatory cytokine was three times and two times higher in the Cx43 asODN treated samples compared to NM-exposed samples on day 3 and day 7, respectively. The data suggests that Cx43 asODN increases mRNA level of IL-10 on day 3 and day 7.

7. Immunoblots and Densitometry of Cx43 in Mouse Dorsal Skin Biopsies -Study 1

The protein level of Cx43 decreased in NM exposed groups when compared to the vehicle control groups at days 1, 7 and 10. At day 3, the level of Cx43 in NM exposed group was slightly higher than the vehicle control group (Figure D7). The reduction of Cx43 protein level by Cx43 asODN when compared NM-exposed treated with Cx43 asODN groups (As) to NM-exposed groups (NM) was observed at days 1, 3, 7 and 10 (Figure D7). The results from Western blot analysis are reflected in the densitometry measurements (Figure D8). Densitometry data showed the protein level of Cx43 decreased in NM exposed mouse skin when compared to the vehicle control groups at days 1, 7 and 10. The level of Cx43 was further reduced by Cx43 asODN at days 1, 3, 7 and 10.

Figure D1. Summary of H&E histology and macroscopic appearance from Study 1. Hematoxylin and eosin stained histology of the dorsal skin in SKH-1 mouse following a topical application of 5 µmole NM (in methylene chloride) and post-exposure treatment with 0.15 nmoles of Cx43 asODN. Histological features show the dorsal skin of mice from unexposed control (A), after 1, 7 and 10 days of NM exposure (B, left panel) and 1, 7 and 10 days post exposure treatment with Cx43 asODN (NM + As) (B, right panel). Bar represents 50 or 200 µm. The boxed area represented what is magnified at right panels. The macroscopic appearance of the dorsal skin of mice from unexposed control is depicted in (A) and lesions in the skin at day 10 are depicted in (C).

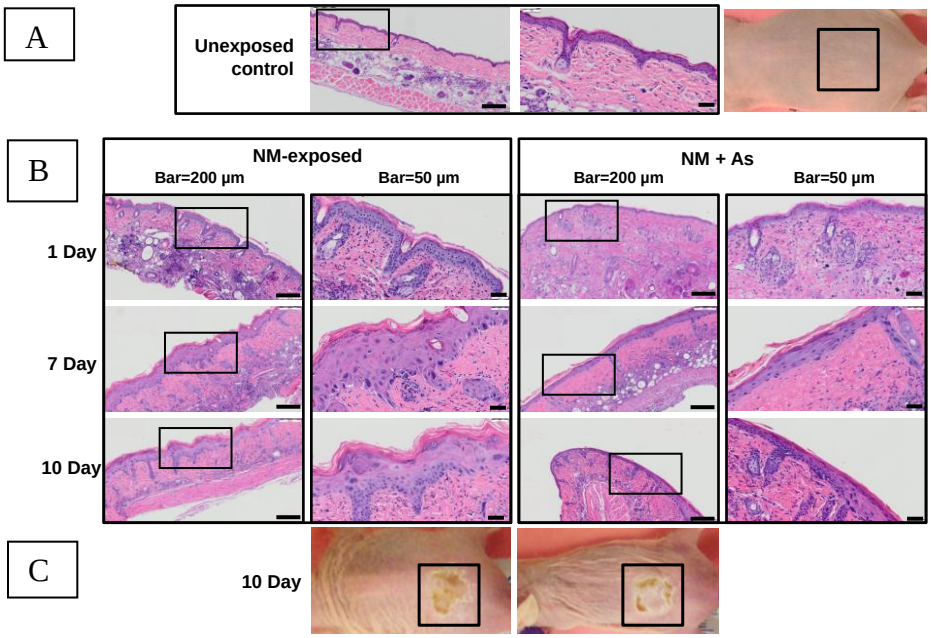

Figure D2. qRT-PCR analysis of Cx43 (Study 1). qRT-PCR analysis of Cx43 gene expression for mouse skin for 1, 3, 7, 10 days post NM-exposure (5 μmole in methylene chloride). mRNA expression of Cx43 was normalized to GAPDH and expressed as fold changes relative to vehicle control (mRNA of vehicle control divided by vehicle control arbitrarily assigned the number 1 and is shown as a dotted line). Data reported as mean ± SE. VC: Vehicle Control; NM: NM-exposed; NM+As: NM-exposed treated with Cx43 asODN (0.15 nmoles). * $p < 0.05$ (NM+As *vs* NM).

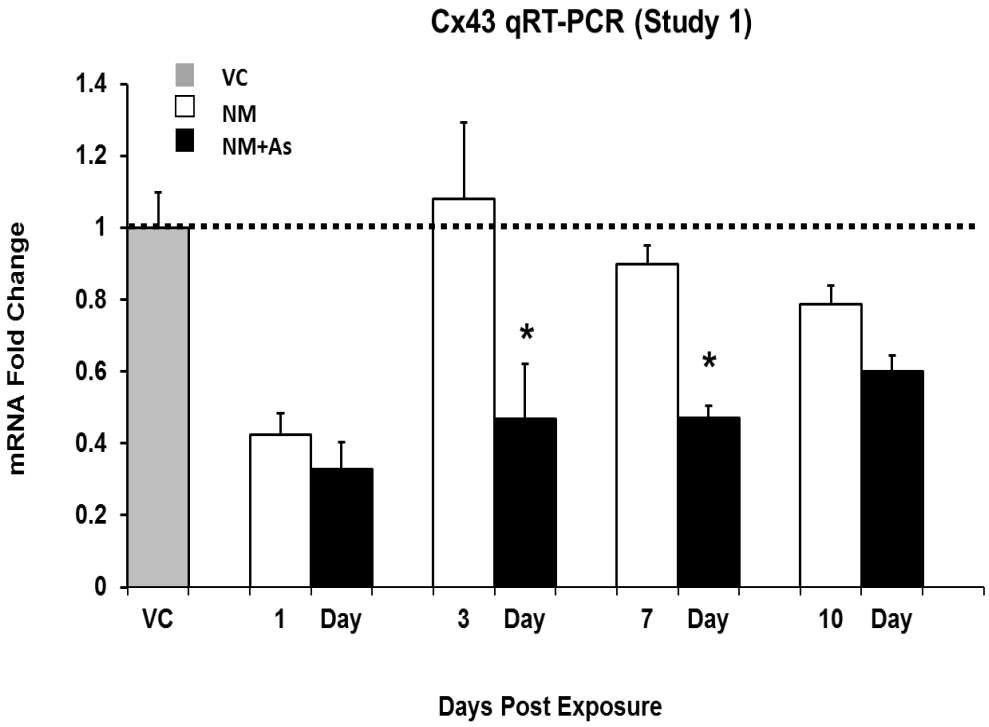

Figure D3. qRT-PCR analysis of Cx26 (Study 1). qRT-PCR analysis of Cx26 gene expression for mouse skin for 1, 3, 7, 10 days post NM-exposure (5 μmole in methylene chloride). mRNA expression of Cx26 was normalized to GAPDH and expressed as fold changes relative to vehicle control (mRNA of vehicle control divided by vehicle control arbitrarily assigned the number 1 and is shown as a dotted line). Data reported as mean ± SE. VC: Vehicle Control; NM: NM-exposed; NM+As: NM-exposed treated with Cx43 asODN (0.15 nmoles). * p< 0.05 (NM+As *vs* NM).

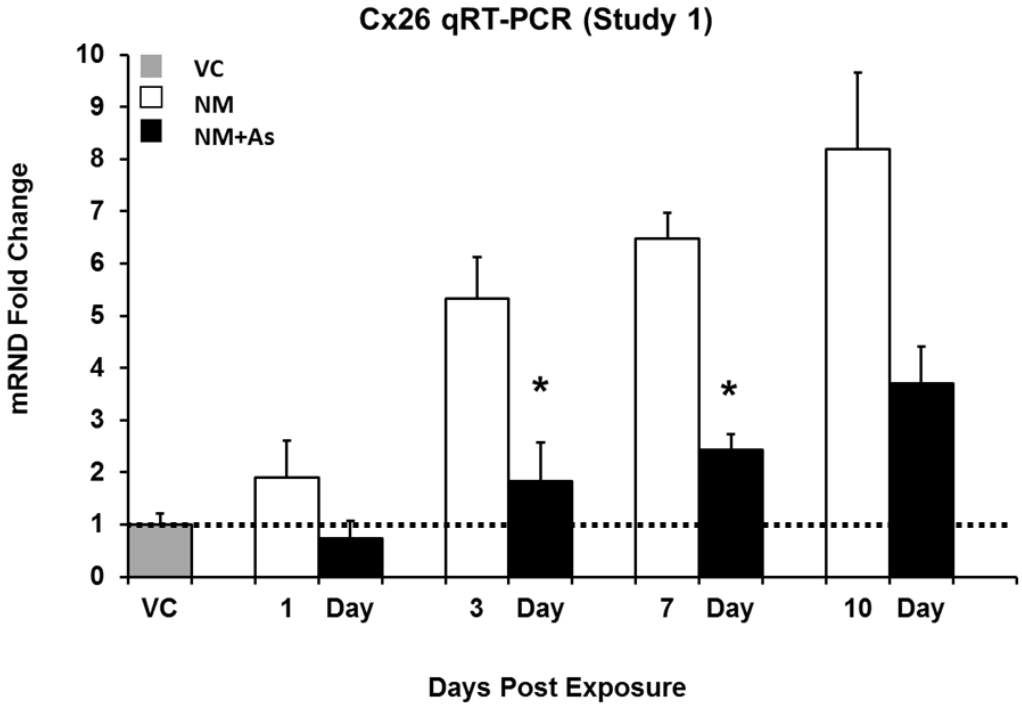

Figure D4. qRT-PCR analysis of Cx30 (Study 1). qRT-PCR analysis of Cx30 gene expression for mouse skin for 1, 3, 7, 10 days post NM-exposure (5 μmole in methylene chloride). mRNA expression of Cx30 was normalized to GAPDH and expressed as fold changes relative to vehicle control (mRNA of vehicle control divided by vehicle control arbitrarily assigned the number 1 and is shown as a dotted line). Data reported as mean ± SE. VC: Vehicle Control; NM: NM-exposed; NM+As: NM-exposed treated with Cx43 asODN (0.15 nmoles). * p< 0.05 (NM+As *vs* NM).

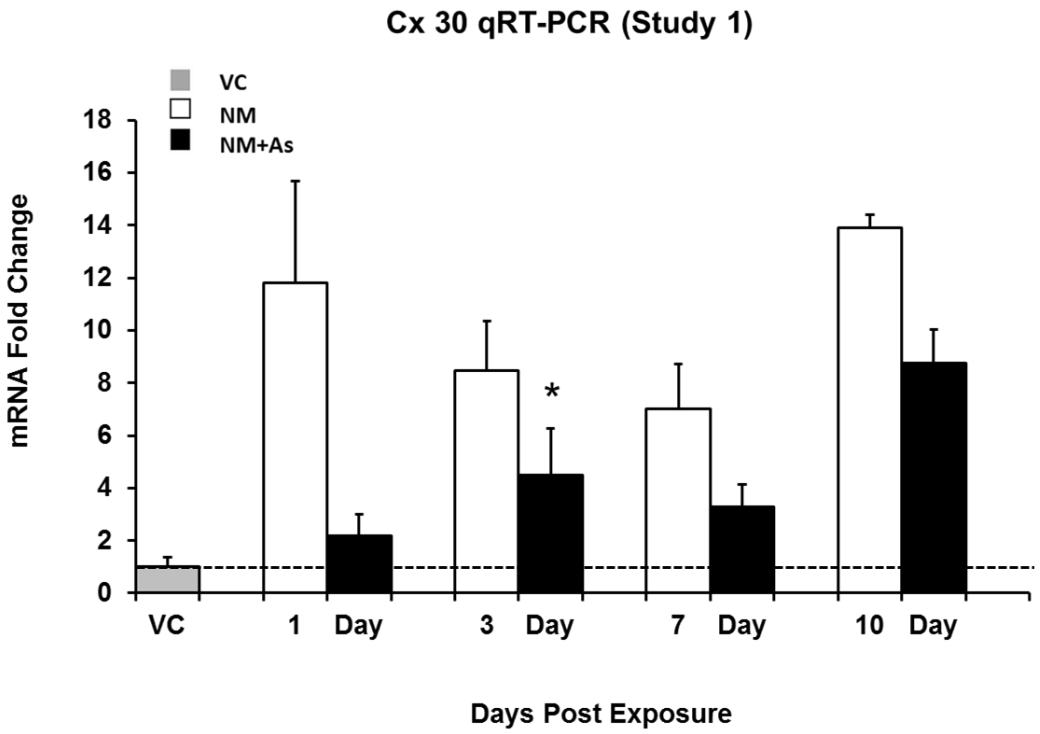

Figure D5. qRT-PCR analysis of IL-1B (Study 1). qRT-PCR analysis of IL-1B gene expression for mouse skin for 1, 3, 7, 10 days post NM-exposure (5 μmole in methylene chloride). mRNA expression of IL-1B was normalized to GAPDH and expressed as fold changes relative to vehicle control (mRNA of vehicle control divided by vehicle control arbitrarily assigned the number 1 and is shown as a dotted line). Data reported as mean ± SE. VC: Vehicle Control; NM: NM-exposed; NM+As: NM-exposed treated with Cx43 asODN (0.15 nmoles). * $p < 0.05$ (NM+As *vs* NM).

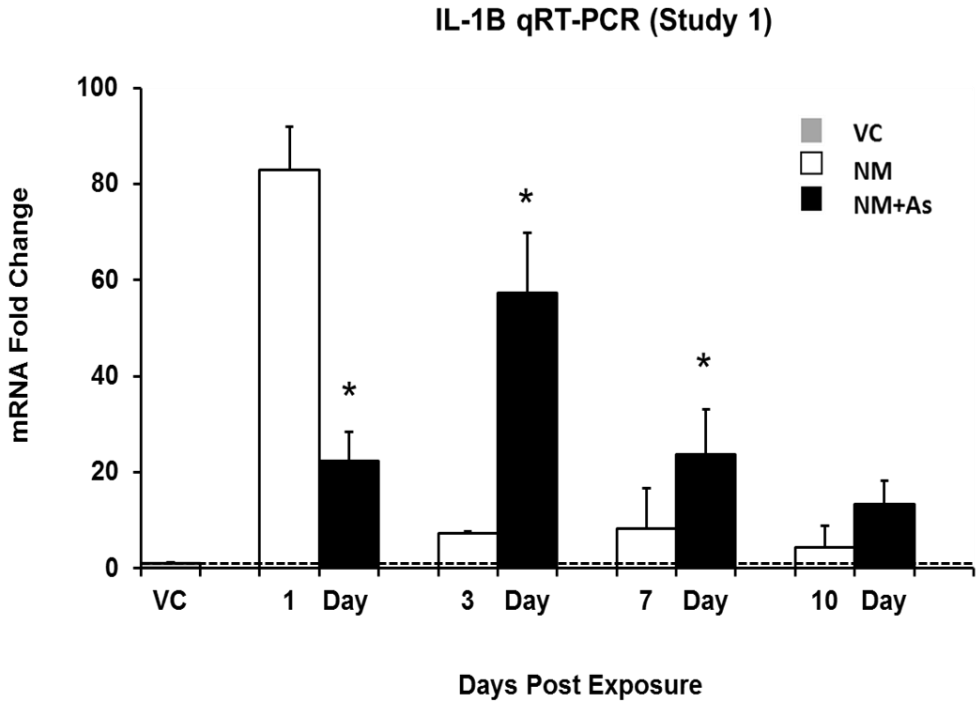

Figure D6. **qRT-PCR analysis of IL-10 (Study 1).** qRT-PCR analysis of IL-10 gene expression for mouse skin for 1, 3, 7, 10 days post NM-exposure (5 μmole in methylene chloride). mRNA expression of IL-10 was normalized to GAPDH and expressed as fold changes relative to vehicle control (mRNA of vehicle control divided by vehicle control arbitrarily assigned the number 1 and is shown as a dotted line). Data reported as mean ± SE. VC: Vehicle Control; NM: NM-exposed; NM+As: NM-exposed treated with Cx43 asODN (0.15 nmoles). * p< 0.05 (NM+As *vs* NM).

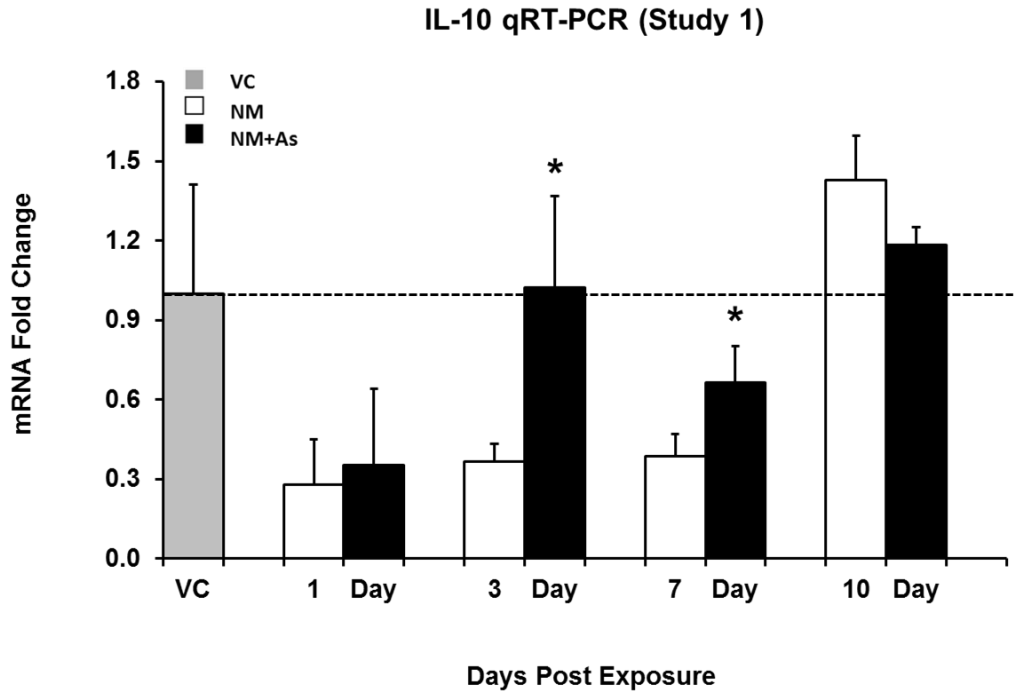

Figure D7. Immunoblots of Cx43 on days 1, 3, 7 and 10 (Study 1). Immunoblots of Cx43 in SKH-1 mouse skin for 1, 3, 7 and 10 days following a topical application of 5 μmole NM in methylene chloride and post-exposure treatment with Cx43 scODN or Cx43 asODN. Protein level of Cx43 in unexposed control (UC), vehicle control (VC), NM exposed (NM), NM exposed treated with Cx43 scODN (sC, 0.15 nmole) and NM exposed treated with Cx43 asODN (As, 0.15 nmole) mice skin at days 1, 3, 7 and 10 post-exposure. GAPDH was used as equal protein loading controls.

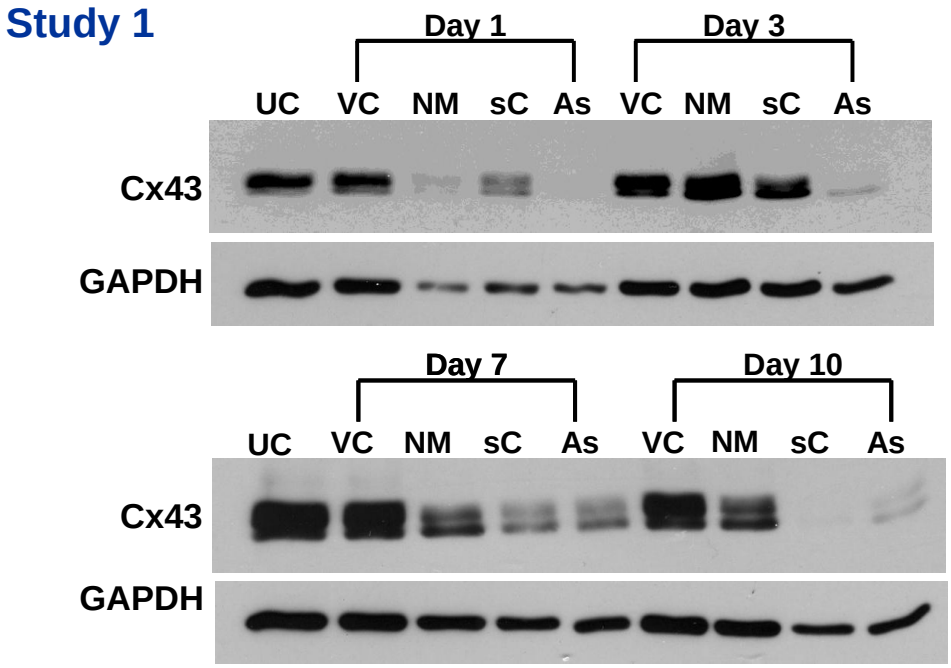

UC: Unexposed Control; **VC**: Vehicle Control; **NM**: Nitrogen Mustard exposed
sC: NM + Sense Control; **As**: NM + Antisense treatment

Figure D8. Densitometry of Cx43 on days 1, 3, 7 and 10 (Study 1). Densitometry of Cx43 in unexposed control (UC), vehicle control (VC), NM exposed (NM, 5 μmole), NM exposed treated with Cx43 scODN (sC, 0.15 nmole) and NM exposed treated with Cx43 asODN (As, 0.15 nmole) mice skin at days 1, 3, 7 and 10 post-exposure.

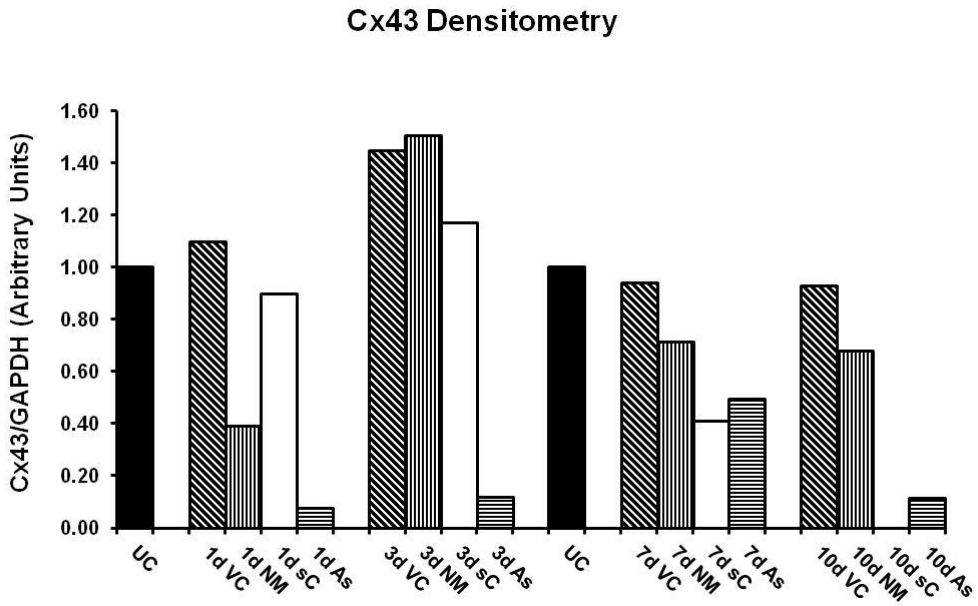

UC: Unexposed Control; **VC**: Vehicle Control; **NM**: Nitrogen Mustard exposed
sC: NM + Sense Control; **As**: NM + Antisense treatment

Appendix E

Overview of Results of Study 1 and Study 2

1. Study 1

The effects of NM-exposure and Cx43 asODN treatment for 1, 3, 7 and 10 days post-exposure on mouse skin based on results from H&E, WB, and qRT-PCR analysis are summarized in Table E1.

Table E1. The effects of NM-exposure and Cx43 asODN treatment for 1, 3, 7 and 10 days post-exposure on mouse skin based on results from H&E, WB and qRT-PCR analysis*

Study 1

Analysis	NM-exposure	Cx43 asODN treatment Day 1	Cx43 asODN treatment Day 3	Cx43 asODN treatment Day 7	Cx43 asODN treatment Day 10
H&E	Increased inflammatory response	Decreased inflammatory response	NA	Decreased inflammatory response	Decreased inflammatory response
WB (Cx43)	-	↓	↓	-	-
RT-PCR					
Cx43	↓	↓	↓ *	↓ *	↓
Cx26	↑	↓	↓ *	↓ *	↓
Cx30	↑	↓	↓ *	↓	↓
IL-1B	↑	↓ *	↑ *	↑ *	↑
IL-10	↓: day1, 3, 7. ↑: day 10	↑	↑ *	↑ *	↓
MMP-12	N.C.: day 1, 3 ↑: day 7,10	↓	↑	↓	↓

***By comparing "NM-exposed treated with Cx43 asODN group" to "NM-exposed group"**

WB denotes Western Blotting
qRT-PCR denotes real-time reverse transcription polymerase chain reaction
N.C.: no change

↑ denotes up-regulated or increased
↓ denotes down-regulated or decreased
* denotes significant ($P<0.05$)

2. Study 2

The effects of NM-exposure and Cx43 asODN treatment for 1, 3, 7 and 10 days post-exposure on mouse skin based on results from H&E, WB and qRT-PCR analysis are summarized in Table E2.

Table E2. The effects of NM-exposure and Cx43 asODN treatment for 1, 3, 7 and 10 days post-exposure on mouse skin based on results from H&E, WB and qRT-PCR analysis*.

Study 2

Analysis	NM-exposure	Cx43 asODN treatment Day 1	Cx43 asODN treatment Day 3	Cx43 asODN treatment Day 7	Cx43 asODN treatment Day 10
H&E	Increased inflammatory response	Decreased inflammatory response	Decreased inflammatory response	Decreased inflammatory response	Decreased inflammatory response
WB (Cx43)	-	↓	↓	↓	↓
RT-PCR					
Cx43	↓	↑	↓*	↓ *	↓
Cx26	↑	↓ *	↓ *	↓	↓
Cx30	↑	↓ *	↓	↓	↓
COX-2	↑	↓ *	↑*	↑	↑
IL-1B	↑	↓	↑*	↑*	↑*
IL-6	↑	↓	↑	↑*	↑
IL-10	↓	↓	↓	↓	↓
MMP-2	↑ day 7, 10	↓	↓	↑	↑
MMP-9	↑ day 7, 10	↑	↑	↑	↑
MMP-12	↑ day 7, 10	↑	↑	↑	↑
PGES-2	↓ day 1, 3, 7 10	↑	↓	↓	↓

***By comparing "NM-exposed treated with Cx43 asODN group" to "NM-exposed group"**

WB denotes Western Blotting
qRT-PCR denotes real-time reverse transcription polymerase chain reaction

↑ denotes up-regulated or increased
↓ denotes down-regulated or decreased
* denotes significant (P<0.05)